Eugene S. Grecheck
Vice President
Nuclear Development

Dominion Energy, Inc. • Dominion Generation
Innsbrook Technical Center
5000 Dominion Boulevard, Glen Allen, VA 23060
Phone: 804-273-2442, Fax: 804-273-3903
E-mail: Eugene.Grecheck@dom.com

Dominion®

August 22, 2011

U. S. Nuclear Regulatory Commission
Attention: Document Control Desk
Washington, D.C. 20555

Serial No. NA3-11-019R
Docket No. 52-017
COL/MWH

DOMINION VIRGINIA POWER
NORTH ANNA UNIT 3 COMBINED LICENSE APPLICATION
SRP 03.07.01 AND 03.07.02: RESPONSE TO RAI LETTER 64

On April 7, 2011, the NRC requested additional information to support the review of certain portions of the North Anna Unit 3 Combined License Application (COLA), which consisted of ten questions. The responses to the following six Request for Additional Information (RAI) Questions are provided in Enclosures 1 through 6:

- RAI 5544 Question 03.07.01-4 Seismic Damping Values for ISRS
- RAI 5546 Question 03.07.02-2 Update of Site-Specific SSI Analyses
- RAI 5546 Question 03.07.02-3 SSI Analysis for Standard Plant Structures
- RAI 5546 Question 03.07.02-4 SSI Analysis for Site-Specific Structures
- RAI 5546 Question 03.07.02-5 Element Connectivity in 3-D Model
- RAI 5546 Question 03.07.02-9 Soil-Structure Separation and Sliding

This information will be incorporated into a future submission of the North Anna Unit 3 COLA, as described in the enclosures.

The responses to the remaining RAI 5544 and 5546 questions are dependent upon potential changes to seismic site response analyses and US-APWR seismic analysis modeling and will be provided in a future submittal following completion of the structural design re-evaluations.

DO89
NRO

Please contact Regina Borsh at (804) 273-2247 (regina.borsh@dom.com) if you have questions.

Very truly yours,

Eugene S. Grecheck

COMMONWEALTH OF VIRGINIA

COUNTY OF HENRICO

The foregoing document was acknowledged before me, in and for the County and Commonwealth aforesaid, today by Eugene S. Grecheck, who is Vice President-Nuclear Development of Virginia Electric and Power Company (Dominion Virginia Power). He has affirmed before me that he is duly authorized to execute and file the foregoing document on behalf of the Company, and that the statements in the document are true to the best of his knowledge and belief.

Acknowledged before me this 22nd day of August, 2011
My registration number is 7173057 and my
Commission expires: August 31, 2012

Wanda L. Marshall
Notary Public

WANDA L. MARSHALL
Notary Public
Commonwealth of Virginia
7173057
My Commission Expires Aug 31, 2012

cc: U. S. Nuclear Regulatory Commission, Region II
C. P. Patel, NRC
T. S. Dozier, NRC
J. T. Reece, NRC

Enclosures:

1. Response to NRC RAI Letter Number 64, RAI 5544 Question 03.07.01-4
2. Response to NRC RAI Letter Number 64, RAI 5546 Question 03.07.02-2
3. Response to NRC RAI Letter Number 64, RAI 5546 Question 03.07.02-3
4. Response to NRC RAI Letter Number 64, RAI 5546 Question 03.07.02-4
5. Response to NRC RAI Letter Number 64, RAI 5546 Question 03.07.02-5
6. Response to NRC RAI Letter Number 64, RAI 5546 Question 03.07.02-9

Commitments made by this letter:

1. Provide COLA markups for RAI 5544 Question 03.07.01-4.
2. Provide responses to RAI 5544, Question 03.07.01-3 and RAI 5546, Questions 03.07.02-6, -7, and -8.
3. Revise COL application as described in the letter.

ENCLOSURE 1

Response to NRC RAI Letter 64

RAI 5544 Question 03.07.01-4

RESPONSE TO REQUEST FOR ADDITIONAL INFORMATION

North Anna Unit 3

Dominion

Docket No. 52-017

RAI NO.: 5544 (RAI Letter 64)

SRP SECTION: 03.07.01 – SEISMIC DESIGN PARAMETERS

QUESTIONS for Structural Engineering Branch 1 (AP1000/EPR Project) (SEB1)

DATE OF RAI ISSUE: 4/7/2011

QUESTION NO.: 03.07.01-4

Section 3.7.1.2 of the NA3 FSAR states that the SSE damping values are used for the calculation of seismic structural demands and in-structure response spectra (ISRS). However, RG 1.61, "Damping Values for Seismic Design of Nuclear Power Plants" sets forth guidance that OBE damping values should be used in calculating ISRS unless a plant-specific technical basis for use of damping values higher than the OBE damping values is submitted. The staff concern is that the use of a higher SSE damping values (if unjustified) may lead to an under-prediction of seismic demands. To address this concern, the staff requests the technical basis for using damping values higher than the OBE damping values in calculating ISRS for Category I structures at the Unit 3 site.

Dominion Response

Dominion will implement OBE damping values for generation of site-specific in-structure response spectra (ISRS), rather than provide additional plant-specific technical basis for use of SSE damping values.

The affected portions of COLA Part 2, which include FSAR Sections 3.7.1.2, 3.7.2.2, 3.7.2.4.1, 3.7.2.5, 3NN.1, 3NN.3, and 3NN.5, and COLA Part 11, which include Sections 3.1.3, 4.1.3, and 5.1.1, will be revised to incorporate the results of this change to damping values. The COLA mark-ups are dependent upon the completion of the revised analyses and will be provided in a supplemental response.

Proposed COLA Revision

To be provided in a future submittal.

ENCLOSURE 2

Response to NRC RAI Letter 64

RAI 5546 Question 03.07.02-2

RESPONSE TO REQUEST FOR ADDITIONAL INFORMATION

North Anna Unit 3

Dominion

Docket No. 52-017

RAI NO.: 5546 (RAI Letter 64)

SRP SECTION: 03.07.02 – SEISMIC SYSTEM ANALYSIS

QUESTIONS for Structural Engineering Branch 1 (AP1000/EPR Project) (SEB1)

DATE OF RAI ISSUE: 4/7/2011

QUESTION NO.: 03.07.02-2

Dominion performed site-specific SSI analyses of the Unit 3 Reactor Building (R/B) complex using the lumped-mass stick model developed by MHI and used for US-APWR standard plant seismic design. However, staff review of US-APWR DCD Sections 3.7 and 3.8 is ongoing. A staff's concern is that Dominion's dynamic analysis model may not reflect the current US-APWR design. To address this concern, the applicant is requested to indentify a technical approach that it will use for SSI model reconciliation between the US-APWR DCA and the Unit 3 COLA and corresponding update of site-specific SSI analyses of Unit 3 R/B complex.

Dominion Response

FSAR Section 3.7.2.4.1 and DCD COL Item 3.7(25) require the COL Applicant referencing the US-APWR standard plant design to perform site-specific soil-structure interaction (SSI) analyses using the same models as those used for site-independent SSI analyses in the standard plant seismic design. When the site-independent SSI analyses are changed, DCD COL 3.7(25) provides the commitment for North Anna Unit 3 to update the site-specific analyses, as necessary.

Proposed COLA Revision

None

ENCLOSURE 3

Response to NRC RAI Letter 64

RAI 5546 Question 03.07.02-3

RESPONSE TO REQUEST FOR ADDITIONAL INFORMATION

North Anna Unit 3

Dominion

Docket No. 52-017

RAI NO.: 5546 (RAI Letter 64)

SRP SECTION: 03.07.02 – SEISMIC SYSTEM ANALYSIS

QUESTIONS for Structural Engineering Branch 1 (AP1000/EPR Project) (SEB1)

DATE OF RAI ISSUE: 4/7/2011

QUESTION NO.: 03.07.02-3

The SRP (NUREG-0800) Section 3.7.2, "Seismic System Analysis," and the Interim Staff Guidance on "Seismic Issues Associated with High Frequency Ground Motion in DC and COL Applications" (ISG-DC/COL-01, 2008) provide guidance the staff will use in evaluating the technical adequacy of the seismic design that takes into account the effects of soil-structure interaction. The NA3 FSAR does not provide sufficient information for the staff to determine the technical adequacy of the seismic SSI analyses of the standard plant Category I structures under the guidance. To address this issue, the applicant is requested to provide the following information:

1) A summary of modal characteristics in the fixed-base condition, including the natural frequencies, effective modal masses, percent of mass participation, cumulative percent of mass participation, total number of modes included in the analysis, and method used to account for missing mass modes, for each of the standard plant Category I structures.

2) The SSI analysis method selected (e.g., flexible volume method, flexible interface method, etc.) and a technical justification for the selection.

3) The cut-off frequencies for each of the SSI analyses performed.

4) The analysis frequencies for each of the SSI analyses performed and basis for the selection of these frequencies.

5) Description of and basis for the selection of transfer function interpolation and smoothing methods.

6) Description of and basis for the selection of phase adjustment option in incoherent SSI analyses.

7) Demonstration of the sufficiency of the number of simulations used in stochastic incoherent SSI analyses.

8) Details of the wave passage effect, if taken into consideration, in incoherent SSI analyses.

9) Details of soil deposit modeling including determination of soil layer thicknesses in view of the minimum cut-off frequency addressed in the guidance.

10) Details of the half-space simulation and the number of generated layers in simulating the half-space.

11) Demonstration of the adequacy of the "selected locations" at which Unit 3 site-specific seismic demands are compared with US-APWR standard design seismic demands. The selected locations should be sufficient to represent various locations throughout the building and should include responses at peripheral locations to detect rocking and torsion, particularly from incoherent ground motion. The selected locations should also include responses to check overturning and sliding stability of the structures.

12) Verification of the adequacy of the Foundation Input Response Spectra (FIRS) as SSI input motions ("NEI Check" as described in FSAR, Section 3OO.1.4) for all embedded structures.

Dominion Response

1) Tables 3NN-11 and 12 of FSAR provide the fixed base natural frequencies of the major modes of vibration for the US APWR standard plant Category I structures, R/B Complex (containment internal structures (CIS), prestressed concrete containment vessel (PCCV) and reactor building (R/B) including the fuel handling area (FH/A)) and power source building (PS/B). Sections 5.3 and 5.4 of MHI US-APWR Technical Report MUAP-10001(R1) (FSAR Reference 3NN-7) provide additional information about the fixed base dynamic properties of the structures and validation of the structural models. Tables 5.3.3.2-1, 2 and 3 of MUAP-10001(R1) provide the natural frequencies, mode participation factors and mode effective masses for the major modes of vibration in N-S, E-W and vertical direction, respectively that were obtained from the fixed base modal analyses of the PCCV detailed FE model. The results of fixed base modal analyses of R/B Complex detailed FE model are presented in Tables 5.3.4.2-1, 2 and 3 of MUAP-10001(R1). Tables 5.3.5.2-1, 2 and 3 of MUAP-10001(R1) summarize the results of fixed base modal analysis of the CIS detailed FE model. The dynamic properties of the PS/B detailed FE model are provided in Tables 5.4.2-3 to 5 of MUAP-10001(R1). Note that the validation of the dynamic properties of the SASSI models is contained in MUAP-10001(R1) and is further addressed in DCD RAI 625-4924 (ML103120403).

   A fixed base modal analysis was performed on the Lumped Mass Stick models used for the North Anna Unit 3 site-specific SSI analyses of R/B Complex in order to extract natural frequencies, effective modal masses, percent of mass participation and cumulative percent of mass participation for the first 500 modes. Figure 1 through Figure 3 present the graphs of the cumulative mass participation vs. frequency for the fixed base response of the R/B Complex in three directions. The larger "jumps" in the plots indicate dominant modes of vibration of the structures with major mass contributions. Table 1 through Table 3 summarize the results for the dominant modes and respective modal characteristics for the response of the R/B Complex lumped mass stick model in N-S, E-W and vertical direction. The dominant modes of vibration of PCCV in each direction and their respective characteristics are presented in Table 4 through Table 6. Table 7 through Table 9 present the dominant modes of vibration in each direction and respective modal characteristics for the CIS lumped mass stick model.

Plots of transfer function amplitudes obtained from the ACS SASSI analysis of the R/B Complex lumped mass stick model resting on the surface of rigid half-space are presented in MUAP-10001(R1). Figures 5.3.3.2-1, 2 and 3 present the plots of transfer function amplitudes for the response of the PCCV lumped mass stick model in N-S, E-W and vertical direction. Figures 5.3.4.2-1, 2 and 3 present the plots of transfer function amplitudes for the response of the R/B Complex lumped mass stick model, and 5.3.5.2-1, 2 and 3 present the plots of transfer function amplitudes for the response of the CIS lumped mass stick model. The plots show peak amplifications in the transfer function amplitudes at frequencies near those of the dominant modes of vibrations provided in the Table 1 through Table 9 below.

A fixed base modal analysis was performed on the PS/B dynamic FE model used for the Unit 3 site-specific SSI analyses in order to extract natural frequencies, effective modal masses, percent of mass participation and cumulative percent of mass participation for the first 500 modes.

Table 10 through Table 12 present the dominant modes of vibration of PS/B dynamic FE model in each direction and the respective modal characteristics. These dominant modes of vibration for PS/B with major mass participations are depicted in Figure 4 through Figure 6 as "jumps" in the cumulative mass participation graphs.

The seismic loads were determined from the results of frequency domain time history SASSI analysis for maximum member forces and maximum nodal accelerations as described in Section 3.6 of MUAP-10006(R0) (FSAR Reference 3NN-8). The method to account for missing mass modes in frequency domain time history analyses is not applicable.

Table 1 - Modal Properties of R/B (including FH/A) of First 2 Dominant Modes, X-Dir. (N-S)

Mode	Frequency (HZ)	Period (sec)	Effective Mass (kips*sec^2/ft)	Cumulative Mass Fraction	Percent of Mass Participation (%)
5	5.6	0.18	2554.5	0.331	18.1
8	7.5	0.13	1415.2	0.432	10.1

Table 2 - Modal Properties of R/B (including FH/A) of First 2 Dominant Modes, Y-Dir. (E-W)

Mode	Frequency (HZ)	Period (sec)	Effective Mass (kips*sec^2/ft)	Cumulative Mass Fraction	Percent of Mass Participation (%)
6	6.0	0.17	4399.7	0.497	31.0
7	7.3	0.14	547.3	0.536	3.9

Table 3 - Modal Properties of R/B (including FH/A) of First 2 Dominant Modes, Z-Dir (Vert)

Mode	Frequency (HZ)	Period (sec)	Effective Mass (kips*sec^2/ft)	Cumulative Mass Fraction	Percent of Mass Participation (%)
74	16.0	0.062	1151.2	0.359	8.3
76	16.5	0.061	772.6	0.414	5.6

Table 4 - Modal Properties of PCCV of First 2 Dominant Modes, X-Direction (N-S)

Mode	Frequency (HZ)	Period (sec)	Effective Mass (kips*sec^2/ft)	Cumulative Mass Fraction	Percent of Mass Participation (%)
2	4.5	0.22	1679.7	0.120	11.9
48	12.8	0.078	431.6	0.763	3.1

Table 5 - Modal Properties of PCCV of First 2 Dominant Modes, Y-Direction (E-W)

Mode	Frequency (HZ)	Period (sec)	Effective Mass (kips*sec^2/ft)	Cumulative Mass Fraction	Percent of Mass Participation (%)
1	4.5	0.22	1679.7	0.118	11.8
47	12.8	0.078	431.6	0.715	3.0

Table 6 - Modal Properties of PCCV of First 2 Dominant Modes, Z-Direction (Vert)

Mode	Frequency (HZ)	Period (sec)	Effective Mass (kips*sec^2/ft)	Cumulative Mass Fraction	Percent of Mass Participation (%)
44	12.2	0.082	1817.4	0.240	13.1
122	22.3	0.045	215.1	0.703	1.6

Table 7 - Modal Properties of CIS of First 2 Dominant Modes, X-Direction (N-S)

Mode	Frequency (HZ)	Period (sec)	Effective Mass (kips*sec^2/ft)	Cumulative Mass Fraction	Percent of Mass Participation (%)
3	5.1	0.20	411.0	0.149	2.9
9	7.5	0.13	894.4	0.495	6.3

Table 8 - Modal Properties of CIS of First 2 Dominant Modes, Y-Direction (E-W)

Mode	Frequency (HZ)	Period (sec)	Effective Mass (kips*sec^2/ft)	Cumulative Mass Fraction	Percent of Mass Participation (%)
4	5.3	0.19	972.4	0.188	6.8
10	7.6	0.13	287.9	0.557	2.0

Table 9 - Modal Properties of CIS of First 2 Dominant Modes, Z-Direction (Vert)

Mode	Frequency (HZ)	Period (sec)	Effective Mass (kips*sec^2/ft)	Cumulative Mass Fraction	Percent of Mass Participation (%)
57	14.4	0.069	227.6	0.269	1.6
86	17.9	0.056	289.1	0.527	2.1

Table 10 - Modal Properties of PS/B of First 2 Dominant Modes, X-Direction (N-S)

Mode	Frequency (HZ)	Period (sec)	Effective Mass (kips*sec^2/ft)	Cumulative Mass Fraction	Percent of Mass Participation (%)
1	8.7	0.11	455.2	0.66	66.0
23	20.2	0.05	62.6	0.80	9.1

Table 11 - Modal Properties of PS/B of First 2 Dominant Modes, Y-Direction (E-W)

Mode	Frequency (HZ)	Period (sec)	Effective Mass (kips*sec^2/ft)	Cumulative Mass Fraction	Percent of Mass Participation (%)
2	10.2	0.10	450.9	0.65	65.0
3	12.1	0.08	70.6	0.75	10.2

Table 12 - Modal Properties of PS/B of First 2 Dominant Modes, Z-Direction (Vert)

Mode	Frequency (HZ)	Period (sec)	Effective Mass (kips*sec^2/ft)	Cumulative Mass Fraction	Percent of Mass Participation (%)
11	15.4	0.07	36.3	0.13	5.7
14	17.1	0.06	115.4	0.33	18.3

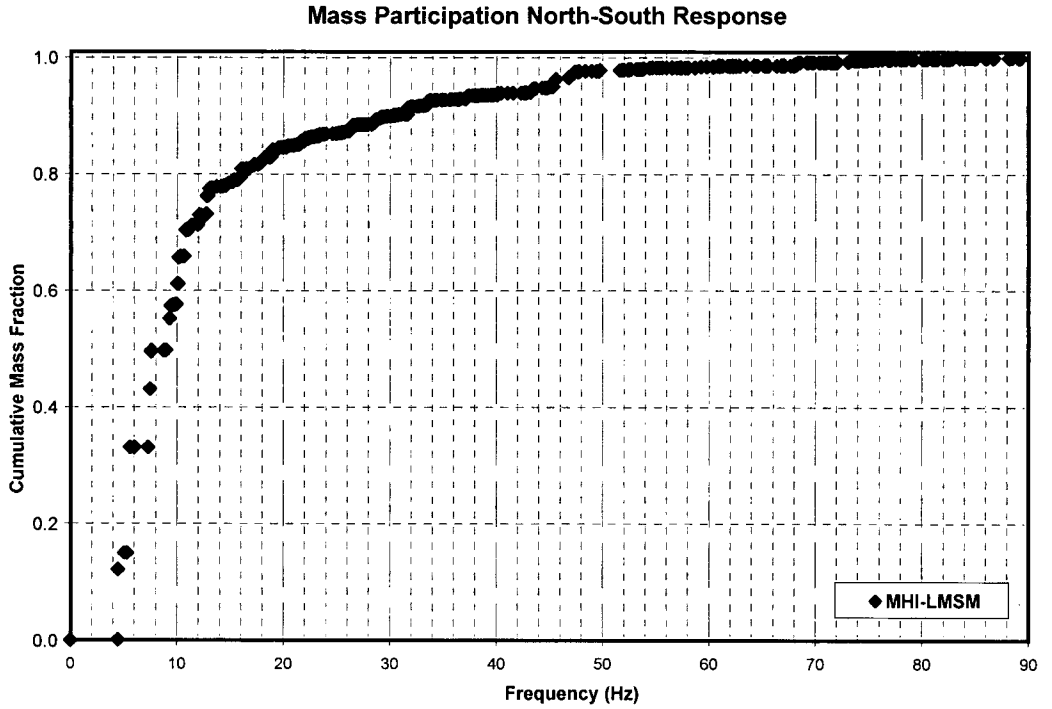

Figure 1 - R/B Complex Mass Participation (N-S direction)

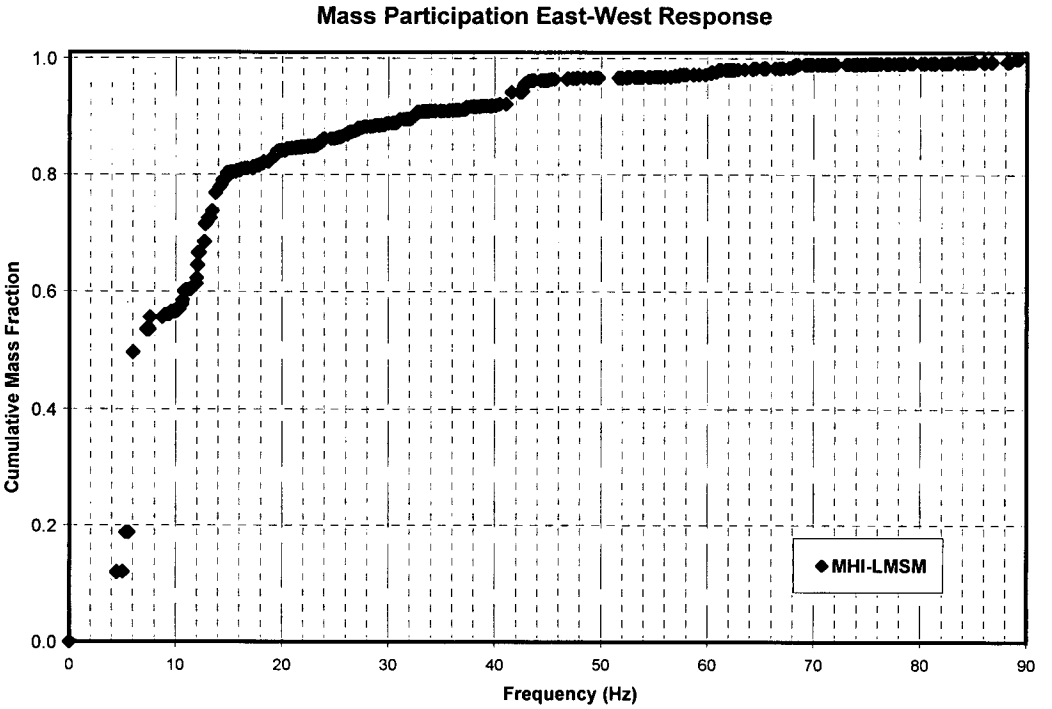

Figure 2 - R/B Complex Mass Participation (E-W direction)

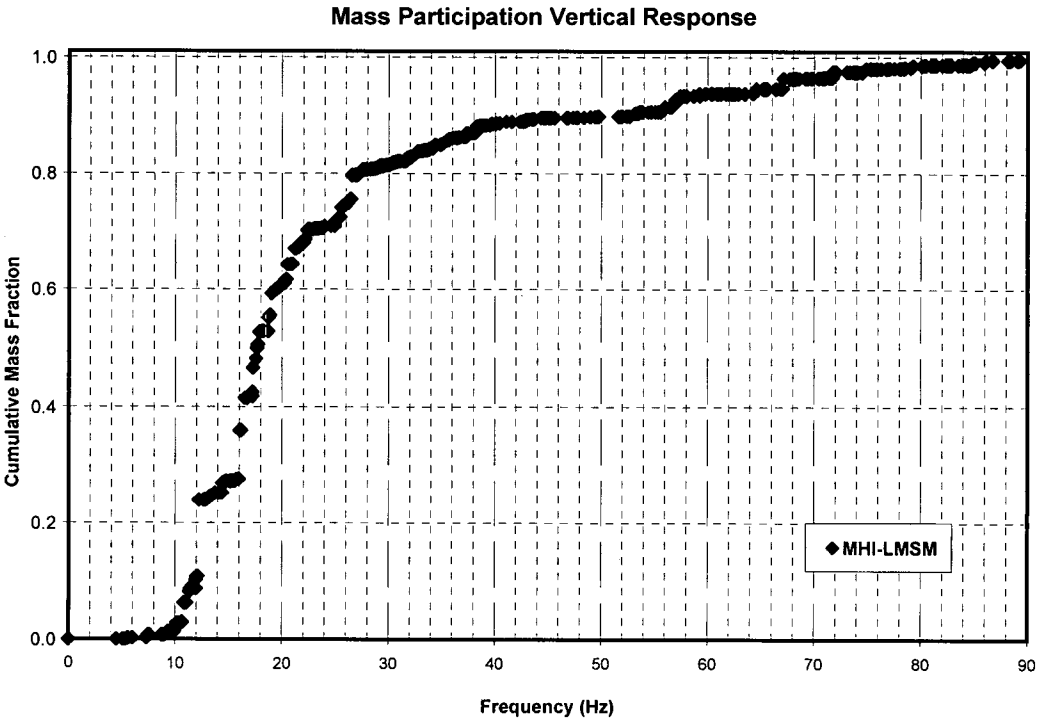

Figure 3 - R/B Complex Mass Participation (Vertical direction)

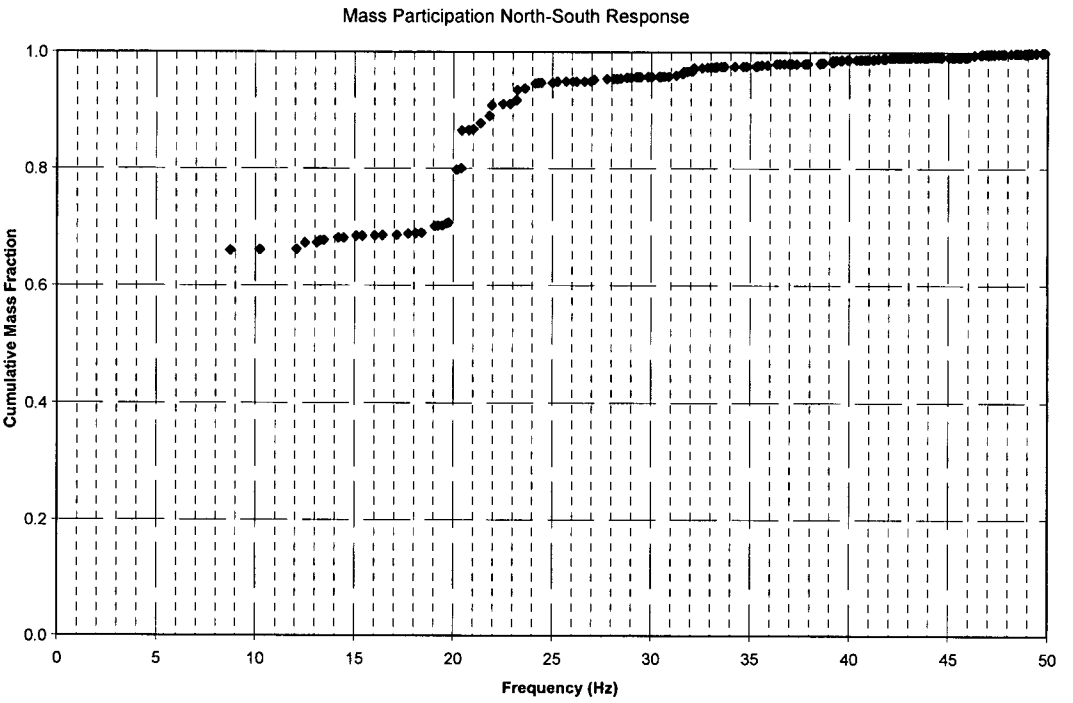

Figure 4 – PS/B Complex Mass Participation (N-S direction)

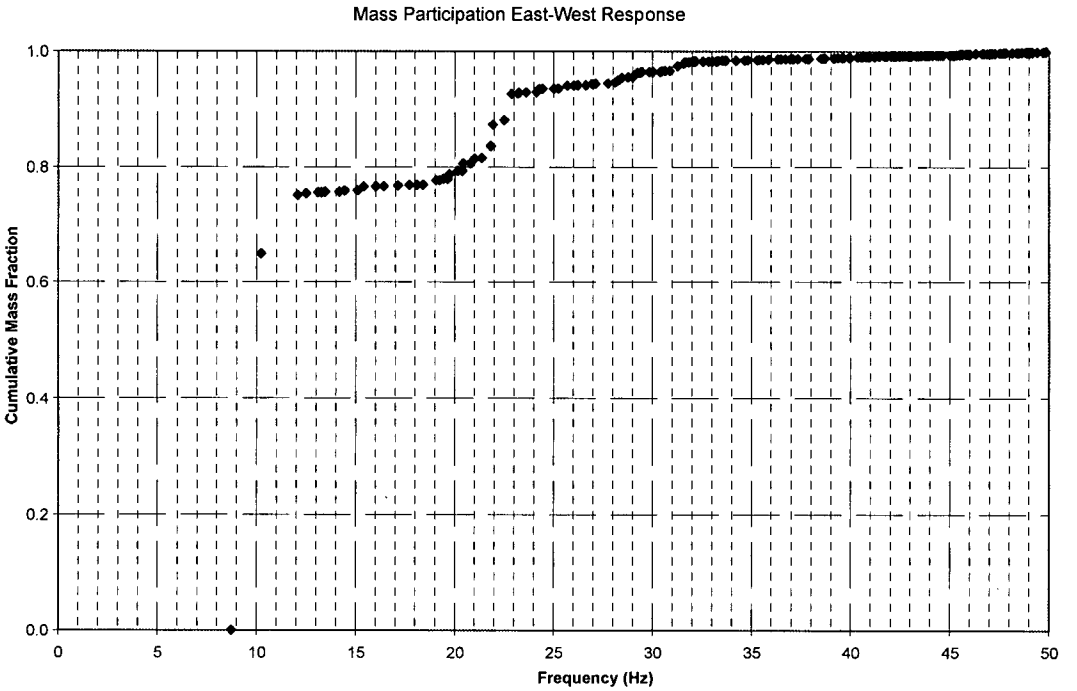

Figure 5 - PS/B Complex Mass Participation (E-W direction)

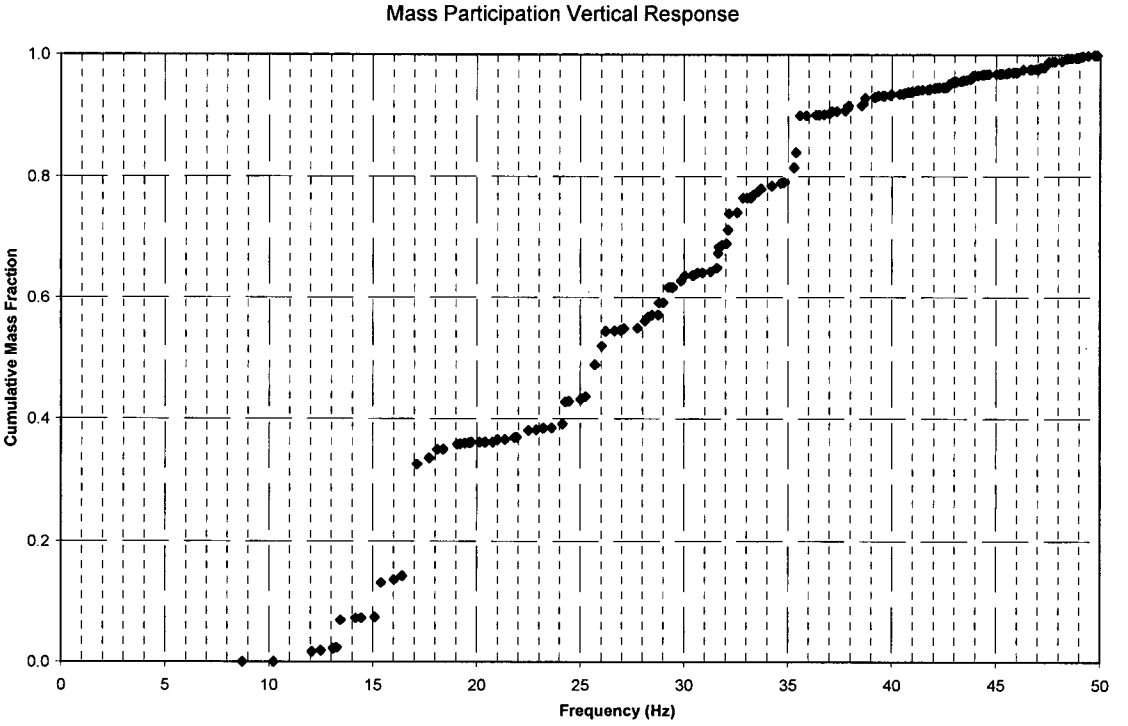

Figure 6 - PS/B Complex Mass Participation (Vertical direction)

2) The Flexible Interface Method with interaction nodes at the foundation-soil interface, also called FI-FSIN (equivalent to Subtraction in SASSI2000) in the ACS SASSI documentation (Reference 1), was used for the North Anna Unit 3 site-specific SSI analyses of both embedded SSI models of the R/B Complex and PS/B.

   In order to investigate the effect of the substructuring methodology on the accuracy of the results, a sensitivity study was performed for the embedded PS/B for the LB soil. These results used a lower level OBE damping to account for the dissipation of energy in the PS/B structure. All three SSI substructuring methods available in the ACS SASSI Version 2.3.0 (Reference 1) were applied: Flexible Volume, FV, Flexible Interface with Foundation-Soil Interface, FI-FSIN and Flexible Interface with Excavation Volume Boundary Nodes, FI-EVBN. Figures 7 through 12 show comparisons of 5% damping ISRS computed at ground surface and roof levels using the three substructuring methods for the embedded PS/B model and the surface PS/B model. The results of this sensitivity study concluded that below 10 Hz, even for the LB soil, FI-FSIN is highly accurate as compared with FI-EVBN and FV. Above 10 Hz, the FI-FSIN method shows some slight deviations, especially in Z-direction, from the FV method solution. However, these slight deviations have no impact on the final ISRS that are defined by the envelope of surface and embedded model ISRS.

   SSI analyses were re-performed on the PS/B model with OBE structural damping using the FI-EBVN method for all soil conditions. The results of these analyses showed that by switching from FI-FSIN to FI-EVBN there was no impact on the final, design basis ISRS. The investigations described above provide the justification for the SSI analyses method selected.

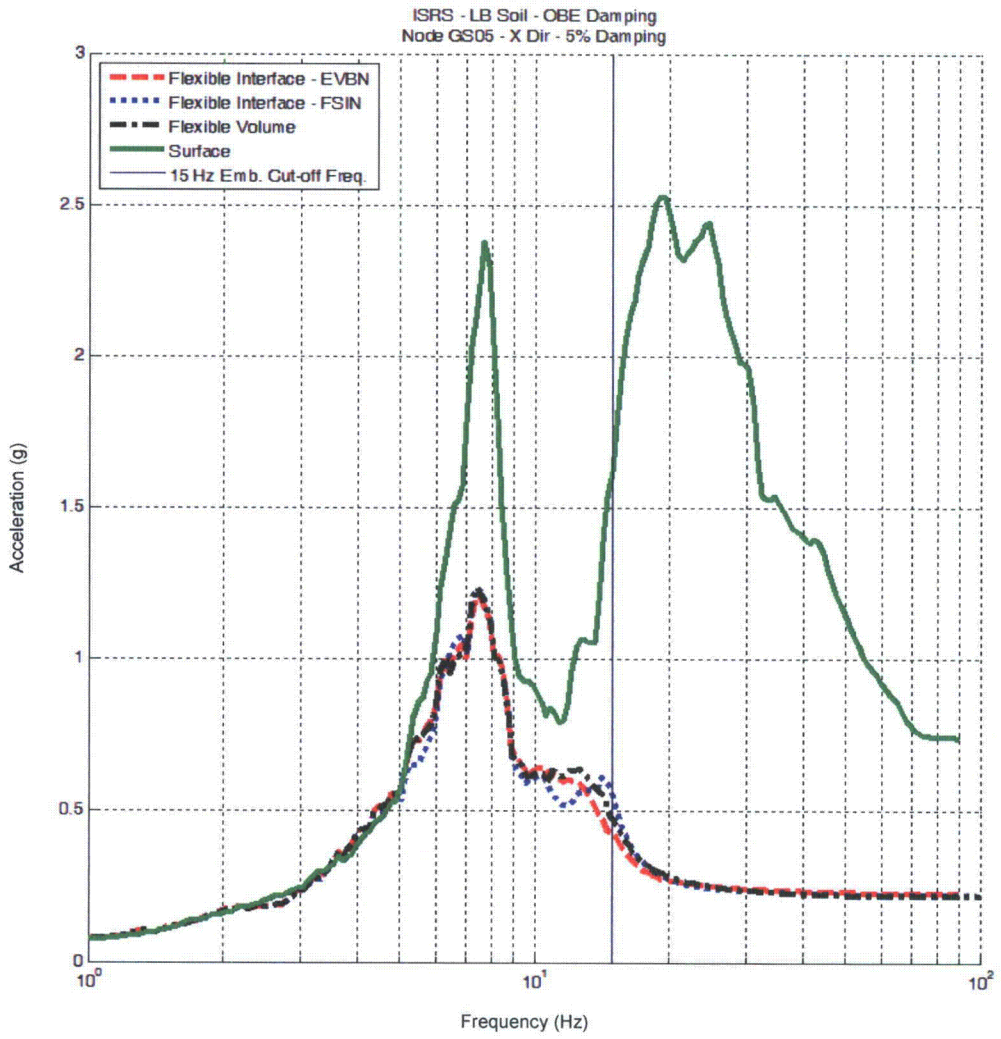

Figure 7 - 5% Damping ISRS at GS05 Location (Ground Level) in X-Direction for Embedded and Surface PS/B Models for the LB soil Using the FI-FSIN, FI-EVBN and FV Methods

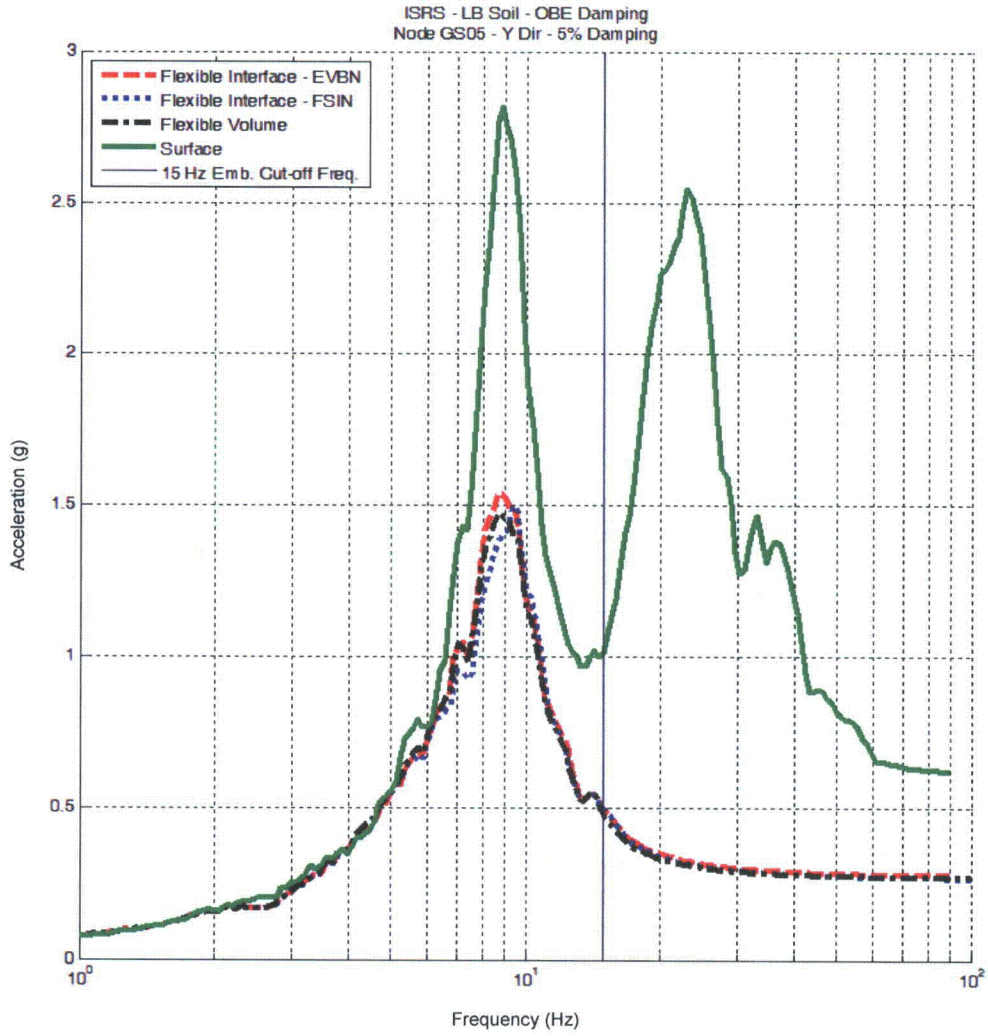

Figure 8 - 5% Damping ISRS at GS05 Location (Ground Level) in Y-Direction for Embedded and Surface PS/B Models for the LB soil Using the FI-FSIN, FI-EVBN and FV Methods

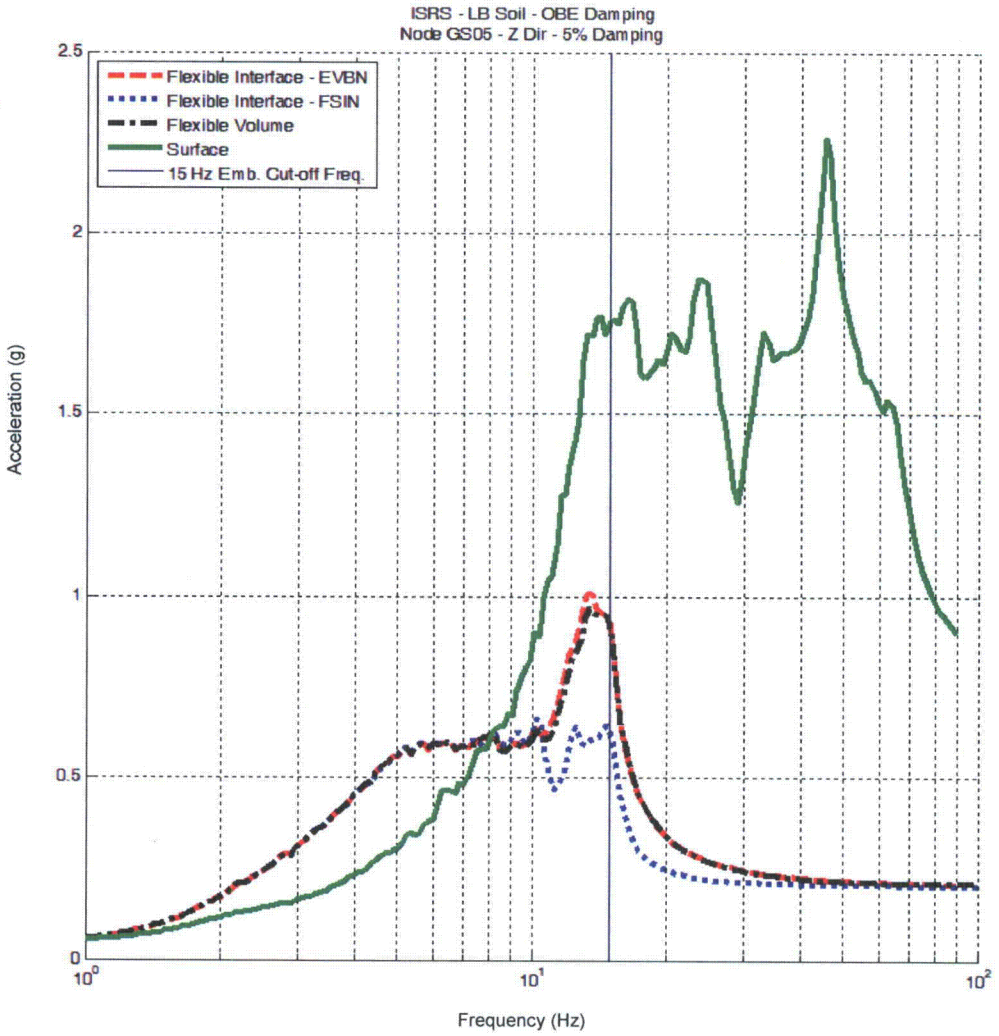

Figure 9 - 5% Damping ISRS at GS05 Location (Ground Level) in Z-Direction for Embedded and Surface PS/B Models for the LB soil Using the FI-FSIN, FI-EVBN and FV Methods

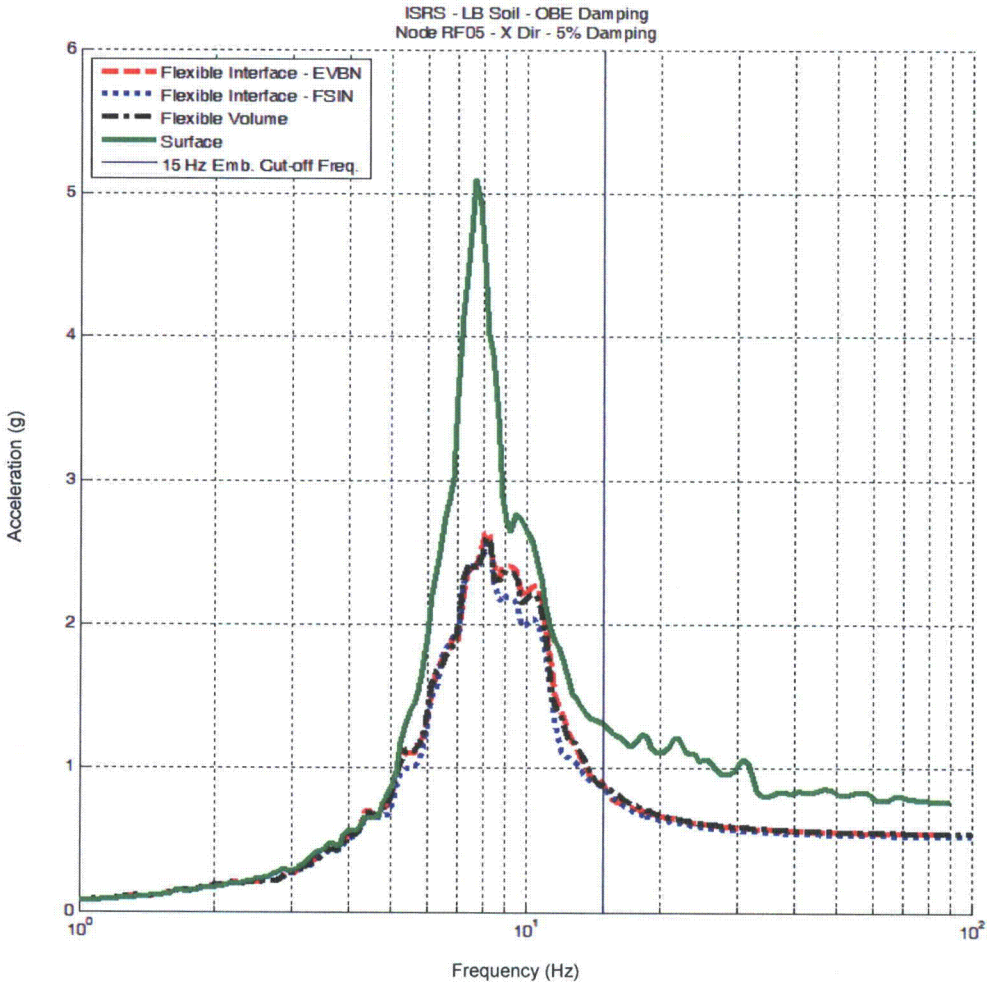

Figure 10 - 5% Damping ISRS at RF05 Location (Roof Level) in X-Direction for Embedded and Surface PS/B Models for the LB soil Using the FI-FSIN, FI-EVBN and FV Methods

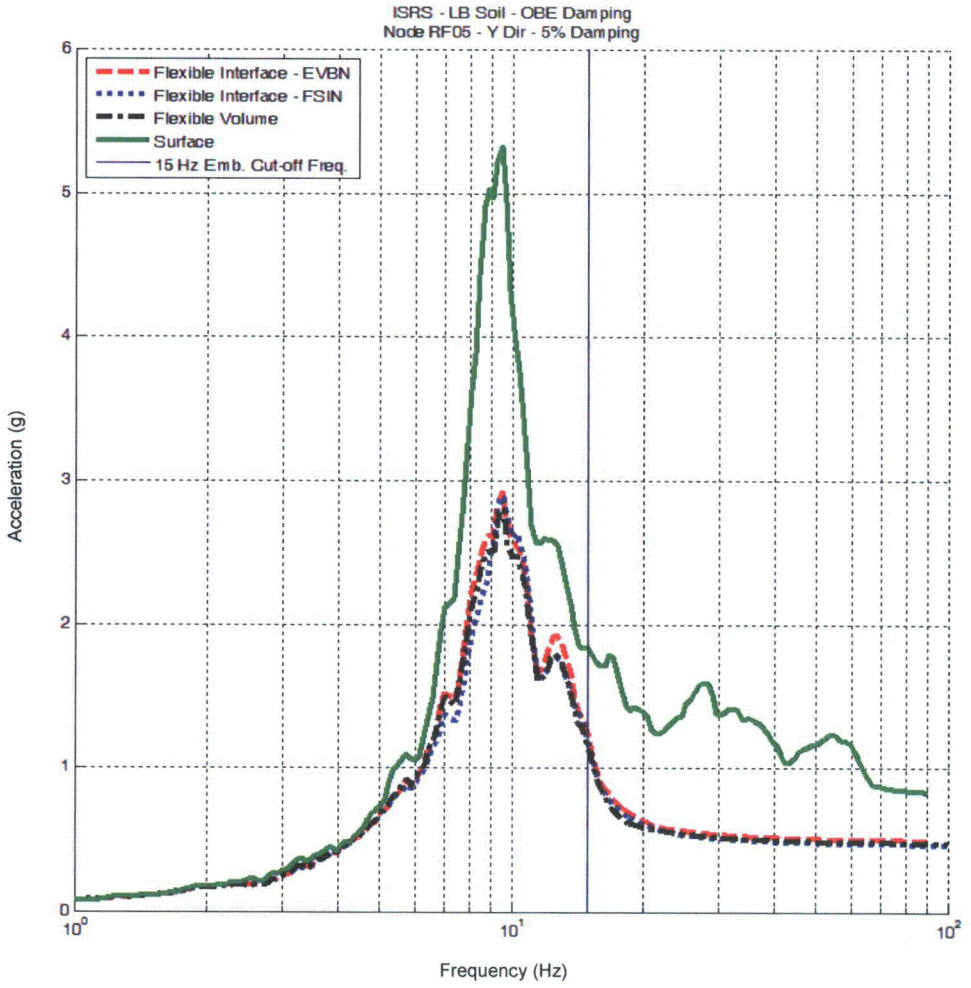

Figure 11 - 5% Damping ISRS at RF05 Location (Roof Level) in Y-Direction for Embedded and Surface PS/B Models for the LB soil Using the FI-FSIN, FI-EVBN and FV Methods

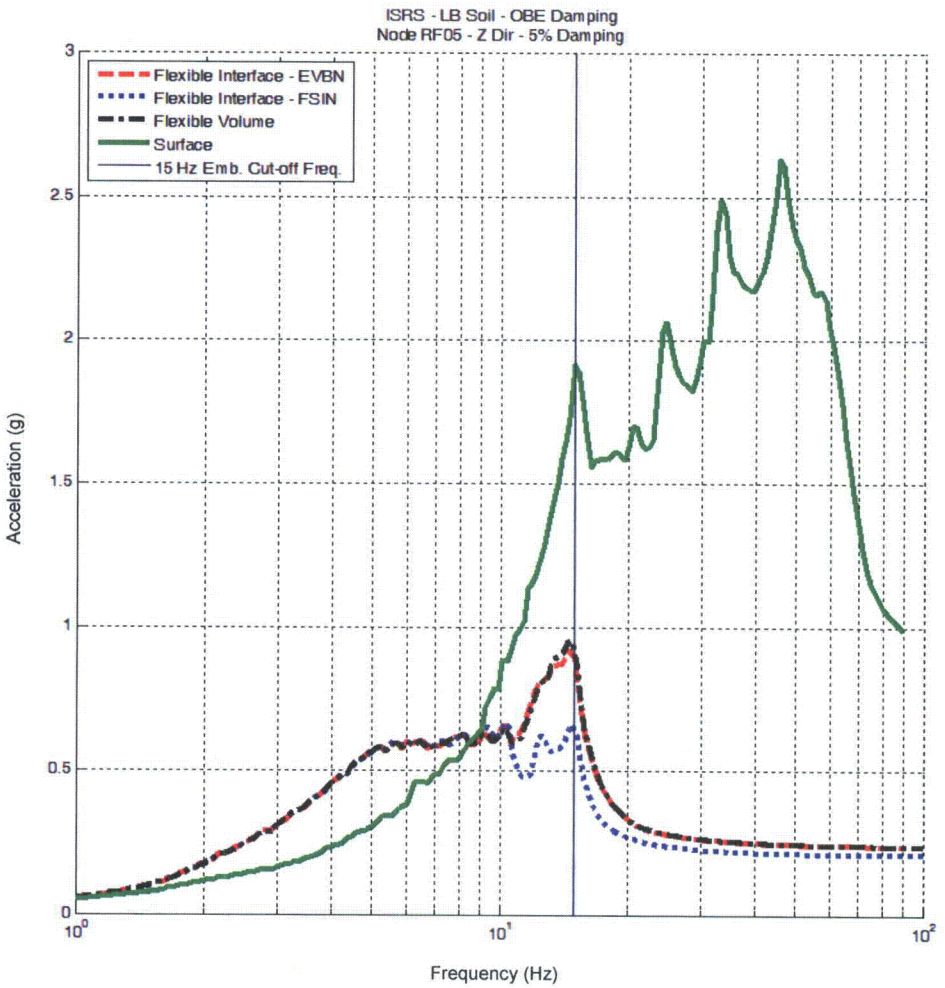

Figure 12 - 5% Damping ISRS at RF05 Location (Roof Level) in Z-Direction for Embedded and Surface PS/B Models for the LB soil Using the FI-FSIN, FI-EVBN and FV Methods

3) The cut-off frequencies for the ACS SASSI analyses for the R/B Complex and PS/B are provided in FSAR Tables 3NN-15 and 3NN-16, respectively.

4) FSAR Tables 3NN-15 and 3NN-16 indicate the total number of frequencies considered. The number of SSI analysis frequencies was selected to be sufficiently dense to allow adequate acceleration transfer function (ATF) interpolation. The computed and interpolated ATF amplitudes were compared for each soil profile (LB, BE and UB soils), for both coherent and incoherent SSI runs. Figures 13 through 16 show the interpolated and computed incoherent ATFs for locations within the R/B Complex and PS/B at both ground level and high elevations for the BE soil profile in the X-direction. The plotted ATFs in these figures are X direction response due to X direction input. Similar accurate results were obtained for the Y and Z. The plotted results correspond to SSI analyses performed with the OBE structural damping. The ATFs plotted in Figures 13 through 16 show that the number of SSI frequencies were adequately selected to prevent any ATF interpolation error.

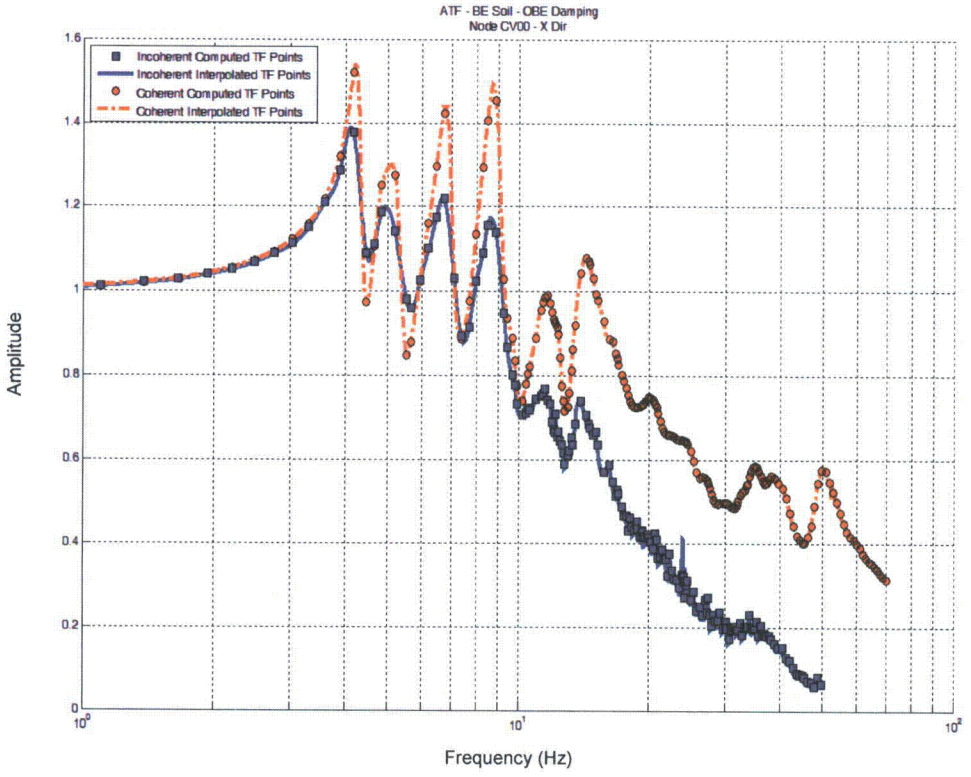

Figure 13 - Coherent and Incoherent Computed and Interpolated ATF for the Surface R/B Complex Model at CV00 Location (Ground) for the BE Soil in X-Direction

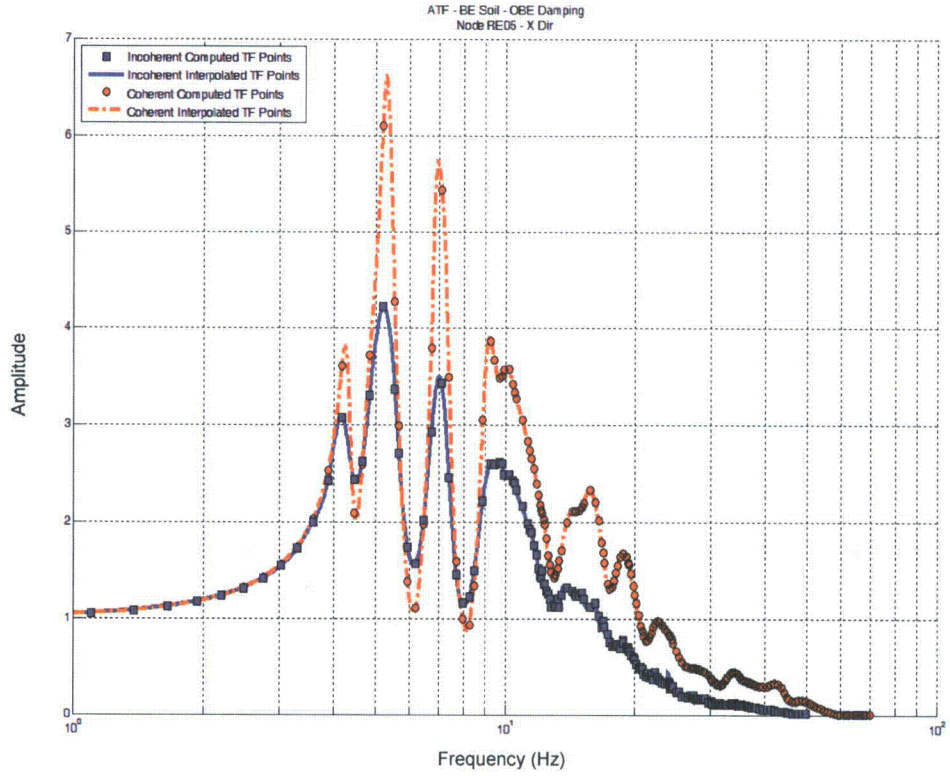

Figure 14 - Coherent and Incoherent Computed and Interpolated ATF for the Surface R/B Complex Model at RE05 Location (High Elevation) for the BE Soil in X-Direction

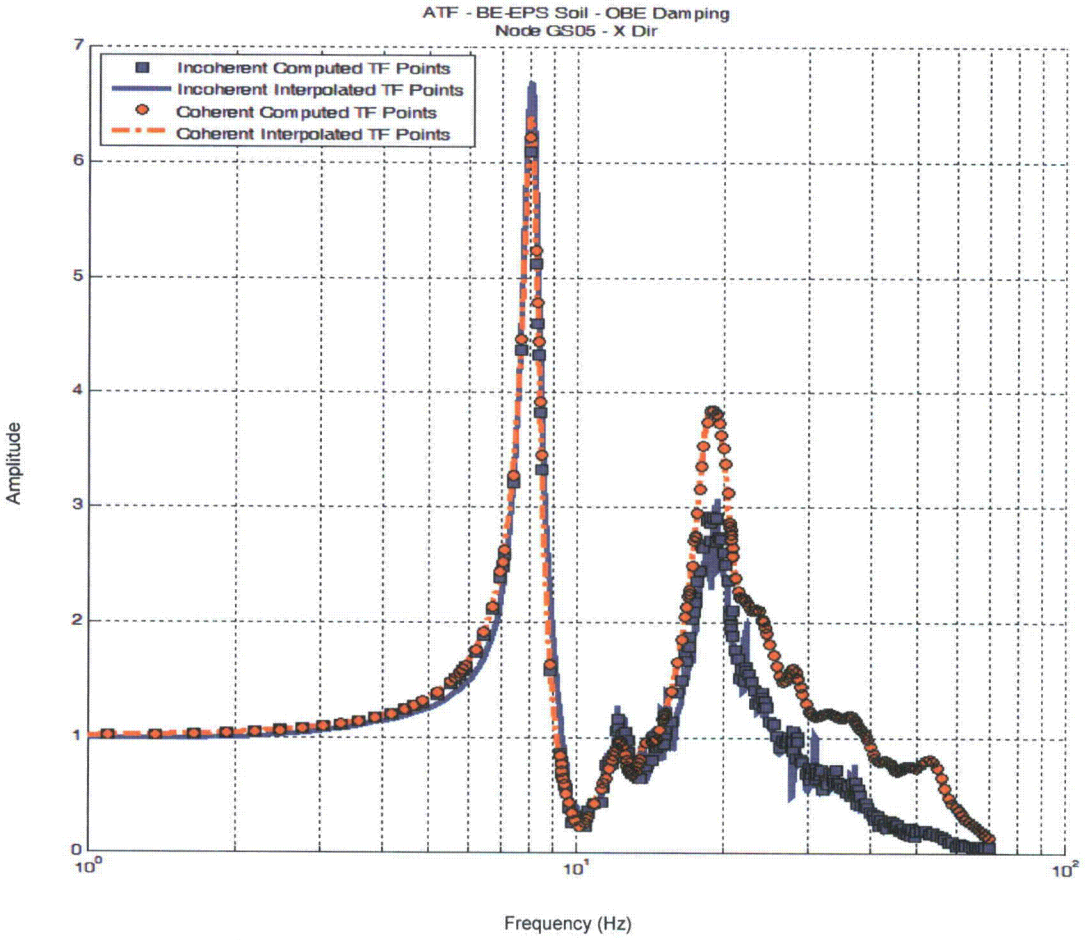

Figure 15 - Coherent and Incoherent Computed and Interpolated ATF for the Surface PS/B Complex Model at GS05 Location (Ground) for the BE-EPS Soil in X-Direction

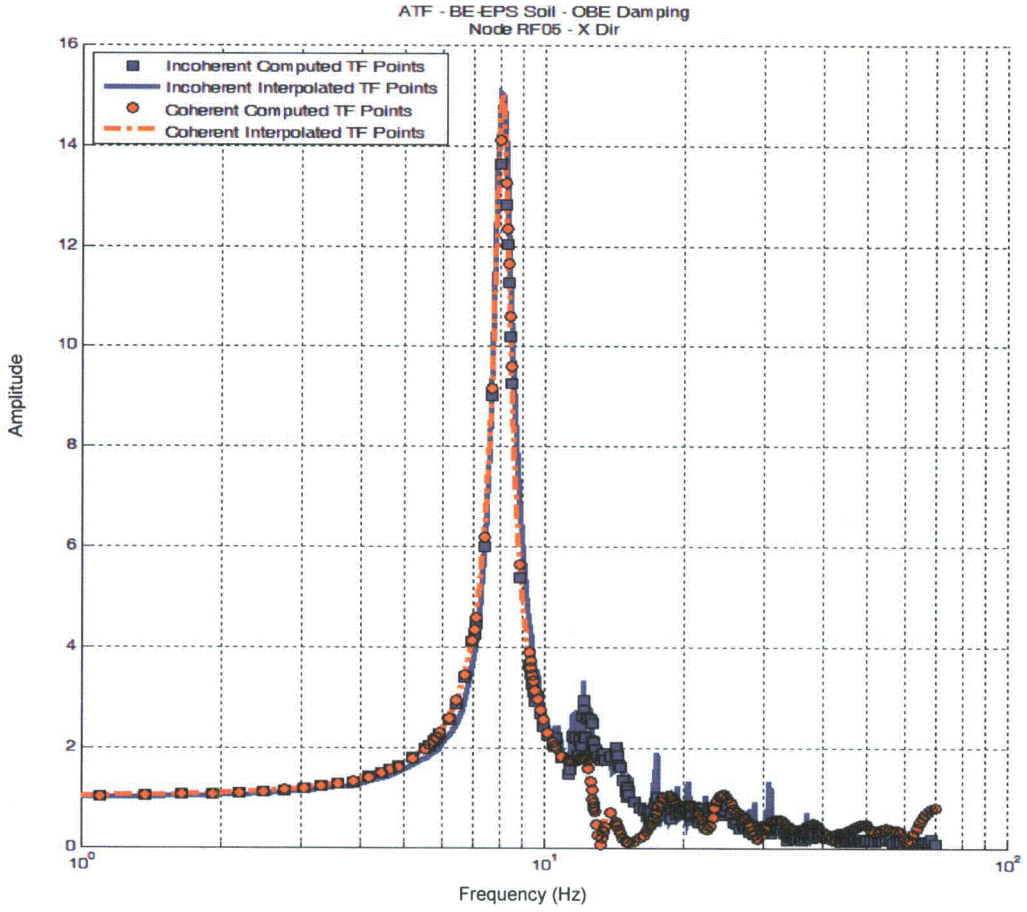

Figure 16 - Coherent and Incoherent Computed and Interpolated ATF for the Surface PS/B Complex Model at RF05 Location (Roof) for the BE-EPS Soil in X-Direction

5) The acceleration transfer functions (ATF) were interpolated using Option 2 in the input of the ACS SASSI MOTION module as described in the user manuals (Reference 1). This is the recommended ATF interpolation option in ACS SASSI for incoherent SSI analyses. This interpolation option includes an unbiased moving average scheme that is well-suited for incoherent SSI analyses. Smoothing was applied only for the incoherent SSI analyses to improve the incoherent ATF interpolation, as recommended by the EPRI studies (References 2 and 3). The transfer function interpolation error smoothing parameter values were selected so that the interpolated ATF curve best fits the computed ATF points from SSI analysis. The acceptable selection of the ATF interpolation scheme option and smoothing parameter is reflected in the matching of the interpolated ATF curve and computed ATF points as shown in Figures 13 through 16 above. The "Analysis Approach" discussion in FSAR Section 3NN.3.1 for the R/B Complex will be expanded to include this information. FSAR Section 3NN.3.2 for the PS/Bs will be modified to add a cross-reference to the same ATF interpolation methodology discussed in Section 3NN.3.1. FSAR Section 3NN.7 will also be revised to add EPRI Report TR-1015111 (Reference 2 in this RAI response) as an FSAR Reference, and to correct the title and report number for FSAR Reference 3NN-3 (Reference 3 in this RAI response).

6) The application of the ATF phase adjustment for incoherent SSI analyses was validated by the EPRI studies (References 2 and 3). All the EPRI incoherent SSI results based on the Stochastic Simulation approach were obtained using the ATF phase adjustment. The effects of the ATF phase adjustment for high-frequency seismic inputs are to increase the interpolated incoherent ATF amplitudes in the high-frequency range as discussed in the Appendix C of the EPRI study (Reference 2). As stated in item 5 above, the "Analysis Approach" discussion in Section 3NN.3.1 FSAR Appendix 3NN will be expanded to include this information.

7) The results of the EPRI studies presented in Figures 4-3 and 4-4 of Reference 2 demonstrate that the use of 5 to 10 stochastic simulations is sufficient for obtaining an accurate computed incoherent ISRS. FSAR Appendix 3NN Section 3NN.2 will be revised to state that the EPRI report (Reference 2) shows that 10 stochastic SSI simulations are sufficient to obtain accurate ISRS from incoherent ground input motion.

   The adequacy of the use the ACS SASSI Stochastic Simulation approach with 10 simulations, as applied to the R/B Complex and PS/B incoherent SSI analyses, is demonstrated herein by comparing the 5% damping incoherent ISRS obtained for 10 simulations with the 5% damping incoherent ISRS obtained for 25 simulations. Figures 17 through 22 show the 5% damping ISRS computed for 10 and 25 simulations, respectively, at two different elevations within the R/B Complex. These locations include the CV00 node at the ground level and the RE05 node at a high elevation.

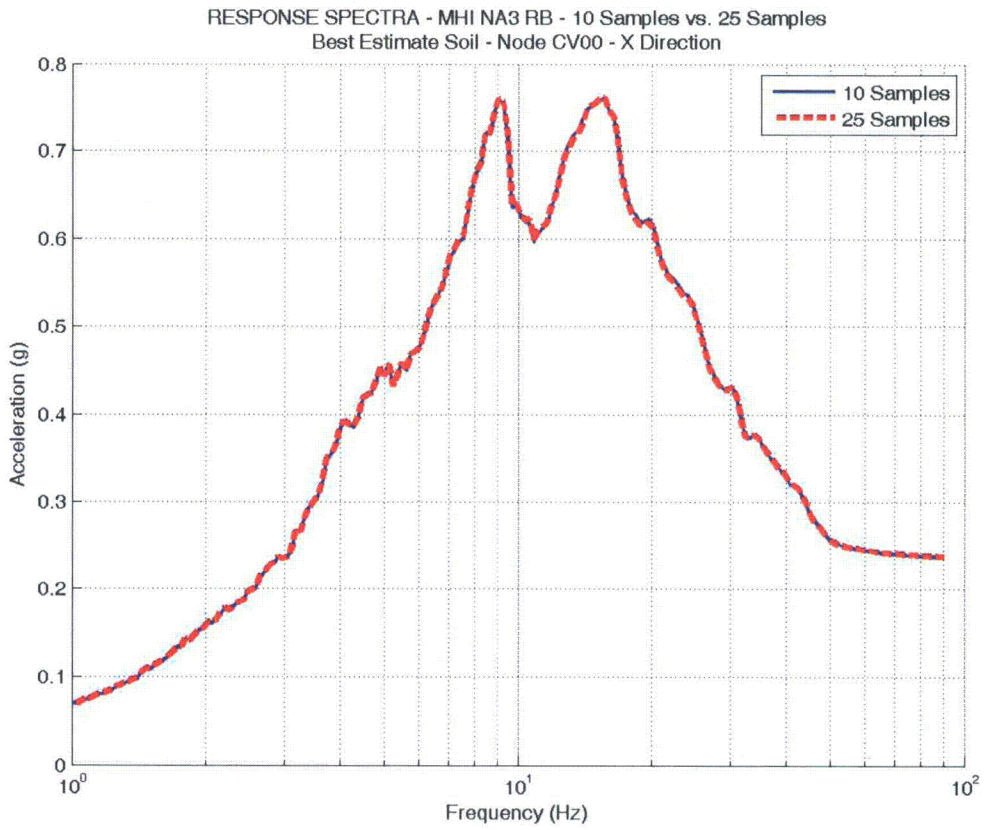

Figure 17 - 5% Damping Incoherent ISRS Computed for 10 and 25 Simulations for the Surface R/B Complex Model at the CV00 Location (Ground) for the BE Soil in X-Direction

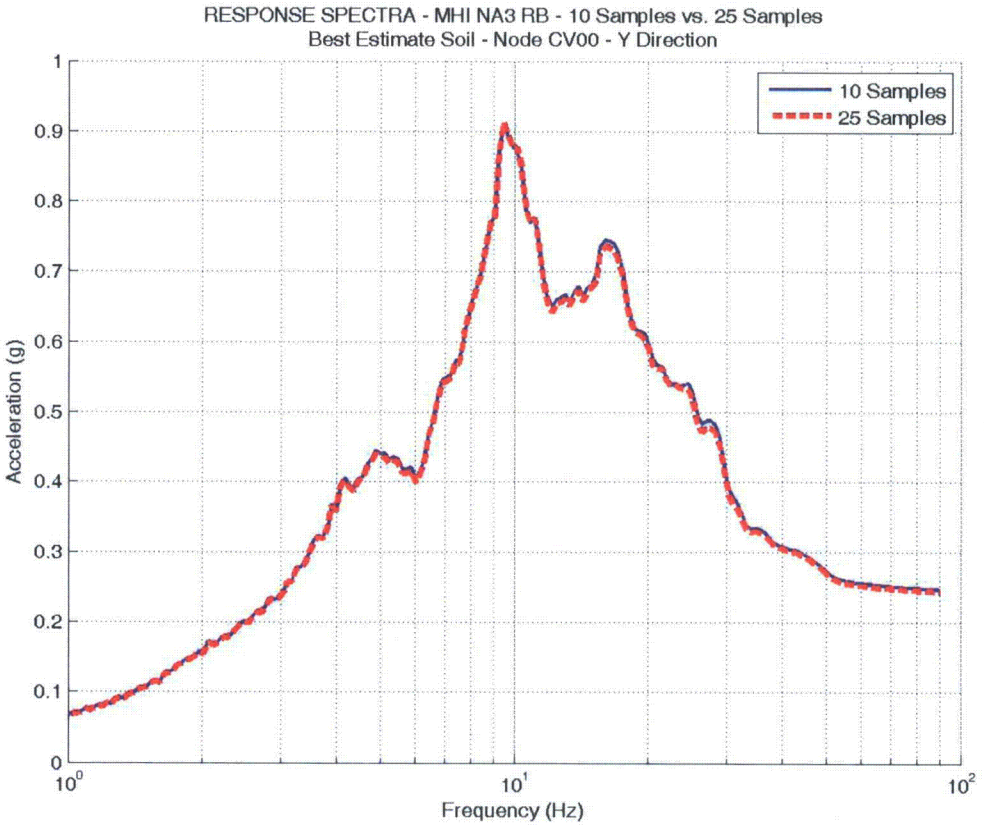

Figure 18 - 5% Damping Incoherent ISRS Computed for 10 and 25 Simulations for the Surface R/B Complex Model at the CV00 Location (Ground) for the BE Soil in Y-Direction

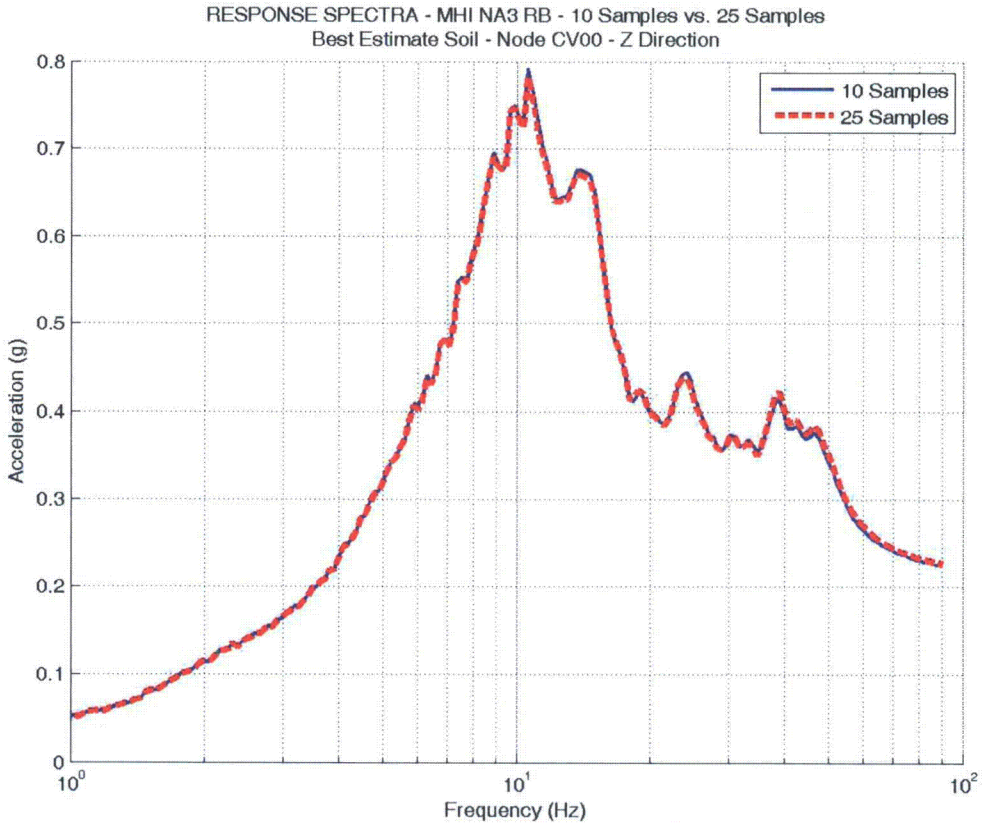

Figure 19 - 5% Damping Incoherent ISRS Computed for 10 and 25 Simulations for the Surface R/B Complex Model at the CV00 Location (Ground) for the BE Soil in Z-Direction

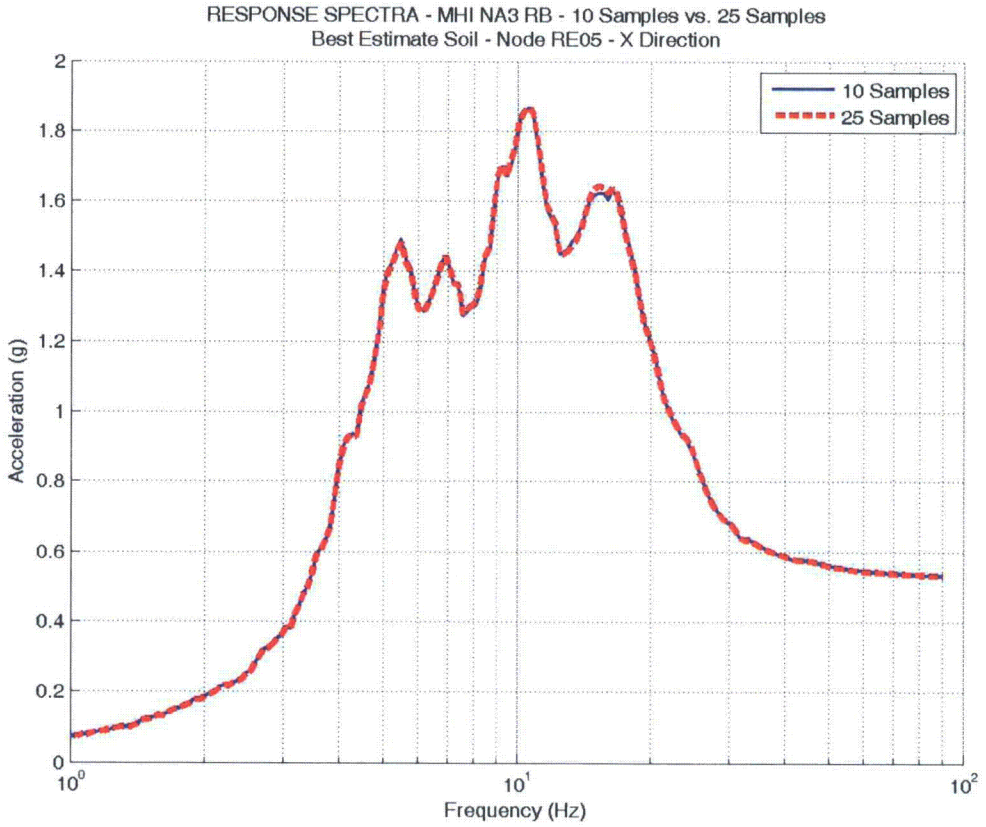

Figure 20 - 5% Damping Incoherent ISRS Computed for 10 and 25 Simulations for the Surface R/B Complex Model at the RE05 Location (High Elevation) for the BE Soil in X-Direction

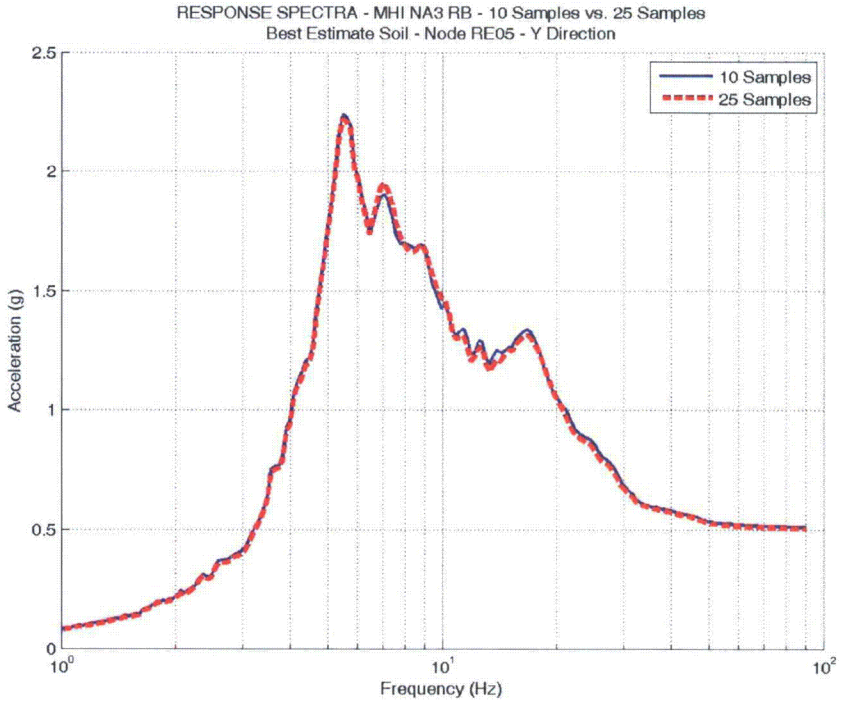

Figure 21 - 5% Damping Incoherent ISRS Computed for 10 and 25 Simulations for the Surface R/B Complex Model at the RE05 Location (High Elevation) for the BE Soil in Y-Direction

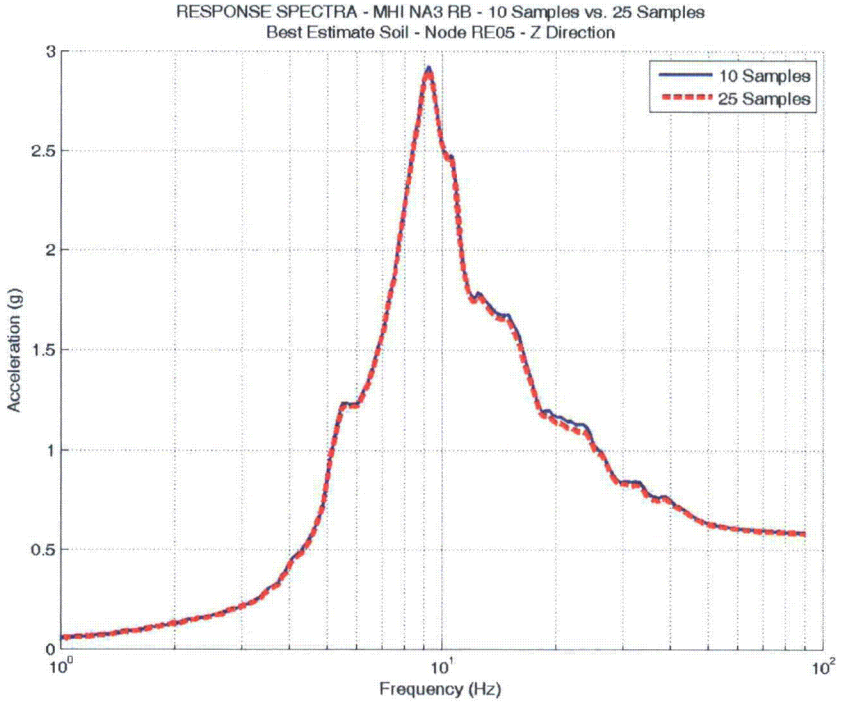

Figure 22 - 5% Damping Incoherent ISRS Computed for 10 and 25 Simulations for the Surface R/B Complex Model at the RE05 Location (High Elevation) for the BE Soil in Z-Direction

8) The wave passage effect was not considered for the incoherent SSI analyses performed for the North Anna Unit 3 site. In general, for rock sites, the effects of wave passage are negligible, even for large-size foundations such as that of the R/B Complex. The EPRI studies did not include the wave passage effects (References 2 and 3).

9) FSAR Tables 3NN-13 and 3NN-14 list the mesh sizes at the basemat-subgrade interface of the models used for the SSI analyses of the R/B Complex and PS/B, respectively, and the maximum frequencies transmittable through the basemat mesh and the soil profile (subgrade and embedment soil). FSAR Tables 3NN-15 and 3NN-16 list the cut-off frequencies used for the SSI analyses. The mesh sizes and cut-off frequencies are chosen such that the maximum transmittable frequency, with regard to seismic wave passage through the mesh, is compatible with the corresponding cut-off frequency. This assures that the mesh sizes are not a limiting factor with regard to accuracy of the SSI results. As shown in FSAR Tables 3NN-15 and 3NN-16, the minimum cut-off frequency of analysis used for the design-basis surface foundation model SSI analysis cases is approximately 50 Hz, which meets guidance in NRC ISG-01. Further, additional confirmatory analyses were also performed on the surface foundation models with cut-off frequencies extended beyond 50 Hz, to capture the energy of the ground motion at frequencies higher than 50 Hz.

   The cut-off frequencies for embedded models are discussed in the response to RAI 5546 Question 03.07.02-6, which will be provided in a separate submittal.

10) As discussed in Appendix 3NN Section 3NN.2, a ten layer half-space is used in the SASSI analysis. The SASSI half-space simulation consists of additional layers with viscous dashpots added at the base of the half-space. The half-space layer has a thickness of 1.5 Vs/ f / number of half-space layers, where Vs is the shear wave velocity of the half-space and f is the frequency of analysis. FSAR Appendix 3NN Section 3NN.2 will be revised to expand the description of the half-space as discussed in this response.

11) As described in FSAR Section 3NN.5, the methodology used to generate the site specific ISRS is the same as described in Section 3.5 of MUAP-10006 (FSAR Reference 3NN-8) and the methodology used to calculate seismic loads (including effects due to rocking and torsion) is the same as described in Section 3.6 of MUAP-10006. The locations selected for comparison of the seismic demands are the same locations as those selected for performing the standard plant analyses as given in MUAP-10006. The locations used in this methodology include peripheral locations to capture the effects of rocking and torsion.

12) The NEI check process is described in detail in FSAR Section 3OO.1.4. The NEI check and adjusted Foundation Input Response Spectra (FIRS) for the horizontal and vertical directions for Reactor Building (R/B) Complex are presented in FSAR Figures 3OO-235 and 3OO-236, respectively. The adjustment for horizontal spectrum occurs at frequencies less than 0.27 Hz with the maximum factor of 1.09. For the vertical spectrum the modification is more pronounced and occurs at frequencies less than 8.7 Hz with a maximum factor of 1.72 at 4.2 Hz.

    The NEI check and adjusted FIRS for East Power Source Building (PS/B) in the horizontal and vertical directions are provided in Figure 23 and Figure 24, respectively. The adjustment for horizontal spectrum occurs at frequencies less than 0.30 Hz with the maximum factor of 1.09. For the vertical spectrum the modification is more pronounced and occurs at frequencies less than 7.8 Hz with a maximum factor of 1.83 at 3.5 Hz.

The NEI check and adjusted FIRS for West PS/B in the horizontal and vertical directions are provided in Figure 25 and Figure 26, respectively. As described in FSAR 3OO.1.4, the adjusted FIRS are smoothed to obtain Soil Structure Interaction (SSI) input motions. Note that the adjusted FIRS for the East and West PS/Bs are enveloped prior to smoothing to constitute the SSI input motion for the PS/Bs. The adjustment for horizontal spectrum occurs at frequencies less than 0.29 Hz with the maximum factor of 1.09. For the vertical spectrum the modification is more pronounced and occurs at frequencies less than 9.3 Hz with a maximum factor of 1.93 at 4.6 Hz.

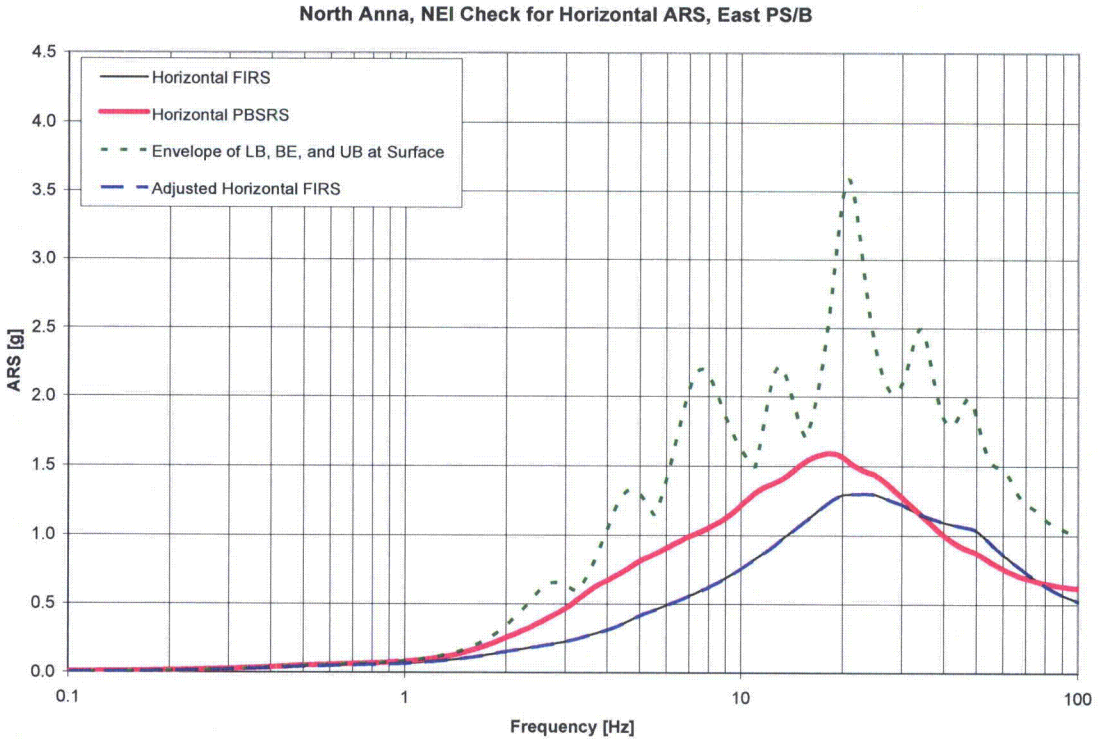

Figure 23 - NEI Check of Horizontal FIRS for East PS/B

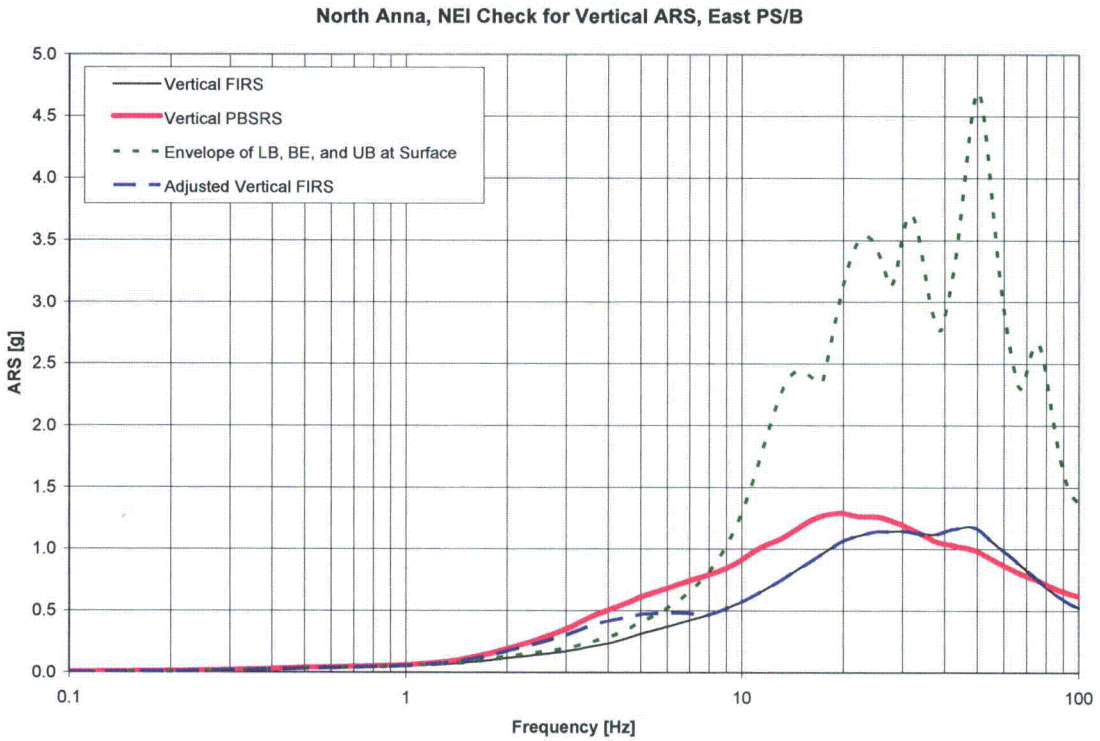

Figure 24 - NEI Check of Vertical FIRS for East PS/B

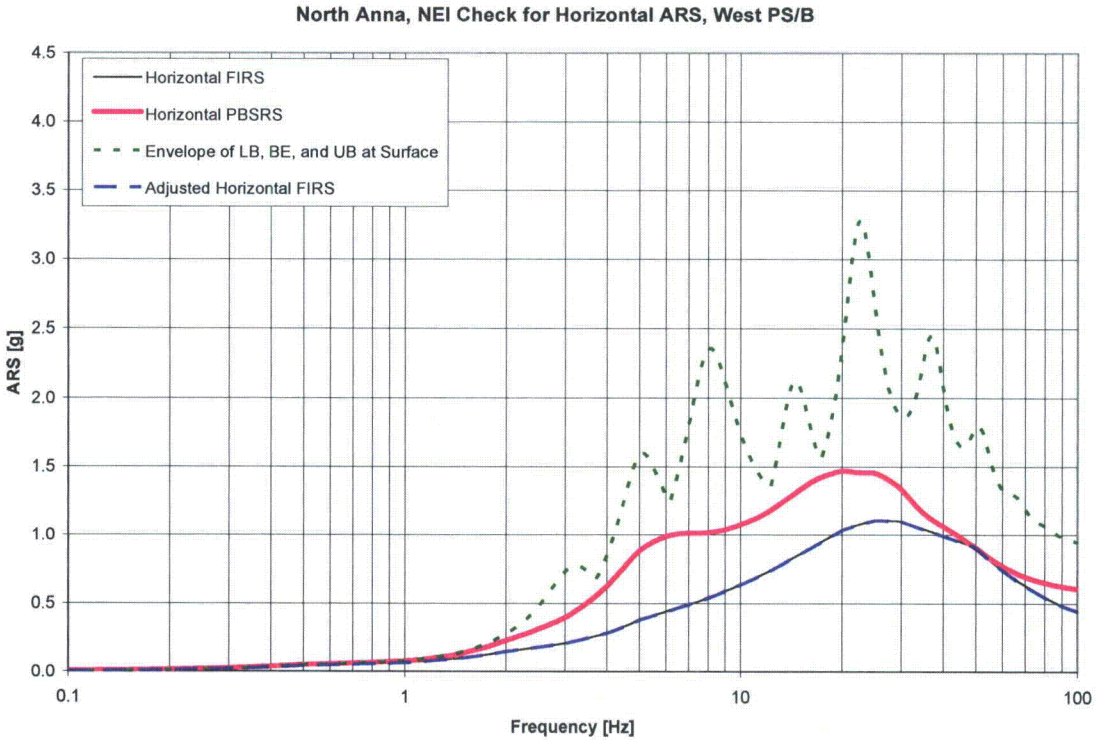

Figure 25 - NEI Check of Horizontal FIRS for West PS/B

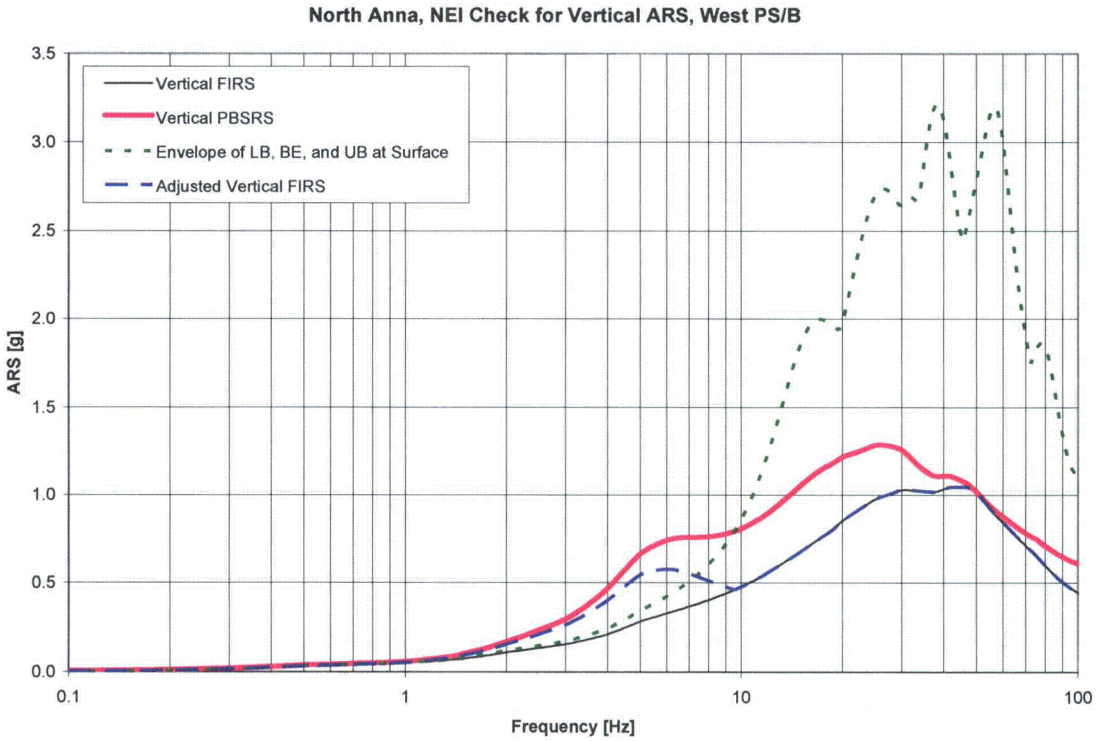

Figure 26 - NEI Check of Vertical FIRS for West PS/B

References:

1 ACS SASSI Version 2.3.0. "An Advanced Computational Software for 3D Dynamic Analysis Including Soil Structure Interaction", User Manuals, Revision 3, Ghiocel Predictive Technologies, Inc., Rochester, New York, December 30, 2010

2 EPRI Report TR-1015111, "Validation of CLASSI and SASSI to Treat Seismic Wave Incoherence in SSI Analysis of NPP Structures," G. Hardy, K. Merz, S. Short, J. Johnson, November, 2007

3 EPRI Report TR-1015110, "Program on Technology Innovation: Effects of Spatial Incoherence on Seismic Ground Motions," N. Abrahamson, December, 2007

Proposed COLA Revision

FSAR Appendix 3NN Sections 3NN.2, 3NN.3, and 3NN.7 will be revised as indicated on the attached markup.

Markup of North Anna COLA

The attached markup represents Dominion's good faith effort to show how the COLA will be revised in a future COLA submittal in response to the subject RAI. However, the same COLA content may be impacted by revisions to the DCD, responses to other COLA RAIs, other COLA changes, plant design changes, editorial or typographical corrections, etc. As a result, the final COLA content that appears in a future submittal may be somewhat different than as presented herein.

The comparison of the results obtained from the first two sets of SSI analyses shows the effects of the incoherency of the input ground motion on the seismic response of the surface foundation R/B complex model. The results obtained from the second two sets of SSI analyses performed with the coherent input motion are compared to assess the effect of embedment on the seismic response.

The results of the site-specific SSI analyses are used to develop seismic demands that are specific for the Unit 3 site. The site-specific seismic demands/loads obtained from the three sets of SSI analyses considering surface and embedded foundation and coherent and incoherent motion are all enveloped by the input seismic loads used for the standard design of R/B complex and PS/B structures. This validates the applicability of the standard seismic design of structural members and components for Unit 3.

The site-specific SSI analyses provide results for the response of the R/B complex and the PS/Bs at different locations within the buildings in terms of broadened in-structure response spectra (ISRS). The ISRS that define the site-specific seismic demands on substructures, subsystems, mechanical components and equipment include the combined effects of embedment and incoherency. The 5 percent damping ISRS obtained from the site-specific SSI analyses of the R/B complex and PS/Bs are compared with the corresponding ISRS that serve as the basis for the standard seismic design of Seismic Category I substructures, subsystems, mechanical components and equipment. In general, the standard design ISRS envelope the site specific ISRS with exceptions where the Unit 3 ISRS exceed the standard plant ISRS at frequencies higher than 10 Hz.

3NN.2 Seismological and Geotechnical Considerations

The R/B complex and PS/Bs are founded on Zone III-IV rock or on a layer of fill concrete placed on Zone III-IV rock. The bottom of foundations is at nominal elevation of 251'-2" NAVD88 (252.02 ft NGVD29). NAVD88 is used throughout this Appendix and it is noted that NGVD29 is +0.86 ft. above NAVD88. The foundation sidewalls are backfilled with a 40 ft. (nominal) thick layer of engineered fill material to establish the nominal elevation of the plant ground surface at 290 ft.

In order to take into account the variation of soil properties and the uncertainties associated with the measurement of the properties of the

site materials, three sets of properties are used for each set of SSI analyses of R/B complex. Four sets of profiles represent the site conditions at the Unit 3 east and west PS/B (these and all other directions used in this report are with respect to Plant North which is at 142.46 degrees counter-clock wise from the State North). Two best estimate (BE) sets of profiles, BE-EPSB and BE-WPSB, represent the properties of the subgrade and embedment for the east and west PS/Bs, respectively. Besides the BE values, the site-specific analyses address the variation of the subgrade properties by considering lower bound (LB) and upper bound (UB) properties. The LB and UB properties are presented in Appendix 3OO, Section 3OO.2. The layering and the dynamic properties of the subgrade materials such as unit weight, strain compatible S-wave and P-wave velocities and damping are obtained from the site response analyses described in Appendix 3OO. The site models for SSI analysis of the R/B complex use a total of 41 horizontally infinite layers to represent the top 560 ft of subgrade materials. 23 horizontally infinite layers model the top 134 ft of subgrade under the East and West PS/B. The properties of the subgrade at greater depths are represented by an elastic half-space. The SSI site models use 10 visco-elastic layers to represent the elastic half space. Each half-space layer has a thickness of :

$$\text{layer thickness} = \frac{(1.5\,Vs) \div f}{n}$$

where:

Vs = the shear wave velocity of the half-space
f = the frequency of analysis
n = the number of half-space layers

Viscous dashpots are modeled at the base of the simulated half-space.

Figures 3NN-1, 3NN-2, and 3NN-3 show the LB, BE and UB profiles for the S-wave velocity (Vs), P-wave velocity (Vp) and damping properties of the subgrade under the R/B complex. Figures 3NN-7, 3NN-8, and 3NN-9 present the four profiles of the S-wave velocity, P-wave velocity, and damping properties of the subgrade under the east and west PS/Bs. Identical damping values are assigned to the profiles used to model the dissipation of energy in the subgrade material associated with both S-wave and P-wave velocities.

under incoherent ground motion is obtained as an average of the results obtained from a set of 10 stochastic SSI simulations similar to Monte Carlo simulations used for probabilistic analyses. The stochastic simulation approach ~~has been included in the NRC interim staff guidance (Reference 3NN-5)~~ is described in EPRI 1015111 (Reference 3NN-9).

3NN.3 ACS SASSI Model Description and Analysis Approach

3NN.3.1 R/B Complex

Model Description

The geometry, stiffness and mass inertia properties of the model used for site-specific SSI analyses of Unit 3 R/B complex are identical to those of the model used for the R/B complex of standard plant SSI analyses and seismic design. The lumped-mass stick models representing the dynamic properties of the structures and equipment above ground level are identical to those of the stick models used for the standard design analyses described in Section 3.7.2.4 and Technical Reports MUAP-10001 and MUAP-10006 (References 3NN-7 and 3NN-8).

The only difference between the standard and Unit 3 site-specific models is in the basement mesh size of the Unit 3 R/B complex model, which is adjusted to ensure that the size of the basemat FE mesh meets the maximum frequency requirements for the Unit 3 subgrade properties. The maximum frequency of analysis is determined from the rule in Reference 3NN-1 that the size of the soil layers or the FE model elements in contact with soil should not be bigger than 20 percent of the seismic wavelength for the given soil material. Table 3NN-13 provides the maximum frequencies of analyses that the FE mesh of the R/B complex basement model can capture for different soil cases considered.

The mesh size of the subgrade is sufficiently refined to capture the transmittal of seismic waves with frequencies up to 50 Hz through the subgrade and the base of the foundation. For the embedded SSI model, the mesh size affects the accuracy of the SSI model to capture the transmittal of high frequency seismic input motion through the relatively soft embedment soil. This limits the accuracy of the ISRS results in the high-frequency range for the embedded conditions. However, the SSI analyses of embedded foundations capture the critical effects of the embedment in the lower frequency range, up to 10 Hz.

the input motion and the nodal responses of the system between frequency and time domain.

The ACS SASSI analysis employs the flexible interface or substructuring method to obtain the SSI impedance at interaction nodes. All the nodes at the contact of the building basement with the subgrade and the sidewall backfill serve as interaction nodes. The design earthquake is input at the center of the common basemat foundation of the R/B complex at the level of foundation bottom nominal elevation of 251'-2", where the SSI input motion in Appendix 3OO for Unit 3 R/B complex is defined. The S-waves propagating upward represent the two horizontal components of the design earthquake motion H1 and H2 that are applied in N-S and E-W direction, respectively. The vertical component of the design earthquake (V) is represented by vertically propagating P-waves. The three components of the earthquake are applied to the model separately. The acceleration time histories compatible to the horizontal and vertical FIRS described in Section 3NN.2 are used as input for the analyses.

The basement of the Unit 3 R/B complex is separated from the buildings around it by expansion joints to prevent their interaction during an earthquake. The R/B foundation is embedded in sidewall backfill of engineered granular material.

The site-specific SSI analyses address the effects of these site-specific conditions by considering both a surface foundation and a foundation basement embedded in sidewall backfill that is modeled as infinite in the horizontal direction. Three profiles with BE, lower bound (LB) and upper bound (UB) subgrade and embedment soil properties are considered in order to account for the variation of the properties of the site materials. The layering and the strain compatible dynamic properties of the site used as input for the site-specific SSI analyses are described in Section 3NN.2. Two sets of analyses, with coherent and incoherent input ground motion, are performed on the SSI model of the R/B complex as a surface foundation. Table 3NN-15 presents the matrix of the nine sets of site-specific SSI analyses performed to provide the seismic response of the R/B complex at the Unit 3 site. The ACS SASSI analyses provide the following results that are post-processed to evaluate the response of the R/B Complex structures:

- ~~Transfer~~ Acceleration transfer functions at major floor mass nodes.

- Maximum accelerations at major floor mass nodes.
- Maximum displacements at major floor mass or outrigger nodes relative to free field motion.
- Maximum member forces and moments in the stick elements modeling the stiffness of the PCCV, CIS and R/B structures.
- 5 percent damping acceleration response spectra of the response in the three orthogonal direction at the lumped mass and outrigger nodes of PCCV, CIS and R/B structures including out-of-plane SDOF mass nodes.

The acceleration transfer functions were interpolated using the recommended interpolation approach Option 2 in the ACS SASSI MOTION module (Reference 3NN-1) for analyses using incoherent input ground motion. This interpolation option includes an unbiased moving average scheme that is well-suited for incoherent SSI analyses. The transfer function interpolation error smoothing parameter values were selected so that the interpolated acceleration transfer function curve best fits the computed acceleration transfer function points from the SSI analyses. The application of the acceleration transfer functions phase adjustment for incoherent SSI analyses was validated by Reference 3NN-9. The effect of the acceleration transfer functions phase adjustment for high-frequency seismic inputs is to increase the interpolated incoherent acceleration transfer functions' amplitudes in the high-frequency range as discussed in Reference 3NN-9, Appendix C.

The results for maximum accelerations at PCCV, CIS and R/B lumped-mass floor locations obtained from different sets of SSI runs are calculated and tabulated to help determine effects of different site conditions on the seismic response. The results of the site-specific SSI analyses for maximum displacements serve to confirm that the gap between the buildings is sufficient to prevent them from colliding during an earthquake.

The results of the site-specific SSI analyses for maximum member forces/moments in the stick elements of the lumped-mass-stick models serve as basis for development of the site-specific seismic demands on the R/B complex structures. The following procedure is used for calculation of site-specific seismic demands for each major floor elevation:

5. For each soil case considered, combine the seismic base reactions that are due to three components of the earthquake using the Newmark 100:40:40 method.

The developed base reactions serve as input for seismic stability evaluations and calculation of dynamic bearing pressures.

3NN.3.2 PS/B

Model Description

The site-specific SSI analyses of the east and west PS/B use two 3-D finite element models. Figure 3NN-17 presents the model used for the SSI analyses of the building as surface foundation, and Figure 3H.2-1R is used for SSI analyses of the building as an embedded foundation. The models reflect the geometry and dynamic properties of the west PS/B of the US-APWR documented in Technical Report MUAP-10001 (Reference 3NN-7).

Since the east and west PS/Bs are nearly identical, the models of the east PS/B are also used for the analyses of the west PS/B. The geometry and the dynamic properties of the models used for site-specific SSI analyses of PS/B are identical to that of the model used for the standard plant SSI analyses described in Section 3.7.2.4 and Technical Reports MUAP-10001 and MUAP-10006 (References 3NN-7 and 3NN-8).

The PS/B models use shell elements to represent the stiffness and inertia properties of structural walls and slabs, including the floor slabs and roof slabs. The properties of the shell elements are adjusted to consider the effect of the concrete cracking on the out-of-plane stiffness of the slab elements. The mass density properties of the slab shell elements are adjusted to include the mass of the equipment, the mass associated with additional dead and live loads. The mass of the equipment is distributed over a representative floor area or equipment support footprint area. Beam elements model the structural beams and columns of the PS/B. Solid brick elements with eight nodes represent the basemat of the building. At the connections between the basemat and the walls, the shell elements extend into the basemat solid elements to transmit nodal rotations. The extended elements share nodes with the corresponding face of the solid elements but have no mass. The model of embedded structure also includes a row of solid elements representing the sidewall backfill around the building basement as shown in Figure 3H.2-1R. These solid elements provide stress results that serve for calculation of

- ~~Transfer~~ Acceleration transfer functions at selected locations. The acceleration transfer functions were interpolated using the same methodology as discussed in Section 3NN.3.1.
- Maximum accelerations at all structural nodes.
- Maximum displacements at building corner at major floor elevation relative to free field motion.
- 5 percent damping acceleration response spectra of the response in selected locations.
- Stresses in the soil elements modeling the embedment soil in contact with the PS/B basement exterior walls.

The results for maximum accelerations at selected locations obtained from different sets of SSI analyses are tabulated and compared to assess the effects of different site conditions on the seismic response. The maximum displacements results serve to demonstrate that the gap between the buildings is sufficient to prevent them from colliding during an earthquake.

The site-specific demands on the PS/B structural members are developed in the form of equivalent static accelerations as follows:

1. Calculate maximum accelerations in each of the three response directions due to each of the three direction input motions from the results of the SSI results of PS/B as surface foundation.

2. Envelope the results the maximum nodal accelerations results from the four surface foundation soil cases.

3. Create nine plots of the envelope maximum accelerations in three directions representing the response of the PS/B at particular floor elevation due to the three components of the earthquake.

4. Apply the SRSS rule to combine the enveloped nodal maximum accelerations due to the three directions of the earthquake. Plot the SRSS of the maximum acceleration responses in the three orthogonal directions.

5. Calculate weighted average accelerations at floor elevation "f" as follows:

$$A_i^f = \frac{\sum a_i^k \cdot w_k}{W_f}$$

3NN.6 ~~Seismic/Dynamic~~ Lateral Earth Pressure

The standard plant is based on ~~a dynamic~~ lateral earth pressure for a water table location of 1 ft below grade. The site specific observations are as follows:

- The post-construction piezometric head contour map (Figure 2.4-216) indicates that maximum groundwater level elevations in the power block area range from about 83.4 to 86.0 m (270.0 to 284.4 ft)
- The maximum groundwater level elevation in the power block RB/PCCV area of Unit 3 is 282.3 ft or 7.7 ft below the design plant grade elevation of 290 ft NAVD88 (290.86 ft NGVD29).
- The maximum groundwater level elevation near the UHSRS is 284.4 ft or 5.6 ft below the design plant grade elevation.
- Figure 2.4-216 shows that the water levels for the PS/Bs and PSFSVs are below Elevation 282.3 ft. However site specific analysis presented below was performed based on a ground water level of 283 ft.

Lateral earth pressure loads are applied to all below-grade exterior walls that are in contact with embedment soil. The earth pressure loads are applied along the whole embedment height of the walls conservatively assuming that during an earthquake there is no separation between the walls and the soil. Hydrostatic pressures are applied at elevations below the nominal water table elevation specified (7 ft below the nominal plant grade i.e., Elevation 283 ft). Hydrostatic pressure due to ground water is also included in the design/analysis of below-grade exterior walls where expansion joints are present. The site-specific dynamic (and static) lateral pressure distributions are calculated using material properties and data for granular structural fill consistent with Table 2.5-212.

The site-specific static lateral earth pressure on the subgrade exterior walls is computed using methods described in Subsection 2.5.4.10.3. The site-specific static lateral earth pressure is computed considering a Rankine at-rest pressure coefficient and using classic formulas in which static earth pressure, including hydrostatic pressure, increases linearly with depth. Lateral load on below-grade walls due to surcharge loading at the surface is also considered. Lateral load due to surcharge loading is computed by multiplying the Rankine at-rest pressure coefficient for granular structural fill times the surcharge area load. Figure 2.5-254 shows a general static earth pressure diagram for nonyielding walls which includes a lateral load due to surcharge.

2. For each soil case, co-linear responses (response in the same direction) from the three directions of input motion are combined using SRSS.

3. The SRSS combined stresses normal to the wall are considered as the soil pressures due to the three direction input motions.

Results of the analysis has been presented graphically in Figure 3NN-22. For comparison, Figure 3NN-22 shows site specific seismic lateral load (curve ~~Unit 3~~ NA3 Dynamic Wood~~'s~~+Westergaard), SASSI analysis results (curves EBE-EPS SRSS, EBEWPS SRSS, ELB SRSS and EUB SRSS), and the seismic earth pressure loading used in the standard design (Standard Plant Design curve) for a typical section of NS direction wall. ~~It demonstrates~~ Figure 3NN-22 also includes plots of the Unit 3 total lateral earth pressure and the standard plant total lateral earth pressure which include both the static and dynamic components. These plots demonstrate that the ~~seismic~~ total (static and dynamic) earth pressure loading used in the standard design envelopes the site-specific loading on the basement wall, which includes the effect of the SRSS soil pressures obtained from site-specific SASSI analyses. ~~It may be noted that, in Figure 3NN-22, at some lower elevations, the SASSI analysis result curve slightly exceeds the Standard Plant Design seismic lateral loading curve. However, this exceedance is compensated for by a larger difference in the upper portion of the wall between SSI analysis results and site specific loadings as determined using Wood's and Westergaard's pressure distributions.~~

3NN.7 References

3NN-1 *An Advanced Computational Software for 3D Dynamic Analysis Including Soil Structure Interaction*, ACS SASSI Version 2.3.0, Ghiocel Predictive Technologies, Inc., September, 2009.

3NN-2 *Seismic Analysis of Safety-Related Nuclear Structures*, American Society of Civil Engineers, ASCE 4-98, Reston, Virginia, 2000.

3NN-3 ~~Abrahamson, N. 2007. "*Effects of Seismic Motion Incoherency Effects*" Palo Alto, CA, EPRI TR-1015111.~~ EPRI Report TR-1015110, "Program on Technology Innovation: Effects of Spatial Incoherence on Seismic Ground Motions," N. Abrahamson, December 2007.

3NN-4 Tseng and Lilhanand.1997. "*Soil-Structure Interaction Analysis Incorporating Spatial Incoherence of Ground Motions*", Electric Power Research Institute, Palo Alto, CA, EPRI TR-102631.

3NN-5 ~~US NRC Interim Staff Guidance ISG-01, "*Seismic Issues Associated with High Frequency Ground Motion in Design Certification and Combined License Applications*", ML081330698, May 19, 2008.~~ [Deleted]

3NN-6 Westergaard, H., 1933. "*Water Pressures on Dams during Earthquakes*," Transactions of ASCE, Paper No. 1835, pp418-433.

3NN-7 *Seismic Design Bases of the US-APWR Standard Plant*, MUAP-10001, Revision 1, Mitsubishi Heavy Industries, Ltd., May 2010.

3NN-8 *Soil-Structure Interaction Analyses and Results for the US-APWR Standard Plant*, MUAP-10006, Revision 0, Mitsubishi Heavy Industries, Ltd., April 2010.

3NN-9 EPRI Report TR-1015111, "Validation of CLASSI and SASSI to Treat Seismic Wave Incoherence in SSI Analysis of NPP Structures," G. Hardy, K. Merz, S. Short, J. Johnson, November, 2007.

ENCLOSURE 4

Response to NRC RAI Letter 64

RAI 5546 Question 03.07.02-4

RESPONSE TO REQUEST FOR ADDITIONAL INFORMATION

North Anna Unit 3

Dominion

Docket No. 52-017

RAI NO.: 5546 (RAI Letter 64)

SRP SECTION: 03.07.02 – SEISMIC SYSTEM ANALYSIS

QUESTIONS for Structural Engineering Branch 1 (AP1000/EPR Project) (SEB1)

DATE OF RAI ISSUE: 4/7/2011

QUESTION NO.: 03.07.02-4

The SRP Section 3.7.2, "Seismic System Analysis," and the Interim Staff Guidance on "Seismic Issues Associated with High Frequency Ground Motion in DC and COL Applications" (ISG-DC/COL-01, 2008) provide guidance the staff will use in evaluating the technical adequacy of the seismic design that takes into account the effects of soil-structure interaction. The NA3 FSAR does not provide sufficient information for the staff to determine the technical adequacy of the seismic SSI analyses of Unit 3 site-specific Category I structures under the guidance. To address this issue, the applicant is requested to provide the following information:

1) A summary of modal characteristics in the fixed-base condition, including the natural frequencies, effective modal masses, percent of mass participation, cumulative percent of mass participation, total number of modes included in the analysis, and method used to account for missing mass modes, for each of the Unit 3 site-specific Category I structures.

2) The SSI analysis method selected (e.g., flexible volume method, flexible interface method, etc.) and a technical justification for the selection.

3) The cut-off frequencies for each of the SSI analyses performed.

4) The analysis frequencies for each of the SSI analyses performed and basis for the selection of these frequencies.

5) Description of and basis for the selection of transfer function interpolation and smoothing methods.

6) Details of soil deposit modeling including determination of soil layer thicknesses in view of the minimum cut-off frequency addressed in the guidance.

7) Details of the half-space simulation and the number of generated layers in simulating the half-space.

8) Demonstration of the adequacy of the "selected locations" at which the seismic demands of Unit 3 site-specific Category I structures are computed. The selected locations should be sufficient to represent various locations throughout the building and should include responses at peripheral locations to detect rocking and torsion. The selected locations should also include responses to check overturning and sliding stability of the structures.

9) Verification of the adequacy of FIRS as SSI input motions ("NEI Check") for all embedded structures.

Dominion Response

North Anna Unit 3 site-specific Category I structures are the Essential Service Water Pipe Tunnel (ESWPT), Ultimate Heat Sink Related Structures (UHSRS), and the Power Source Fuel Storage Vaults (PSFSVs) as described in Part 2 FSAR Subsections 3.8.4.1.3.1, 3.8.4.1.3.2, and 3.8.4.1.3.3, respectively.

1) The modal analyses for the Essential Service Water Pipe Tunnel (ESWPT) investigated two separate sections of the structure, Section E (Pipe Chase), which considered structural response for the first 28 modes, and Section F (Segment 2), which considered structural response for the first 108 modes.

   Table 1 through Table 3 represents the dominant modes and respective characteristics in each direction for Section E (Pipe Chase) of the tunnel. Table 4 through Table 6 represents the dominant modes and respective characteristics in each direction for Section F (Segment 2) of the tunnel. These main modes for the structures are depicted on the cumulative mass vs. frequency graphs (Figure 1 through Figure 3 for Section E and Figure 4 through Figure 6 for Section F) and are represented by the "jumps" in the plots, thus indicating a mode with a major mass contribution.

   The fixed based modal analysis for the Power Source Fuel Storage Vault (PSFSV) considers structural response for the first 204 modes. Table 7 through Table 9 represents the dominant modes and respective characteristics in each direction for the PSFSV. These main modes for the structure are depicted on the cumulative mass vs. frequency graphs (Figure 7 through Figure 9) and are represented by the "jumps" in the plots, thus indicating a mode with a major mass contribution.

   A fixed based modal analysis for the Ultimate Heat Sink Related Structures (UHSRS) investigates the structural response for the first 1000 modes. Table 10 through Table 12 represents the dominant modes and respective characteristics in each direction for the UHS. These main modes for the structure are depicted on the cumulative mass vs. frequency graphs (Figure 10 through Figure 12) and are represented by the "jumps" in the plots, thus indicating a mode with a major mass contribution.

   The seismic loads were determined from the results of frequency domain time history SASSI analysis for maximum member forces and maximum nodal accelerations. The method to account for missing mass modes in frequency domain time history analyses is not applicable.

Table 1 - Modal Properties of ESWPT Section E (Pipe Chase) of First 2 Dominant Modes, X-Direction (NS)

Mode	Frequency (HZ)	Period (sec)	Effective Mass (Lbs*sec^2/ft)	Cumulative Mass Fraction	Percent of Mass Participation (%)
1	15.8	0.063	39.9	0.560	56.0
5	42.2	0.024	1.7	0.585	2.4

Table 2 - Modal Properties of ESWPT Section E (Pipe Chase) of First 2 Dominant Modes, Y-Direction (EW)

Mode	Frequency (HZ)	Period (sec)	Effective Mass (Lbs*sec^2/ft)	Cumulative Mass Fraction	Percent of Mass Participation (%)
3	34.6	0.029	25.9	0.377	37.6
6	47.5	0.021	35.6	0.894	51.7

Table 3 - Modal Properties of ESWPT Section E (Pipe Chase) of First 2 Dominant Modes, Z-Direction (Vert)

Mode	Frequency (HZ)	Period (sec)	Effective Mass (Lbs*sec^2/ft)	Cumulative Mass Fraction	Percent of Mass Participation (%)
4	37.6	0.027	66.3	0.930	93.0
5	42.2	0.024	0.58	0.938	0.8

Table 4 - Modal Properties of ESWPT Section F (Segment 2) of First 2 Dominant Modes, X-Dir. (NS)

Mode	Frequency (HZ)	Period (sec)	Effective Mass (Lbs*sec^2/ft)	Cumulative Mass Fraction	Percent of Mass Participation (%)
1	8.3	0.12	138.2	0.324	32.4
6	30.1	0.033	110.4	0.584	25.9

Table 5 - Modal Properties of ESWPT Section F (Segment 2) of First 2 Dominant Modes, Y-Dir. (EW)

Mode	Frequency (HZ)	Period (sec)	Effective Mass (Lbs*sec^2/ft)	Cumulative Mass Fraction	Percent of Mass Participation (%)
5	29.3	0.034	172.1	0.404	40.4
20	40.9	0.024	130.7	0.930	30.7

Table 6 - Modal Properties of ESWPT Section F (Segment 2) of First 2 Dominant Modes, Z-Dir. (Vert)

Mode	Frequency (HZ)	Period (sec)	Effective Mass (Lbs*sec^2/ft)	Cumulative Mass Fraction	Percent of Mass Participation (%)
7	31.2	.032	158.4	0.377	37.1
9	31.9	.031	259.5	0.986	60.9

Table 7 - Modal Properties of PSFSV of First 2 Dominant Modes, X-Dir. (NS)

Mode	Frequency (HZ)	Period (sec)	Effective Mass (Lbs*sec^2/ft)	Cumulative Mass Fraction	Percent of Mass Participation (%)
4	15.7	0.064	111.1	0.088	8.6
10	19.5	0.051	230.5	0.407	18.0

Table 8 - Modal Properties of PSFSV of First 2 Dominant Modes, Y-Dir. (EW)

Mode	Frequency (HZ)	Period (sec)	Effective Mass (Lbs*sec^2/ft)	Cumulative Mass Fraction	Percent of Mass Participation (%)
1	12.8	0.078	234.9	0.195	19.5
3	15.0	0.067	100.7	0.279	8.4

Table 9 - Modal Properties of PSFSV of First 2 Dominant Modes, Z-Dir. (Vert)

Mode	Frequency (HZ)	Period (sec)	Effective Mass (Lbs*sec^2/ft)	Cumulative Mass Fraction	Percent of Mass Participation (%)
7	16.4	0.061	17.6	0.027	2.4
16	21.2	0.047	52.7	0.101	7.2

Table 10 - Modal Properties of UHS of First 2 Dominant Modes, X-Dir. (NS)

Mode	Frequency (HZ)	Period (sec)	Effective Mass (Lbs*sec^2/ft)	Cumulative Mass Fraction	Percent of Mass Participation (%)
22	5.2	0.193	108.2	0.207	4.9
23	6.3	0.160	162.8	0.280	7.4

Table 11 - Modal Properties of UHS of First 2 Dominant Modes, Y-Dir. (EW)

Mode	Frequency (HZ)	Period (sec)	Effective Mass (Lbs*sec^2/ft)	Cumulative Mass Fraction	Percent of Mass Participation (%)
34	6.5	0.153	68.2	0.268	3.1
47	9.1	0.110	476.0	0.513	22.0

Table 12 - Modal Properties of UHS of First 2 Dominant Modes, Z-Dir. (Vert)

Mode	Frequency (HZ)	Period (sec)	Effective Mass (Lbs*sec^2/ft)	Cumulative Mass Fraction	Percent of Mass Participation (%)
87	16.0	0.063	97.0	0.139	7.5
230	29.4	0.034	97.5	0.410	7.6

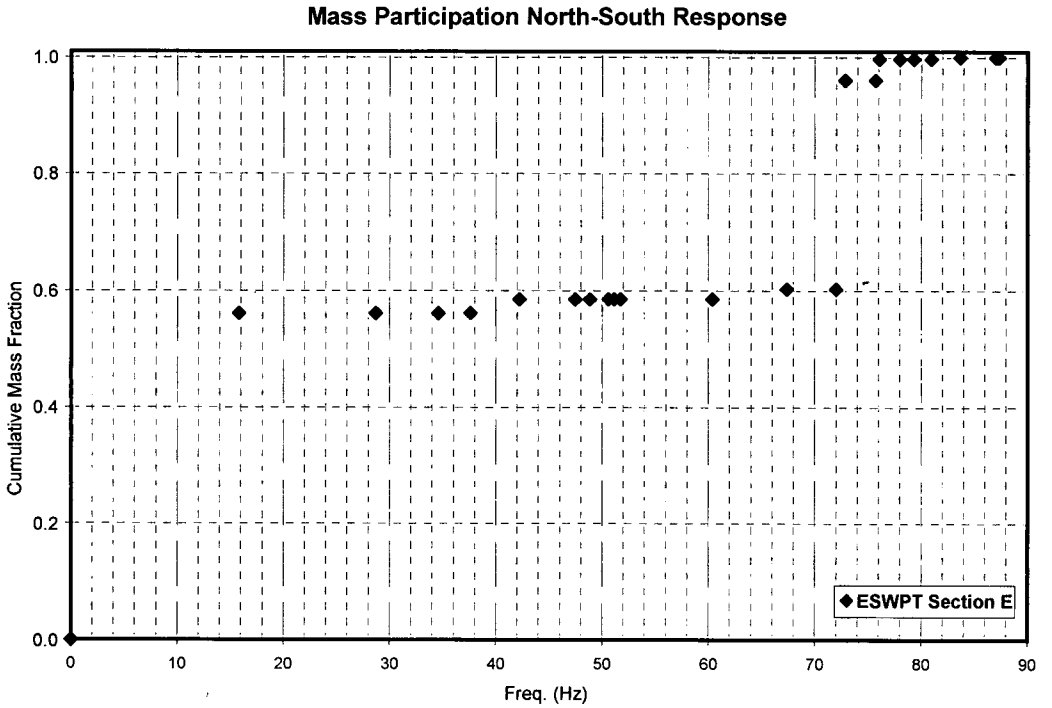

Figure 1 – ESWPT Section E (Pipe Chase) Mass Participation (NS dir.)

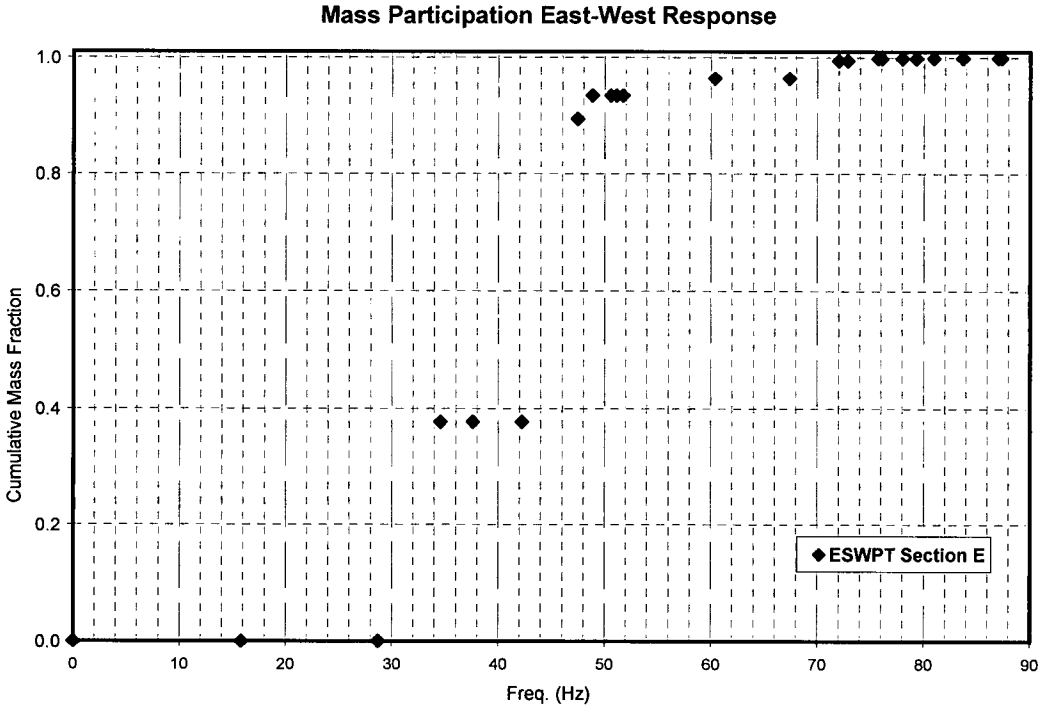

Figure 2 - ESWPT Section E (Pipe Chase) Mass Participation (EW dir.)

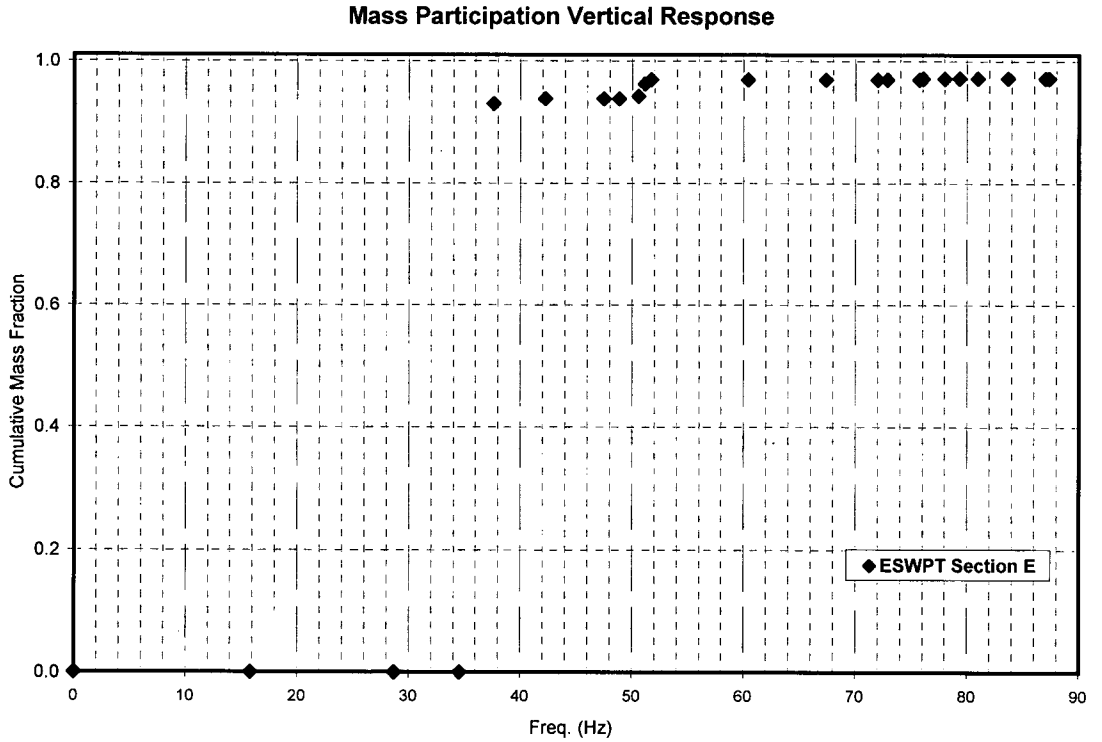

Figure 3 - ESWPT Section E (Pipe Chase) Mass Participation (Vert. dir.)

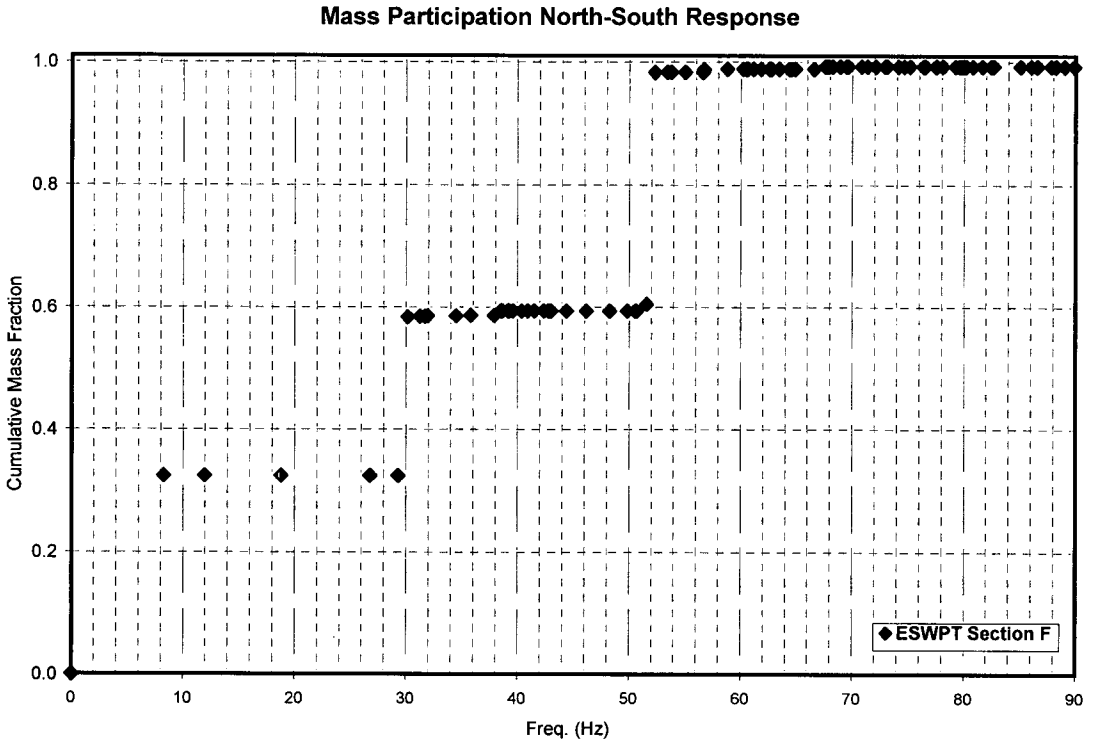

Figure 4 – ESWPT Section F (Segment 2) Mass Participation (NS dir.)

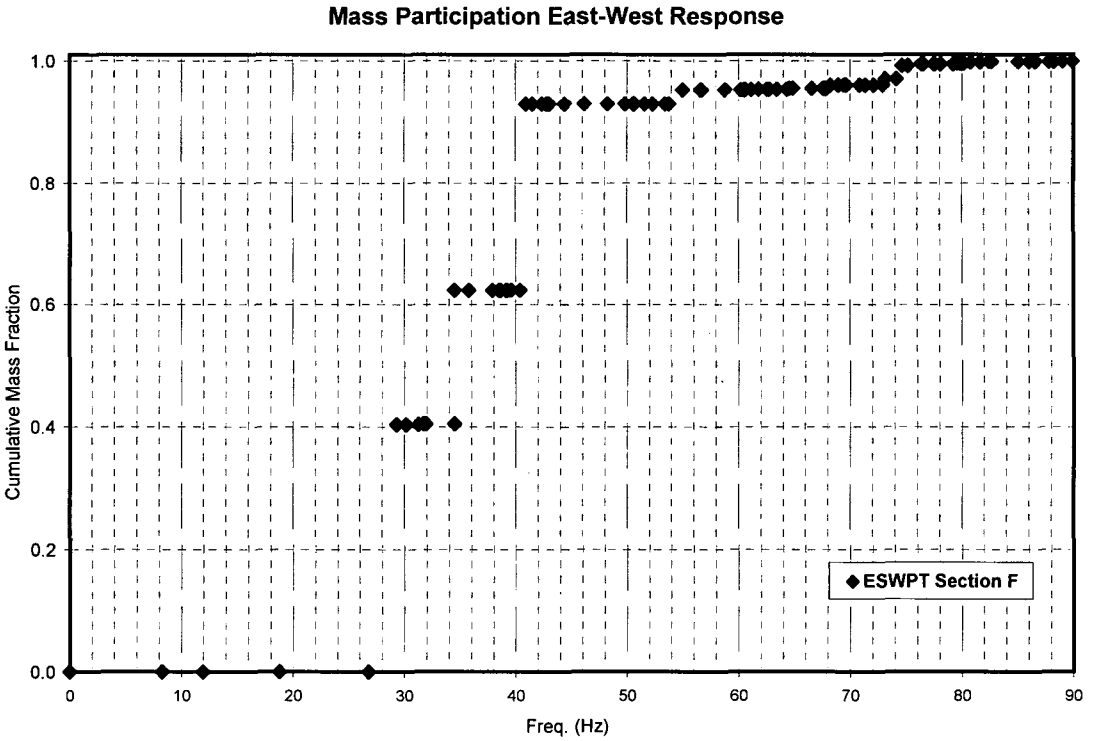

Figure 5 - ESWPT Section F (Segment 2) Mass Participation (EW dir.)

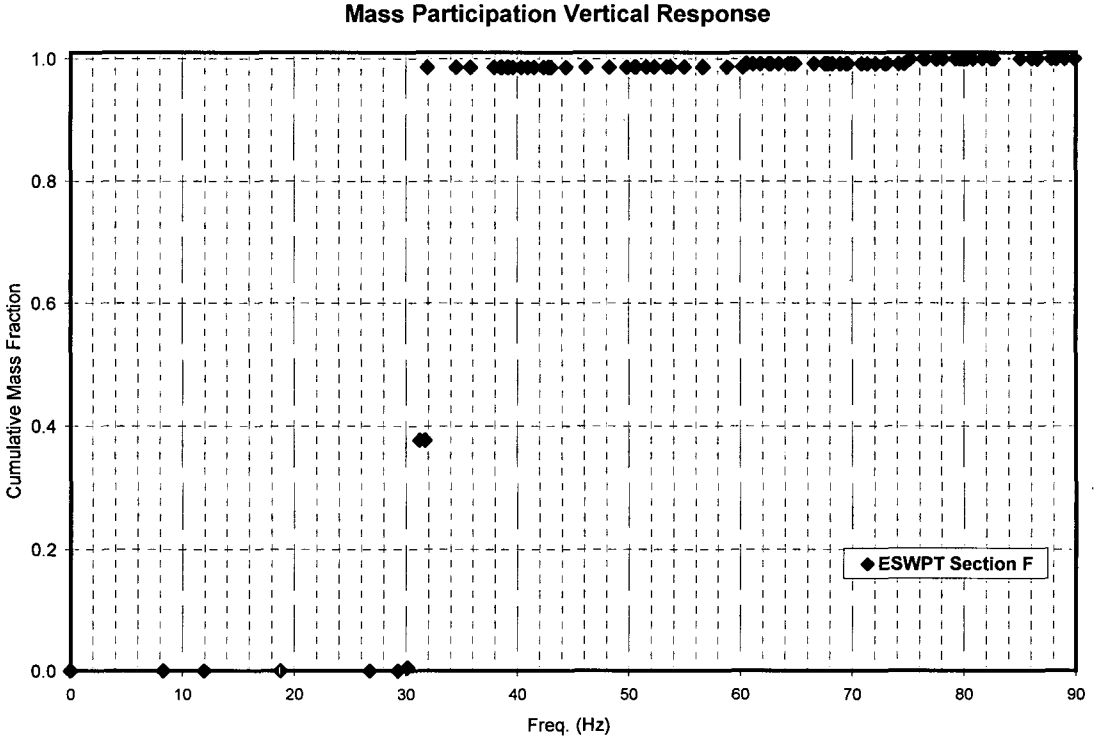

Figure 6 - ESWPT Section F (Segment 2) Mass Participation (Vert. dir.)

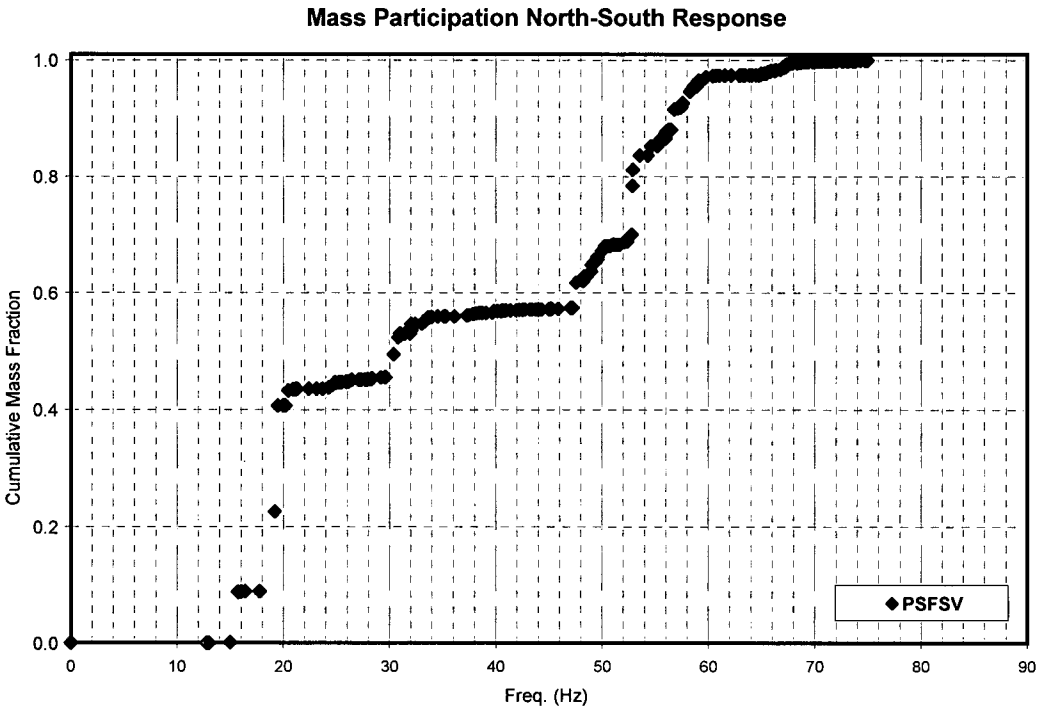

Figure 7 – PSFSV Mass Participation (NS dir.)

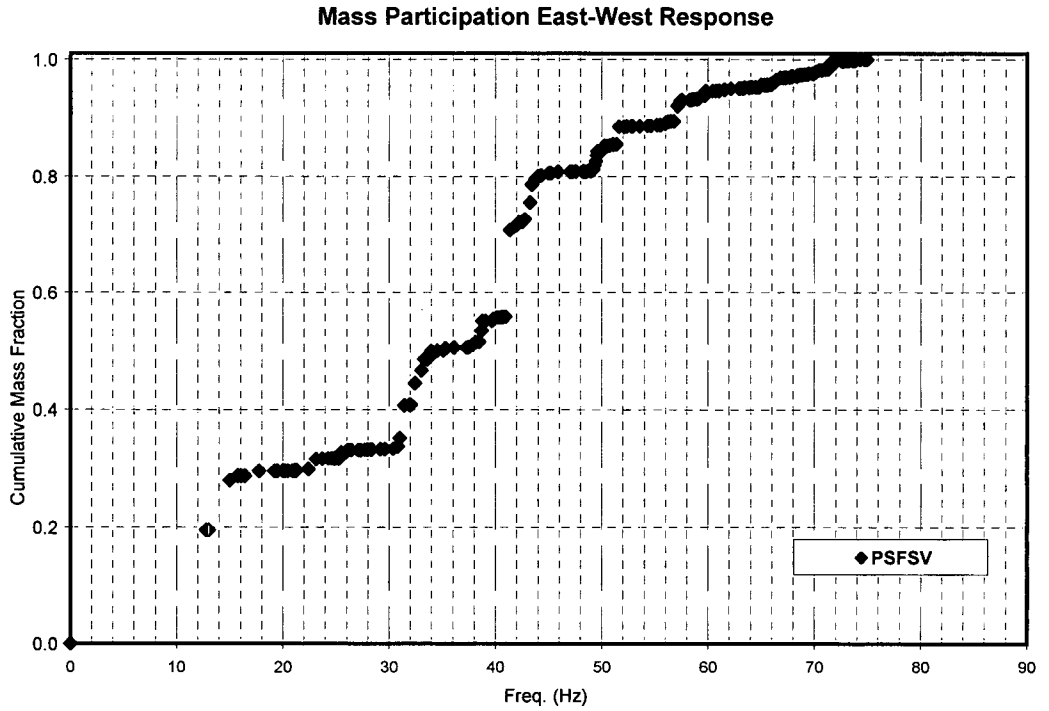

Figure 8 - PSFSV Mass Participation (EW dir.)

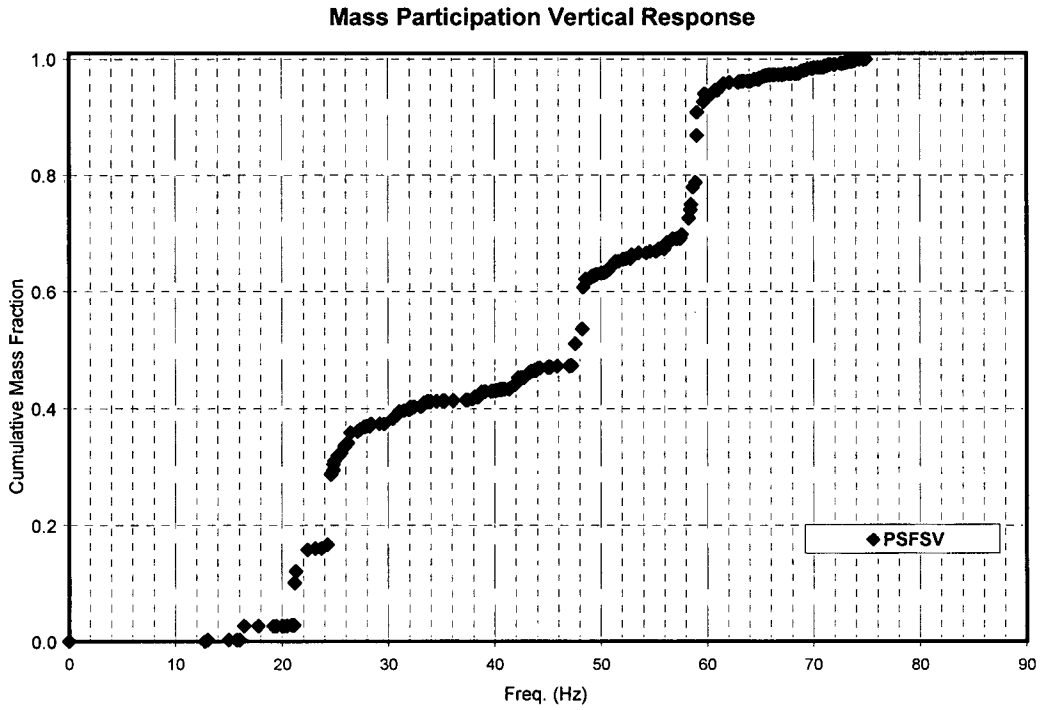

Figure 9 - PSFSV Mass Participation (Vert. dir.)

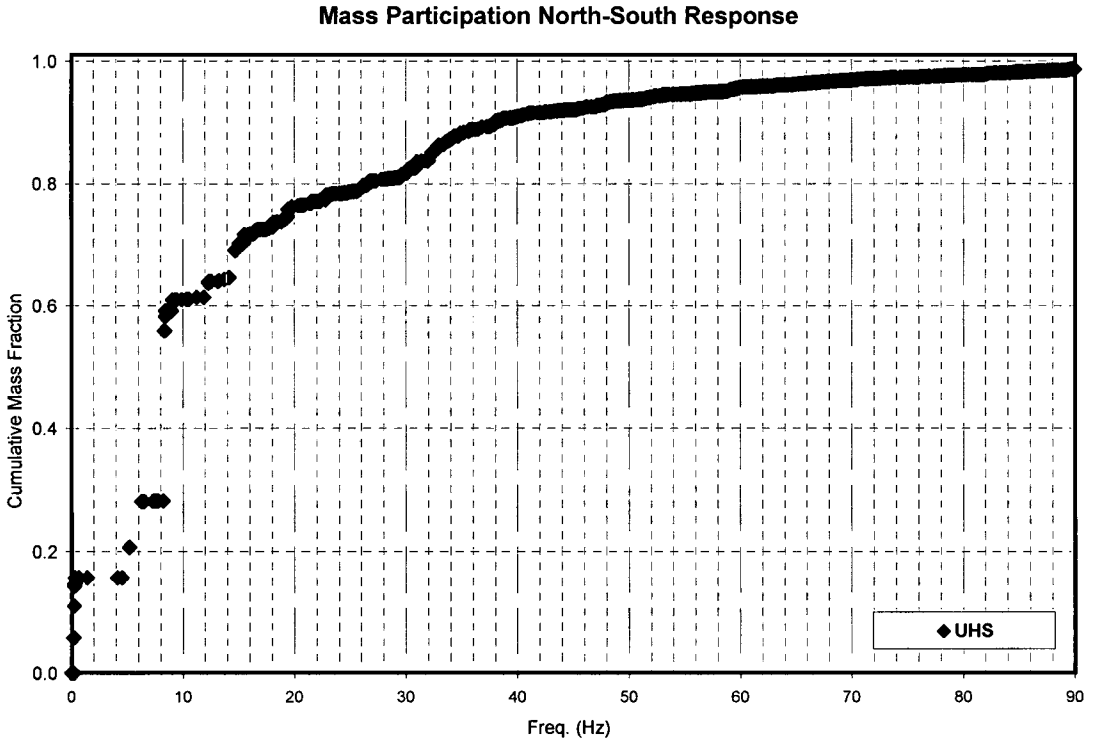

Figure 10 – UHS Mass Participation (NS dir.)

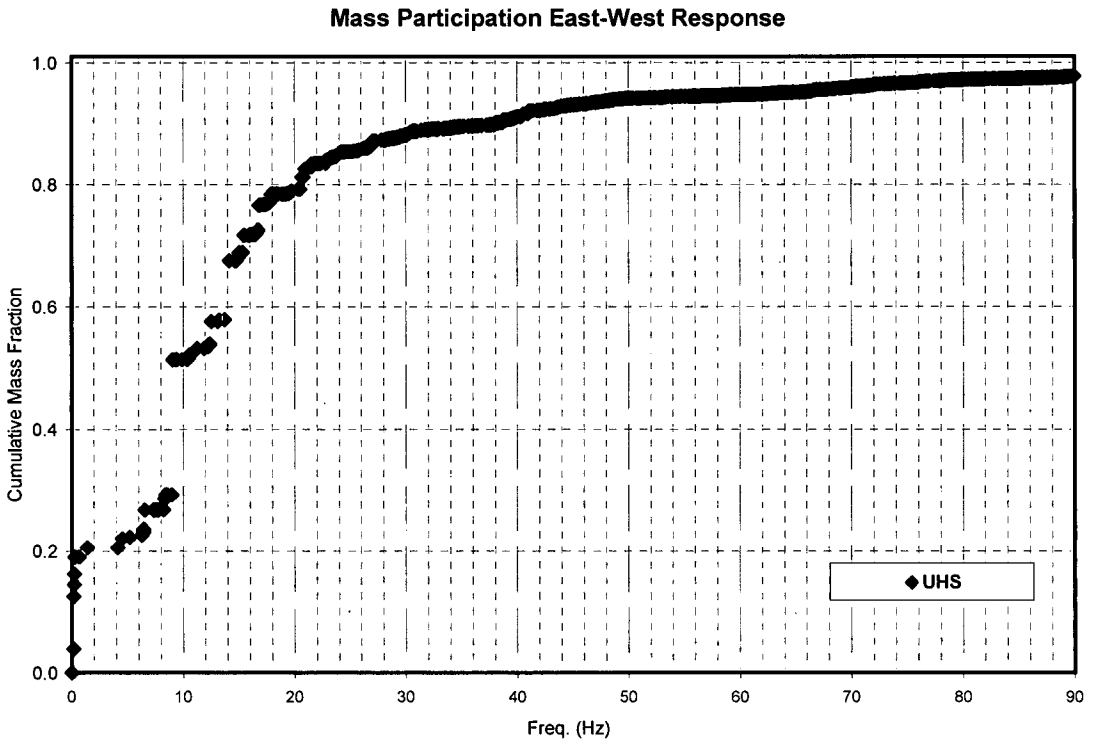

Figure 11 - UHS Mass Participation (EW dir.)

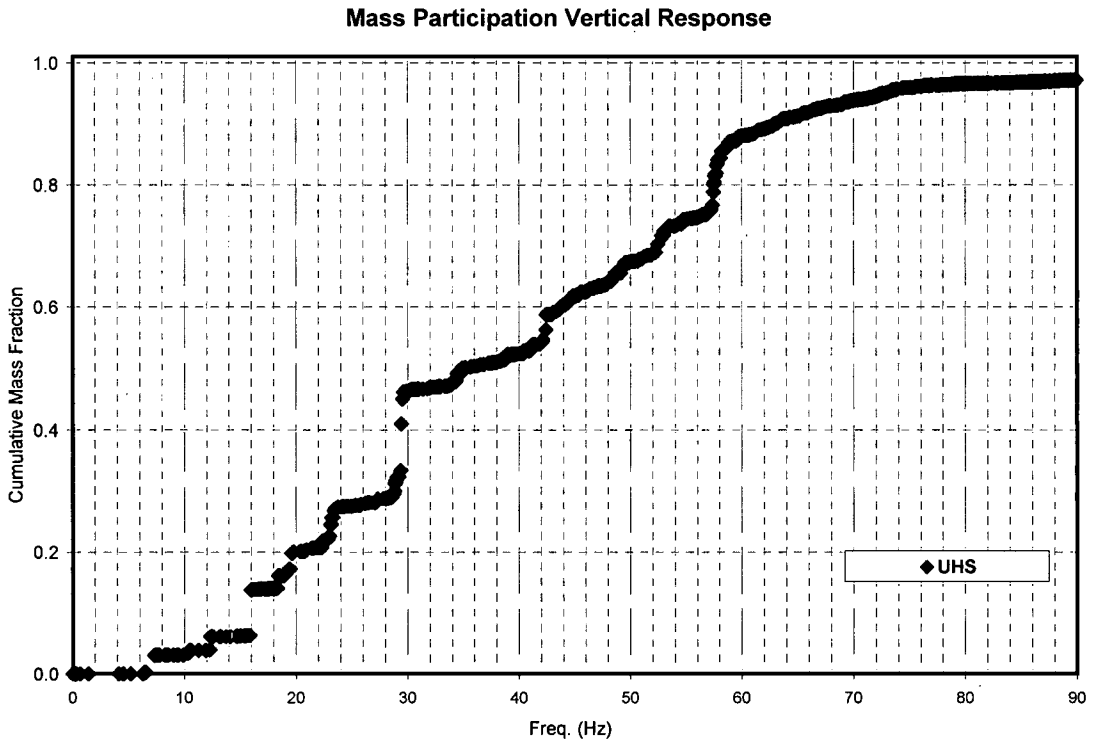

Figure 12 - UHS Mass Participation (Vert. dir.)

2) The flexible interface method, with interaction nodes at the foundation-soil interface, was used for the analyses of the PSFSV and ESWPT models. The choice of this method is based on sensitivity studies and investigations that were performed for the Unit 3 site-specific analyses of the standard plant structures as explained in the response to RAI 5546, Question 03.07.02-3 subpart 2. Note that the UHSRS were analyzed as surface-mounted structures only and therefore neither the flexible interface nor the flexible volume method is applicable.

   FSAR Part 11 Sections 4.1.3 and 5.1.1 will be revised to clarify that the flexible interface method was used in the SSI analyses of the PSFSV and ESWPT.

3) The cut-off frequencies for the surface models for the PSFSV are 50 Hz as stated in FSAR Part 11 Section 4.1.3, and the cut-off frequencies for the PSFSV embedded models are given in FSAR Part 11 Table 4.0-7.

   The cut-off frequencies for all SSI models for the UHSRS are 50 Hz as stated in FSAR Part 11 Section 3.1.3.

   The cut-off frequencies for the surface models for the ESWPT are given in FSAR Part 11 Table 5.0-5.

4) The SASSI analysis frequencies were selected to cover the range between around 1 Hz and the cutoff frequency. This frequency range includes the SSI frequency and primary structural frequencies. The 1Hz lower limit was shown to be low enough to be outside the range of SSI or structural mode amplification. Initially, the frequencies are selected evenly spaced. Frequencies were added as needed to produce smooth interpolation of the transfer functions and accurately capture peaks. As verification, additional frequencies were added to observe that the results did not change.

   The frequencies selected for the Unit 3 site-specific Category I structures are listed in the Tables below:

   There are 101 frequencies of analysis for the surface models for the PSFSV as stated in FSAR Part 11 Section 4.1.3. The number of frequencies of analysis for each PSFSV embedded model is presented in FSAR Part 11 Table 4.0-7, and the frequencies of analysis are shown below.

PSFSV - Power Source Fuel Storage Vaults

Freq #	Frequency of Analysis (Hz)							
	SBEE	SBEW	SUBEW	SLBEW	EBE1	EBE2	ELB	EUB
1	0.05	0.05	0.05	0.05	0.05	0.05	0.05	0.05
2	0.5	0.5	0.5	0.5	0.5	0.5	0.5	0.5
3	1.0	1.0	1.0	1.0	1.0	1.0	1.0	1.0
4	1.5	1.5	1.5	1.5	1.5	1.5	1.5	1.5
5	2.0	2.0	2.0	2.0	2.0	2.0	2.0	2.0

Freq #	Frequency of Analysis (Hz)							
	SBEE	SBEW	SUBEW	SLBEW	EBE1	EBE2	ELB	EUB
6	2.5	2.5	2.5	2.5	2.5	2.5	2.5	2.5
7	3.0	3.0	3.0	3.0	3.0	3.0	3.0	3.0
8	3.5	3.5	3.5	3.5	3.5	3.5	3.5	3.5
9	4.0	4.0	4.0	4.0	4.0	4.0	4.0	4.0
10	4.5	4.5	4.5	4.5	4.5	4.5	4.5	4.5
11	5.0	5.0	5.0	5.0	5.0	5.0	5.0	5.0
12	5.5	5.5	5.5	5.5	5.5	5.5	5.5	5.5
13	6.0	6.0	6.0	6.0	6.0	6.0	6.0	6.0
14	6.5	6.5	6.5	6.5	6.5	6.5	6.5	6.5
15	7.0	7.0	7.0	7.0	7.0	7.0	7.0	7.0
16	7.5	7.5	7.5	7.5	7.5	7.5	7.5	7.5
17	8.0	8.0	8.0	8.0	8.0	8.0	8.0	8.0
18	8.5	8.5	8.5	8.5	8.5	8.5	8.5	8.5
19	9.0	9.0	9.0	9.0	9.0	9.0	9.0	9.0
20	9.5	9.5	9.5	9.5	9.5	9.5	9.5	9.5
21	10.0	10.0	10.0	10.0	10.0	10.0	10.0	10.0
22	10.5	10.5	10.5	10.5	10.5	10.5	10.5	10.5
23	11.0	11.0	11.0	11.0	11.0	11.0	11.0	11.0
24	11.5	11.5	11.5	11.5	11.5	11.5	11.5	11.5
25	12.0	12.0	12.0	12.0	12.0	12.0	12.0	12.0
26	12.5	12.5	12.5	12.5	12.5	12.5		12.5
27	13.0	13.0	13.0	13.0	13.0	13.0		13.0
28	13.5	13.5	13.5	13.5	13.5	13.5		13.5
29	14.0	14.0	14.0	14.0	14.0	14.0		14.0
30	14.5	14.5	14.5	14.5	14.5	14.5		14.5
31	15.0	15.0	15.0	15.0	15.0	15.0		15.0
32	15.5	15.5	15.5	15.5	15.5	15.5		15.5
33	16.0	16.0	16.0	16.0	16.0	16.0		16.0
34	16.5	16.5	16.5	16.5	16.5	16.5		16.5
35	17.0	17.0	17.0	17.0	17.0	17.0		17.0
36	17.5	17.5	17.5	17.5	17.5	17.5		17.5
37	18.0	18.0	18.0	18.0	18.0	18.0		18.0

Freq #	Frequency of Analysis (Hz)							
	SBEE	SBEW	SUBEW	SLBEW	EBE1	EBE2	ELB	EUB
38	18.5	18.5	18.5	18.5	18.5	18.5		18.5
39	19.0	19.0	19.0	19.0	19.0	19.0		19.0
40	19.5	19.5	19.5	19.5	19.5	19.5		19.5
41	20.0	20.0	20.0	20.0	20.0	20.0		20.0
42	20.5	20.5	20.5	20.5		20.5		20.5
43	21.0	21.0	21.0	21.0		21.0		21.0
44	21.5	21.5	21.5	21.5				21.5
45	22.0	22.0	22.0	22.0				22.0
46	22.5	22.5	22.5	22.5				22.5
47	23.0	23.0	23.0	23.0				23.0
48	23.5	23.5	23.5	23.5				23.5
49	24.0	24.0	24.0	24.0				24.0
50	24.5	24.5	24.5	24.5				24.5
51	25.0	25.0	25.0	25.0				25.0
52	25.5	25.5	25.5	25.5				25.5
53	26.0	26.0	26.0	26.0				26.0
54	26.5	26.5	26.5	26.5				26.5
55	27.0	27.0	27.0	27.0				27.0
56	27.5	27.5	27.5	27.5				27.5
57	28.0	28.0	28.0	28.0				28.0
58	28.5	28.5	28.5	28.5				28.5
59	29.0	29.0	29.0	29.0				29.0
60	29.5	29.5	29.5	29.5				29.5
61	30.0	30.0	30.0	30.0				30.0
62	30.5	30.5	30.5	30.5				30.5
63	31.0	31.0	31.0	31.0				31.0
64	31.5	31.5	31.5	31.5				31.5
65	32.0	32.0	32.0	32.0				32.0
66	32.5	32.5	32.5	32.5				32.5
67	33.0	33.0	33.0	33.0				33.0
68	33.5	33.5	33.5	33.5				33.5
69	34.0	34.0	34.0	34.0				34.0

Freq #	Frequency of Analysis (Hz)							
	SBEE	SBEW	SUBEW	SLBEW	EBE1	EBE2	ELB	EUB
70	34.5	34.5	34.5	34.5				
71	35.0	35.0	35.0	35.0				
72	35.5	35.5	35.5	35.5				
73	36.0	36.0	36.0	36.0				
74	36.5	36.5	36.5	36.5				
75	37.0	37.0	37.0	37.0				
76	37.5	37.5	37.5	37.5				
77	38.0	38.0	38.0	38.0				
78	38.5	38.5	38.5	38.5				
79	39.0	39.0	39.0	39.0				
80	39.5	39.5	39.5	39.5				
81	40.0	40.0	40.0	40.0				
82	40.5	40.5	40.5	40.5				
83	41.0	41.0	41.0	41.0				
84	41.5	41.5	41.5	41.5				
85	42.0	42.0	42.0	42.0				
86	42.5	42.5	42.5	42.5				
87	43.0	43.0	43.0	43.0				
88	43.5	43.5	43.5	43.5				
89	44.0	44.0	44.0	44.0				
90	44.5	44.5	44.5	44.5				
91	45.0	45.0	45.0	45.0				
92	45.5	45.5	45.5	45.5				
93	46.0	46.0	46.0	46.0				
94	46.5	46.5	46.5	46.5				
95	47.0	47.0	47.0	47.0				
96	47.5	47.5	47.5	47.5				
97	48.0	48.0	48.0	48.0				
98	48.5	48.5	48.5	48.5				
99	49.0	49.0	49.0	49.0				
100	49.5	49.5	49.5	49.5				
101	50.0	50.0	50.0	50.0				

There are a total of 101 frequencies of analysis for the surface models for the UHSRS as stated in FSAR Part 11 Section 3.1.3, and the frequencies of analysis are shown below.

UHSRS - Ultimate Heat Sink Related Structures

Freq #	Frequency of Analysis (Hz)							
	SBEA	SBEB	SBEC	SBED	SLBA	SLBD	SUBA	SUBD
1	0.05	0.05	0.05	0.05	0.05	0.05	0.05	0.05
2	0.5	0.5	0.5	0.5	0.5	0.5	0.5	0.5
3	1.0	1.0	1.0	1.0	1.0	1.0	1.0	1.0
4	1.5	1.5	1.5	1.5	1.5	1.5	1.5	1.5
5	2.0	2.0	2.0	2.0	2.0	2.0	2.0	2.0
6	2.5	2.5	2.5	2.5	2.5	2.5	2.5	2.5
7	3.0	3.0	3.0	3.0	3.0	3.0	3.0	3.0
8	3.5	3.5	3.5	3.5	3.5	3.5	3.5	3.5
9	4.0	4.0	4.0	4.0	4.0	4.0	4.0	4.0
10	4.5	4.5	4.5	4.5	4.5	4.5	4.5	4.5
11	5.0	5.0	5.0	5.0	5.0	5.0	5.0	5.0
12	5.5	5.5	5.5	5.5	5.5	5.5	5.5	5.5
13	6.0	6.0	6.0	6.0	6.0	6.0	6.0	6.0
14	6.5	6.5	6.5	6.5	6.5	6.5	6.5	6.5
15	7.0	7.0	7.0	7.0	7.0	7.0	7.0	7.0
16	7.5	7.5	7.5	7.5	7.5	7.5	7.5	7.5
17	8.0	8.0	8.0	8.0	8.0	8.0	8.0	8.0
18	8.5	8.5	8.5	8.5	8.5	8.5	8.5	8.5
19	9.0	9.0	9.0	9.0	9.0	9.0	9.0	9.0
20	9.5	9.5	9.5	9.5	9.5	9.5	9.5	9.5
21	10.0	10.0	10.0	10.0	10.0	10.0	10.0	10.0
22	10.5	10.5	10.5	10.5	10.5	10.5	10.5	10.5
23	11.0	11.0	11.0	11.0	11.0	11.0	11.0	11.0
24	11.5	11.5	11.5	11.5	11.5	11.5	11.5	11.5
25	12.0	12.0	12.0	12.0	12.0	12.0	12.0	12.0
26	12.5	12.5	12.5	12.5	12.5	12.5	12.5	12.5
27	13.0	13.0	13.0	13.0	13.0	13.0	13.0	13.0
28	13.5	13.5	13.5	13.5	13.5	13.5	13.5	13.5

Freq #	Frequency of Analysis (Hz)							
	SBEA	SBEB	SBEC	SBED	SLBA	SLBD	SUBA	SUBD
29	14.0	14.0	14.0	14.0	14.0	14.0	14.0	14.0
30	14.5	14.5	14.5	14.5	14.5	14.5	14.5	14.5
31	15.0	15.0	15.0	15.0	15.0	15.0	15.0	15.0
32	15.5	15.5	15.5	15.5	15.5	15.5	15.5	15.5
33	16.0	16.0	16.0	16.0	16.0	16.0	16.0	16.0
34	16.5	16.5	16.5	16.5	16.5	16.5	16.5	16.5
35	17.0	17.0	17.0	17.0	17.0	17.0	17.0	17.0
36	17.5	17.5	17.5	17.5	17.5	17.5	17.5	17.5
37	18.0	18.0	18.0	18.0	18.0	18.0	18.0	18.0
38	18.5	18.5	18.5	18.5	18.5	18.5	18.5	18.5
39	19.0	19.0	19.0	19.0	19.0	19.0	19.0	19.0
40	19.5	19.5	19.5	19.5	19.5	19.5	19.5	19.5
41	20.0	20.0	20.0	20.0	20.0	20.0	20.0	20.0
42	20.5	20.5	20.5	20.5	20.5	20.5	20.5	20.5
43	21.0	21.0	21.0	21.0	21.0	21.0	21.0	21.0
44	21.5	21.5	21.5	21.5	21.5	21.5	21.5	21.5
45	22.0	22.0	22.0	22.0	22.0	22.0	22.0	22.0
46	22.5	22.5	22.5	22.5	22.5	22.5	22.5	22.5
47	23.0	23.0	23.0	23.0	23.0	23.0	23.0	23.0
48	23.5	23.5	23.5	23.5	23.5	23.5	23.5	23.5
49	24.0	24.0	24.0	24.0	24.0	24.0	24.0	24.0
50	24.5	24.5	24.5	24.5	24.5	24.5	24.5	24.5
51	25.0	25.0	25.0	25.0	25.0	25.0	25.0	25.0
52	25.5	25.5	25.5	25.5	25.5	25.5	25.5	25.5
53	26.0	26.0	26.0	26.0	26.0	26.0	26.0	26.0
54	26.5	26.5	26.5	26.5	26.5	26.5	26.5	26.5
55	27.0	27.0	27.0	27.0	27.0	27.0	27.0	27.0
56	27.5	27.5	27.5	27.5	27.5	27.5	27.5	27.5
57	28.0	28.0	28.0	28.0	28.0	28.0	28.0	28.0
58	28.5	28.5	28.5	28.5	28.5	28.5	28.5	28.5
59	29.0	29.0	29.0	29.0	29.0	29.0	29.0	29.0
60	29.5	29.5	29.5	29.5	29.5	29.5	29.5	29.5

Freq #	Frequency of Analysis (Hz)							
	SBEA	SBEB	SBEC	SBED	SLBA	SLBD	SUBA	SUBD
61	30.0	30.0	30.0	30.0	30.0	30.0	30.0	30.0
62	30.5	30.5	30.5	30.5	30.5	30.5	30.5	30.5
63	31.0	31.0	31.0	31.0	31.0	31.0	31.0	31.0
64	31.5	31.5	31.5	31.5	31.5	31.5	31.5	31.5
65	32.0	32.0	32.0	32.0	32.0	32.0	32.0	32.0
66	32.5	32.5	32.5	32.5	32.5	32.5	32.5	32.5
67	33.0	33.0	33.0	33.0	33.0	33.0	33.0	33.0
68	33.5	33.5	33.5	33.5	33.5	33.5	33.5	33.5
69	34.0	34.0	34.0	34.0	34.0	34.0	34.0	34.0
70	34.5	34.5	34.5	34.5	34.5	34.5	34.5	34.5
71	35.0	35.0	35.0	35.0	35.0	35.0	35.0	35.0
72	35.5	35.5	35.5	35.5	35.5	35.5	35.5	35.5
73	36.0	36.0	36.0	36.0	36.0	36.0	36.0	36.0
74	36.5	36.5	36.5	36.5	36.5	36.5	36.5	36.5
75	37.0	37.0	37.0	37.0	37.0	37.0	37.0	37.0
76	37.5	37.5	37.5	37.5	37.5	37.5	37.5	37.5
77	38.0	38.0	38.0	38.0	38.0	38.0	38.0	38.0
78	38.5	38.5	38.5	38.5	38.5	38.5	38.5	38.5
79	39.0	39.0	39.0	39.0	39.0	39.0	39.0	39.0
80	39.5	39.5	39.5	39.5	39.5	39.5	39.5	39.5
81	40.0	40.0	40.0	40.0	40.0	40.0	40.0	40.0
82	40.5	40.5	40.5	40.5	40.5	40.5	40.5	40.5
83	41.0	41.0	41.0	41.0	41.0	41.0	41.0	41.0
84	41.5	41.5	41.5	41.5	41.5	41.5	41.5	41.5
85	42.0	42.0	42.0	42.0	42.0	42.0	42.0	42.0
86	42.5	42.5	42.5	42.5	42.5	42.5	42.5	42.5
87	43.0	43.0	43.0	43.0	43.0	43.0	43.0	43.0
88	43.5	43.5	43.5	43.5	43.5	43.5	43.5	43.5
89	44.0	44.0	44.0	44.0	44.0	44.0	44.0	44.0
90	44.5	44.5	44.5	44.5	44.5	44.5	44.5	44.5
91	45.0	45.0	45.0	45.0	45.0	45.0	45.0	45.0
92	45.5	45.5	45.5	45.5	45.5	45.5	45.5	45.5

Freq #	Frequency of Analysis (Hz)							
	SBEA	SBEB	SBEC	SBED	SLBA	SLBD	SUBA	SUBD
93	46.0	46.0	46.0	46.0	46.0	46.0	46.0	46.0
94	46.5	46.5	46.5	46.5	46.5	46.5	46.5	46.5
95	47.0	47.0	47.0	47.0	47.0	47.0	47.0	47.0
96	47.5	47.5	47.5	47.5	47.5	47.5	47.5	47.5
97	48.0	48.0	48.0	48.0	48.0	48.0	48.0	48.0
98	48.5	48.5	48.5	48.5	48.5	48.5	48.5	48.5
99	49.0	49.0	49.0	49.0	49.0	49.0	49.0	49.0
100	49.5	49.5	49.5	49.5	49.5	49.5	49.5	49.5
101	50.0	50.0	50.0	50.0	50.0	50.0	50.0	50.0

ESWPT - Essential Service Water Pipe Tunnel

The total number of frequencies of analysis and the cut-off frequency for the different segments of the ESWPT are shown on FSAR Part 11 Table 5.0-5. The frequencies of analysis for each ESWPT segment are shown below.

Tunnel_1a_N			
Freq #	Frequency of Analysis (Hz)		
	EBE-E	ELB	EUB
1	0.01	0.01	0.01
2	1.10	0.49	1.10
3	2.20	1.10	2.20
4	3.05	2.20	3.05
5	4.03	2.56	4.03
6	4.88	3.05	4.88
7	5.80	4.03	5.80
8	6.84	4.52	6.84
9	7.57	4.88	7.57
10	8.69	5.80	8.69
11	9.77	6.84	9.77
12	10.35	7.57	10.35
13	10.99	8.69	10.99
14	11.60	9.77	11.60
15	12.28	10.35	12.28
16	12.77	10.99	12.77
17	13.16	11.60	13.16
18	13.49	12.28	13.49
19	13.88	12.77	13.88
20	14.50	13.16	14.50
21	15.05	13.49	15.05
22	15.69	13.88	15.69
23	16.50	14.50	16.50
24	16.86	15.05	16.86
25	17.65	15.69	17.65
26	18.04	16.50	18.04
27	18.27	16.86	18.27
28	18.51	17.65	18.51

Tunnel_1a_N			
Freq #	Frequency of Analysis (Hz)		
	EBE-E	ELB	EUB
29	18.98	18.04	18.98
30	19.59	18.27	19.59
31	19.95	18.51	19.95
32	20.19	18.98	20.19
33	20.58	19.59	20.58
34	20.94	19.95	20.94
35	21.40	20.19	21.40
36	21.62	20.58	21.62
37	21.86	20.94	21.86
38	21.88	21.40	21.88
39	21.94	21.62	21.94
40	22.33	21.86	22.33
41	22.73	21.88	22.73
42	23.07	21.94	23.07
43	23.40	22.33	23.40
44	23.47	22.73	23.47
45	23.54	23.07	23.54
46	23.93	23.40	23.93
47	24.28	23.47	24.28
48	24.74	23.54	24.74
49	24.98	23.93	24.98
50	25.55	24.28	25.55
51	26.03	24.74	26.03
52	26.76	24.98	26.76
53	27.19		27.19
54	27.60		27.60
55	27.94		27.94
56	28.03		28.03
57	28.44		28.44
58	28.70		28.70
59	28.76		28.76
60	28.98		28.98

Tunnel_1a_N			
Freq #	Frequency of Analysis (Hz)		
	EBE-E	ELB	EUB
61	29.49		29.49
62	29.72		29.72
63	30.03		30.03
64	30.21		30.21
65	31.04		31.04
66	31.24		31.24
67	31.46		31.46
68	31.76		31.76
69	31.85		31.85
70	32.23		32.23
71	32.32		32.32
72	32.50		32.50
73	32.71		32.71
74	32.79		32.79
75	33.02		33.02
76	33.51		33.51
77	34.06		34.06
78	34.61		34.61
79	35.69		35.69
80	36.04		36.04
81	36.61		36.61
82	36.82		36.82
83	37.07		37.07
84	37.84		37.84
85	38.48		38.48
86	39.69		39.69
87	39.90		39.90
88			40.22
89			41.36
90			41.74
91			42.11
92			42.72

Tunnel_1a_N			
Freq #	Frequency of Analysis (Hz)		
	EBE-E	ELB	EUB
93			43.46
94			44.73
95			45.53
96			46.53
97			47.61
98			48.65
99			49.54
100			49.74

Tunnel_1a_S				
Freq #	Frequency of Analysis (Hz)			
	SBE-E	SBE-W	SLB	SUB
1	0.01	0.01	0.01	0.01
2	1.10	1.10	1.10	1.10
3	2.20	2.20	2.20	2.20
4	3.05	3.05	3.05	3.05
5	4.03	4.03	4.03	4.03
6	4.88	4.88	4.88	4.88
7	5.80	5.80	5.80	5.80
8	6.84	6.84	6.84	6.84
9	7.57	7.57	7.57	7.57
10	8.69	8.69	8.69	8.69
11	9.77	9.77	9.77	9.77
12	10.35	10.35	10.35	10.35
13	10.99	10.99	10.99	10.99
14	11.60	11.60	11.60	11.60
15	12.28	12.28	12.28	12.28
16	12.77	12.77	12.77	12.77
17	13.16	13.16	13.16	13.16
18	13.49	13.49	13.49	13.49
19	13.88	13.88	13.88	13.88
20	14.50	14.50	14.50	14.50

Tunnel_1a_S				
Freq #	Frequency of Analysis (Hz)			
	SBE-E	SBE-W	SLB	SUB
21	15.05	15.05	15.05	15.05
22	15.69	15.69	15.69	15.69
23	16.50	16.50	16.50	16.50
24	16.86	16.86	16.86	16.86
25	17.65	17.65	17.65	17.65
26	18.04	18.04	18.04	18.04
27	18.27	18.27	18.27	18.27
28	18.51	18.51	18.51	18.51
29	18.98	18.98	18.98	18.98
30	19.59	19.59	19.59	19.59
31	19.95	19.95	19.95	19.95
32	20.19	20.19	20.19	20.19
33	20.58	20.58	20.58	20.58
34	20.94	20.94	20.94	20.94
35	21.40	21.40	21.40	21.40
36	21.62	21.62	21.62	21.62
37	21.86	21.86	21.86	21.86
38	21.88	21.88	21.88	21.88
39	21.94	21.94	21.94	21.94
40	22.33	22.33	22.33	22.33
41	22.73	22.73	22.73	22.73
42	23.07	23.07	23.07	23.07
43	23.40	23.40	23.40	23.40
44	23.47	23.47	23.47	23.47
45	23.54	23.54	23.54	23.54
46	23.93	23.93	23.93	23.93
47	24.28	24.28	24.28	24.28
48	24.74	24.74	24.74	24.74
49	24.98	24.98	24.98	24.98
50	25.55	25.55	25.55	25.55
51	26.03	26.03	26.03	26.03
52	26.76	26.76	26.76	26.76

Tunnel_1a_S				
Freq #	Frequency of Analysis (Hz)			
	SBE-E	SBE-W	SLB	SUB
53	27.19	27.19	27.19	27.19
54	27.60	27.60	27.60	27.60
55	27.94	27.94	27.94	27.94
56	28.03	28.03	28.03	28.03
57	28.44	28.44	28.44	28.44
58	28.70	28.70	28.70	28.70
59	28.76	28.76	28.76	28.76
60	28.98	28.98	28.98	28.98
61	29.49	29.49	29.49	29.49
62	29.72	29.72	29.72	29.72
63	30.03	30.03	30.03	30.03
64	30.21	30.21	30.21	30.21
65	31.04	31.04	31.04	31.04
66	31.24	31.24	31.24	31.24
67	31.46	31.46	31.46	31.46
68	31.76	31.76	31.76	31.76
69	31.85	31.85	31.85	31.85
70	32.23	32.23	32.23	32.23
71	32.32	32.32	32.32	32.32
72	32.50	32.50	32.50	32.50
73	32.71	32.71	32.71	32.71
74	32.79	32.79	32.79	32.79
75	33.02	33.02	33.02	33.02
76	33.51	33.51	33.51	33.51
77	34.06	34.06	34.06	34.06
78	34.61	34.61	34.61	34.61
79	35.69	35.69	35.69	35.69
80	36.04	36.04	36.04	36.04
81	36.61	36.61	36.61	36.61
82	36.82	36.82	36.82	36.82
83	37.07	37.07	37.07	37.07
84	37.84	37.84	37.84	37.84

Tunnel_1a_S				
Freq #	Frequency of Analysis (Hz)			
	SBE-E	SBE-W	SLB	SUB
85	38.48	38.48	38.48	38.48
86	39.69	39.69	39.69	39.69
87	39.90	39.90	39.90	39.90
88	40.22	40.22	40.22	40.22
89	41.36	41.36	41.36	41.36
90	41.74	41.74	41.74	41.74
91	42.11	42.11	42.11	42.11
92	42.72	42.72	42.72	42.72
93	43.46	43.46	43.46	43.46
94	44.73	44.73	44.73	44.73
95	45.53	45.53	45.53	45.53
96	46.53	46.53	46.53	46.53
97	47.61	47.61	47.61	47.61
98	48.65	48.65	48.65	48.65
99	49.54	49.54	49.54	49.54
100	49.74	49.74	49.74	49.74

Tunnel_1b			
Freq #	Frequency of Analysis (Hz)		
	EBE-W	ELB	EUB
1	0.01	0.01	0.01
2	1.10	0.49	1.10
3	2.20	1.10	2.20
4	3.05	2.20	3.05
5	4.03	2.56	4.03
6	4.88	3.05	4.88
7	5.80	4.03	5.80
8	6.84	4.52	6.84
9	7.57	4.88	7.57
10	8.69	5.80	8.69
11	9.77	6.84	9.77

Tunnel_1b			
Freq #	Frequency of Analysis (Hz)		
	EBE-W	ELB	EUB
12	10.35	7.57	10.35
13	10.99	8.69	10.99
14	11.60	9.77	11.60
15	12.28	10.35	12.28
16	12.77	10.99	12.77
17	13.16	11.60	13.16
18	13.49	12.28	13.49
19	13.88	12.77	13.88
20	14.50	13.16	14.50
21	15.05	13.49	15.05
22	15.69	13.88	15.69
23	16.50	14.50	16.50
24	16.86	15.05	16.86
25	17.65	15.69	17.65
26	18.04	16.50	18.04
27	18.27	16.86	18.27
28	18.51	17.65	18.51
29	18.98	18.04	18.98
30	19.59	18.27	19.59
31	19.95	18.51	19.95
32	20.19	18.98	20.19
33	20.58	19.59	20.58
34	20.94	19.95	20.94
35	21.40	20.19	21.40
36	21.62	20.58	21.62
37	21.86	20.94	21.86
38	21.88	21.40	21.88
39	21.94	21.62	21.94
40	22.33	21.86	22.33
41	22.73	21.88	22.73
42	23.07	22.33	23.07
43	23.40	22.73	23.40

Tunnel_1b			
Freq #	Frequency of Analysis (Hz)		
	EBE-W	ELB	EUB
44	23.47	23.07	23.47
45	23.54	23.40	23.54
46	23.93	23.47	23.93
47	24.28	23.54	24.28
48	24.74	23.93	24.74
49	24.98	24.28	24.98
50	25.55	24.74	25.55
51	26.03	24.98	26.03
52	26.76		26.76
53	27.19		27.19
54	27.60		27.60
55	27.94		27.94
56	28.03		28.03
57	28.44		28.44
58	28.70		28.70
59	28.76		28.76
60	28.98		28.98
61	29.49		29.49
62	29.72		29.72
63	30.03		30.03
64	30.21		30.21
65	31.04		31.04
66	31.24		31.24
67	31.46		31.46
68	31.76		31.76
69	31.85		31.85
70	32.23		32.23
71	32.32		32.32
72	32.50		32.50
73	32.71		32.71
74	32.79		32.79
75	33.02		33.02

Tunnel_1b			
Freq #	Frequency of Analysis (Hz)		
	EBE-W	ELB	EUB
76	33.51		33.51
77	34.06		34.06
78	34.61		34.61
79	35.69		35.69
80	36.04		36.04
81	36.61		36.61
82	36.82		36.82
83	37.07		37.07
84	37.84		37.84
85	38.48		38.48
86	39.69		39.69
87	39.90		39.90
88			40.22
89			41.36
90			41.74
91			42.11
92			42.72
93			43.46
94			44.73
95			45.53
96			46.53
97			47.61
98			48.65
99			49.54
100			49.74

Tunnel_UHSRS Pipe Chase			
Freq #	Frequency of Analysis (Hz)		
	EBE	ELB	EUB
1	0.01	0.01	0.01
2	1.10	1.10	1.10
3	2.20	2.20	2.20

Tunnel_UHSRS Pipe Chase			
Freq #	Frequency of Analysis (Hz)		
	EBE	ELB	EUB
4	3.05	3.05	3.05
5	4.03	4.03	4.03
6	4.88	4.88	4.88
7	5.80	5.80	5.80
8	6.84	6.84	6.84
9	7.57	7.57	7.57
10	8.69	8.69	8.69
11	9.77	9.77	9.77
12	10.35	10.35	10.35
13	10.99	10.99	10.99
14	11.60	11.60	11.60
15	12.28	12.28	12.28
16	12.77	12.77	12.77
17	13.16	13.16	13.16
18	13.49	13.49	13.49
19	13.88	13.88	13.88
20	14.50	14.50	14.50
21	15.05	15.05	15.05
22	15.69	15.69	15.69
23	16.50	16.50	16.50
24	16.86	16.86	16.86
25	17.65	17.65	17.65
26	18.04	18.04	18.04
27	18.27	18.27	18.27
28	18.51	18.51	18.51
29	18.98	18.98	18.98
30	19.59	19.59	19.59
31	19.95	19.95	19.95
32	20.19	20.19	20.19
33	20.58	20.58	20.58
34	20.94	20.94	20.94
35	21.40	21.40	21.40

Tunnel_UHSRS Pipe Chase			
Freq #	Frequency of Analysis (Hz)		
	EBE	ELB	EUB
36	21.62	21.62	21.62
37	21.86	21.86	21.86
38	21.88	21.88	21.88
39	21.94	21.94	21.94
40	22.33	22.33	22.33
41	22.73	22.73	22.73
42	23.07	23.07	23.07
43	23.40	23.40	23.40
44	23.47	23.47	23.47
45	23.54	23.54	23.54
46	23.93	23.93	23.93
47	24.28	24.28	24.28
48	24.74	24.74	24.74
49	24.98	24.98	24.98
50	25.55	25.55	25.55
51	26.03	26.03	26.03
52	26.76	26.76	26.76
53	27.19	27.19	27.19
54	27.60	27.60	27.60
55	27.94	27.94	27.94
56	28.03	28.03	28.03
57	28.44	28.44	28.44
58	28.70	28.70	28.70
59	28.76	28.76	28.76
60	28.98	28.98	28.98
61	29.49	29.49	29.49
62	29.72	29.72	29.72
63	30.03	30.03	30.03
64	30.21	30.21	30.21
65	31.04	31.04	31.04
66	31.24	31.24	31.24
67	31.46	31.46	31.46

Tunnel_UHSRS Pipe Chase			
Freq #	Frequency of Analysis (Hz)		
	EBE	ELB	EUB
68	31.76	31.76	31.76
69	31.85	31.85	31.85
70	32.23	32.23	32.23
71	32.32	32.32	32.32
72	32.50	32.50	32.50
73	32.71	32.71	32.71
74	32.79	32.79	32.79
75	33.02	33.02	33.02
76	33.51	33.51	33.51
77	34.06	34.06	34.06
78	34.61	34.61	34.61
79	35.69	35.69	35.69
80	36.04	36.04	36.04
81	36.61	36.61	36.61
82	36.82	36.82	36.82
83	37.07	37.07	37.07
84	37.84	37.84	37.84
85	38.48	38.48	38.48
86	39.69	39.69	39.69
87	39.90	39.90	39.90
88	40.22	40.22	40.22
89	41.36	41.36	41.36
90	41.74	41.74	41.74
91	42.11	42.11	42.11
92	42.72	42.72	42.72
93	43.46	43.46	43.46
94	44.73	44.73	44.73
95	45.53	45.53	45.53
96	46.53	46.53	46.53
97	47.61	47.61	47.61
98	48.65	48.65	48.65
99	49.54	49.54	49.54

Tunnel_UHSRS Pipe Chase			
Freq #	Frequency of Analysis (Hz)		
	EBE	ELB	EUB
100	49.74	49.74	49.74

Tunnel_2				
Freq #	Frequency of Analysis (Hz)			
	SBE-E	SBE-W	SLB	SUB
1	0.01	0.01	0.01	0.01
2	1.10	1.10	1.10	1.10
3	2.20	2.20	2.20	2.20
4	3.05	3.05	3.05	3.05
5	4.03	4.03	4.03	4.03
6	4.88	4.88	4.88	4.88
7	5.80	5.80	5.80	5.80
8	6.84	6.84	6.84	6.84
9	7.57	7.57	7.57	7.57
10	8.69	8.69	8.69	8.69
11	9.77	9.77	9.77	9.77
12	10.35	10.35	10.35	10.35
13	10.99	10.99	10.99	10.99
14	11.60	11.60	11.60	11.60
15	12.28	12.28	12.28	12.28
16	12.77	12.77	12.77	12.77
17	13.16	13.16	13.16	13.16
18	13.49	13.49	13.49	13.49
19	13.88	13.88	13.88	13.88
20	14.50	14.50	14.50	14.50
21	15.05	15.05	15.05	15.05
22	15.69	15.69	15.69	15.69
23	16.50	16.50	16.50	16.50
24	16.86	16.86	16.86	16.86
25	17.65	17.65	17.65	17.65
26	18.04	18.04	18.04	18.04

Tunnel_2				
Freq #	Frequency of Analysis (Hz)			
	SBE-E	SBE-W	SLB	SUB
27	18.27	18.27	18.27	18.27
28	18.51	18.51	18.51	18.51
29	18.98	18.98	18.98	18.98
30	19.59	19.59	19.59	19.59
31	19.95	19.95	19.95	19.95
32	20.19	20.19	20.19	20.19
33	20.58	20.58	20.58	20.58
34	20.94	20.94	20.94	20.94
35	21.40	21.40	21.40	21.40
36	21.62	21.62	21.62	21.62
37	21.86	21.86	21.86	21.86
38	21.88	21.88	21.88	21.88
39	21.94	21.94	21.94	21.94
40	22.33	22.33	22.33	22.33
41	22.73	22.73	22.73	22.73
42	23.07	23.07	23.07	23.07
43	23.40	23.40	23.40	23.40
44	23.47	23.47	23.47	23.47
45	23.54	23.54	23.54	23.54
46	23.93	23.93	23.93	23.93
47	24.28	24.28	24.28	24.28
48	24.74	24.74	24.74	24.74
49	24.98	24.98	24.98	24.98
50	25.55	25.55	25.55	25.55
51	26.03	26.03	26.03	26.03
52	26.76	26.76	26.76	26.76
53	27.19	27.19	27.19	27.19
54	27.60	27.60	27.60	27.60
55	27.94	27.94	27.94	27.94
56	28.03	28.03	28.03	28.03
57	28.44	28.44	28.44	28.44
58	28.70	28.70	28.70	28.70

Tunnel_2				
Freq #	Frequency of Analysis (Hz)			
	SBE-E	SBE-W	SLB	SUB
59	28.76	28.76	28.76	28.76
60	28.98	28.98	28.98	28.98
61	29.49	29.49	29.49	29.49
62	29.72	29.72	29.72	29.72
63	30.03	30.03	30.03	30.03
64	30.21	30.21	30.21	30.21
65	31.04	31.04	31.04	31.04
66	31.24	31.24	31.24	31.24
67	31.46	31.46	31.46	31.46
68	31.76	31.76	31.76	31.76
69	31.85	31.85	31.85	31.85
70	32.23	32.23	32.23	32.23
71	32.32	32.32	32.32	32.32
72	32.50	32.50	32.50	32.50
73	32.71	32.71	32.71	32.71
74	32.79	32.79	32.79	32.79
75	33.02	33.02	33.02	33.02
76	33.51	33.51	33.51	33.51
77	34.06	34.06	34.06	34.06
78	34.61	34.61	34.61	34.61
79	35.69	35.69	35.69	35.69
80	36.04	36.04	36.04	36.04
81	36.61	36.61	36.61	36.61
82	36.82	36.82	36.82	36.82
83	37.07	37.07	37.07	37.07
84	37.84	37.84	37.84	37.84
85	38.48	38.48	38.48	38.48
86	39.69	39.69	39.69	39.69
87	39.90	39.90	39.90	39.90
88	40.22	40.22	40.22	40.22
89	41.36	41.36	41.36	41.36
90	41.74	41.74	41.74	41.74

Tunnel_2				
Freq #	Frequency of Analysis (Hz)			
	SBE-E	SBE-W	SLB	SUB
91	42.11	42.11	42.11	42.11
92	42.72	42.72	42.72	42.72
93	43.46	43.46	43.46	43.46
94	44.73	44.73	44.73	44.73
95	45.53	45.53	45.53	45.53
96	46.53	46.53	46.53	46.53
97	47.61	47.61	47.61	47.61
98	48.65	48.65	48.65	48.65
99	49.54	49.54	49.54	49.54
100	49.74	49.74	49.74	49.74

5) The amplification transfer functions are interpolated using Option 2 in the ACS SASSI MOTION module input, and no smoothing of the transfer functions is applied. For each analysis, the amplitudes of the acceleration functions are plotted and inspected to check the accuracy of the interpolation and to ensure that the expected structural responses were observed. Frequencies of analyses were added if needed to improve the accuracy. Sample transfer functions for the UHSRS and the PSFSV are provided below to show the adequacy of the interpolation and smoothing used.

FSAR Part 11 Sections 3.1.3, 4.1.3 and 5.1.1 will be revised to incorporate the above information on the use of Option 2 in the ACS SASSI MOTION module input on the amplification transfer functions.

Transfer functions for UHSRS:

1. Pump Room Elevated Slab Node 7

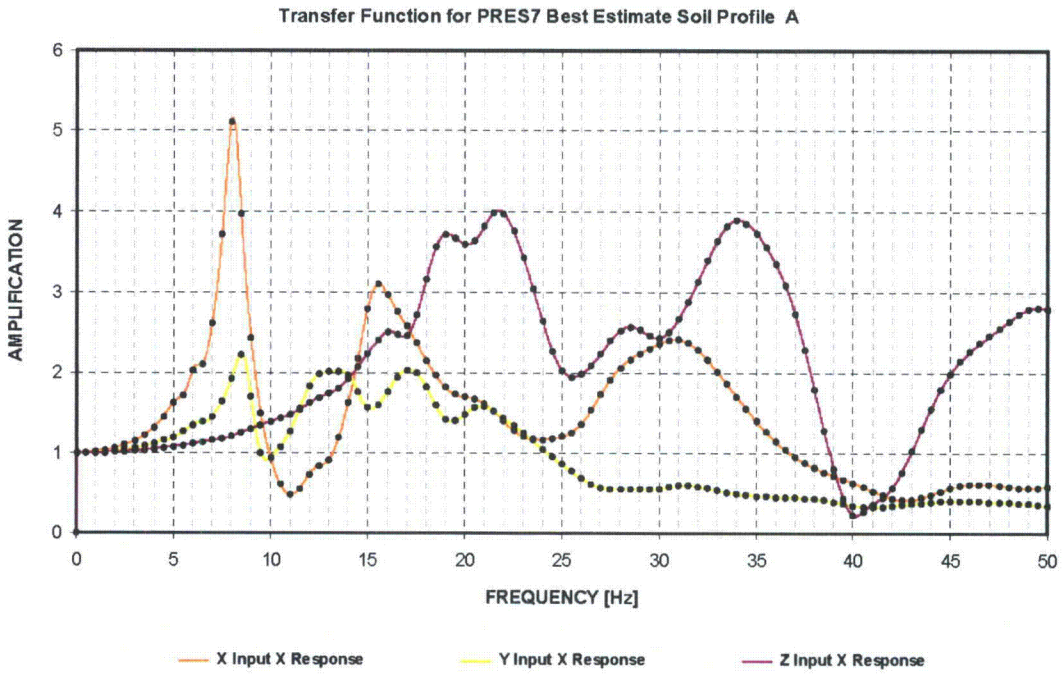

Figure 1. Transfer Function for PRES7, Soil Case Best Estimate Soil Profile A X-Direction Response

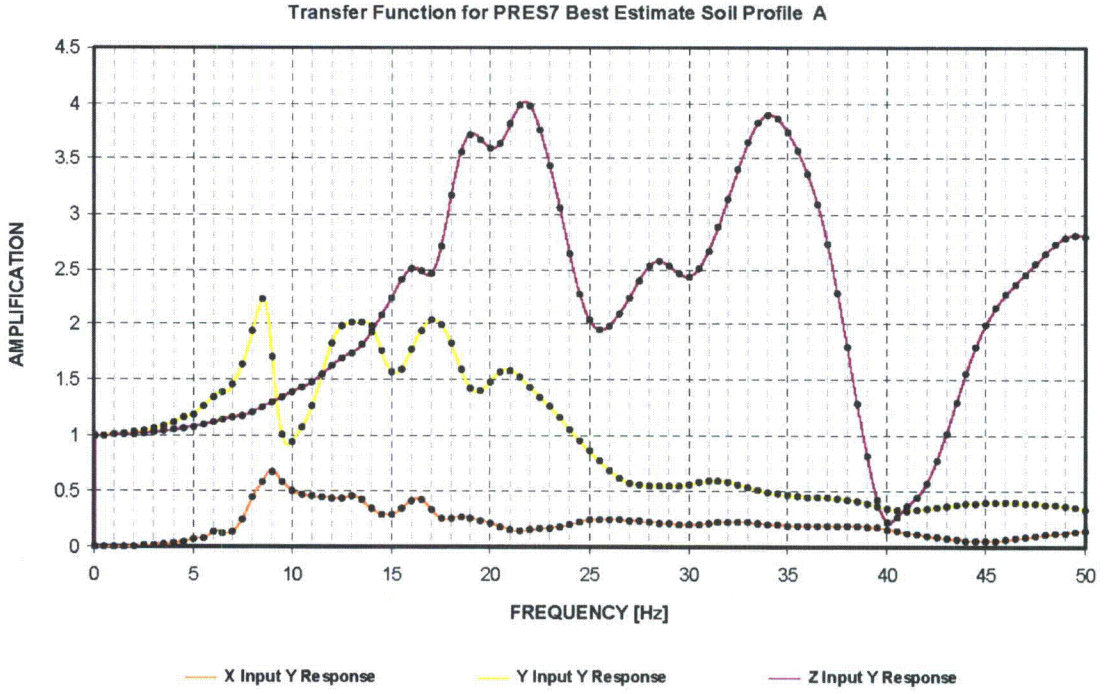

Figure 2. Transfer Function for PRES7, Soil Case Best Estimate Soil Profile A Y-Direction Response

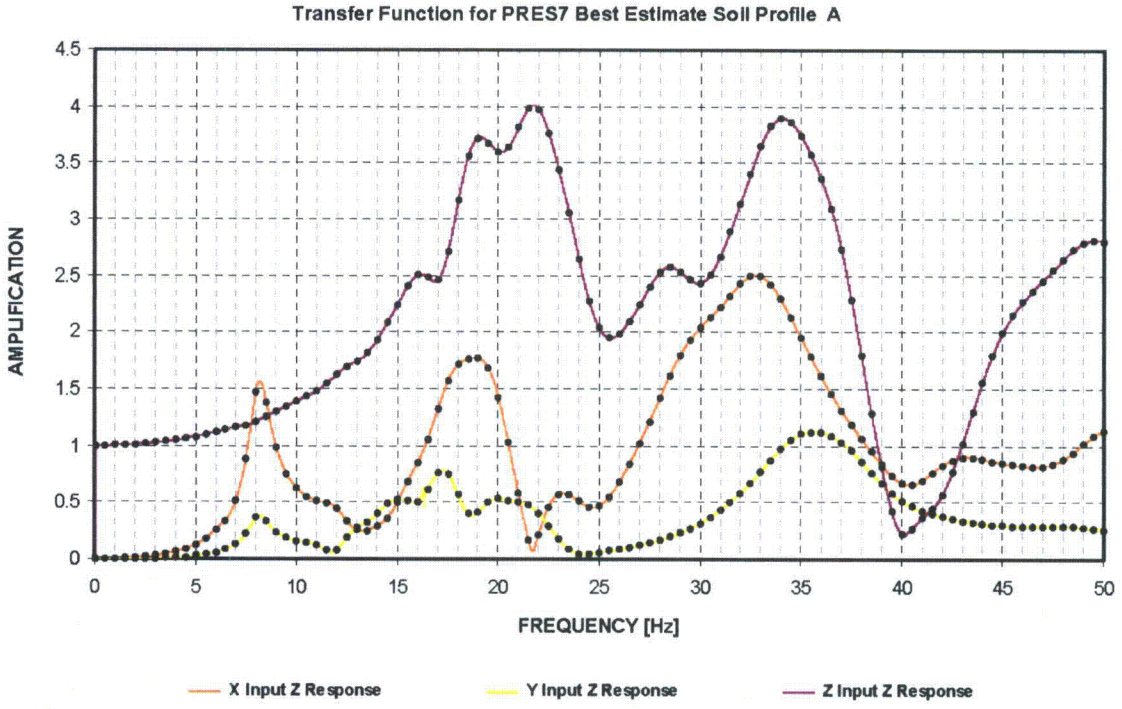

Figure 3. Transfer Function for PRES7, Soil Case Best Estimate Soil Profile A Z-Direction Response

Transfer functions for PSFSV:

1. Vault Roof Surface Node 5

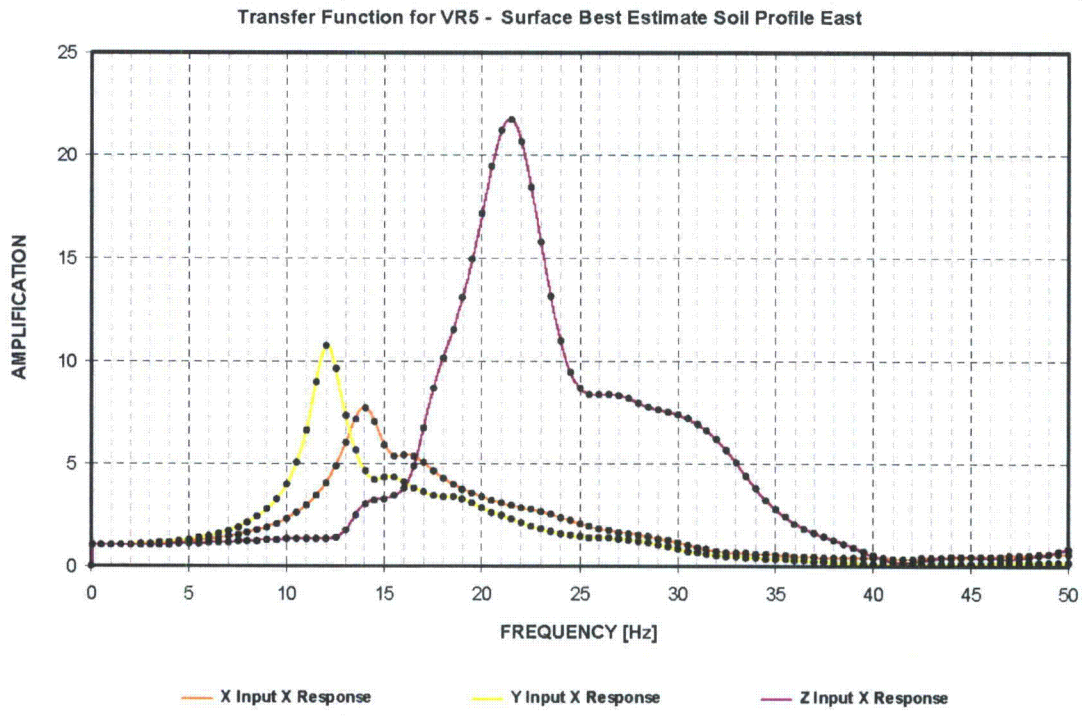

Figure 1. Transfer Function for VRF5, Soil Case Surface Best Estimate Soil Profile East X-Direction Response

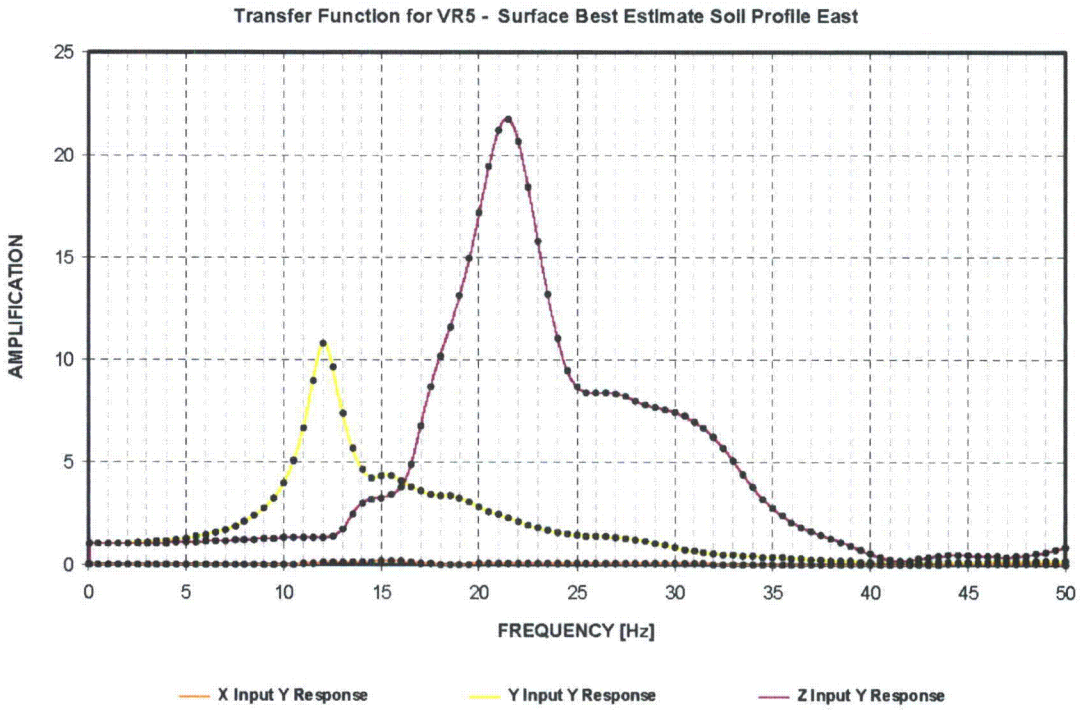

Figure 2. Transfer Function for VRF5, Soil Case Surface Best Estimate Soil Profile East Y-Direction Response

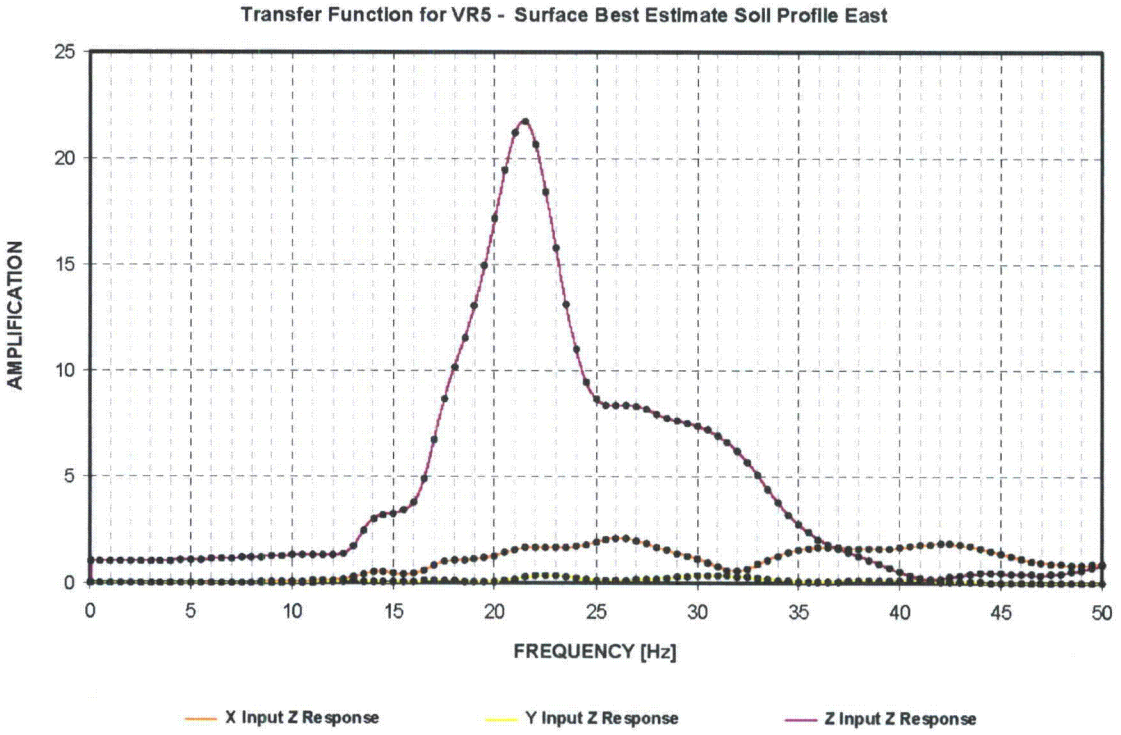

Figure 3. Transfer Function for VRF5, Soil Case Surface Best Estimate Soil Profile East Z-Direction Response

6) The soil layer thicknesses used in the SASSI analyses, and a demonstration that the layer thicknesses comply with the maximum layer thicknesses given by the "1/5 wavelength" guideline as described below. The minimum cutoff frequency was calculated based on the soil site conditions and seismic input frequency content as follows: Vs/5*soil layer thickness. The selected cutoff frequency corresponds to the lowest value calculated for all foundation soil layers. Calculated cutoff frequencies for each layer are presented below.

PSFSV – Surface Structure

Layer	Thickness (ft)	S-wave velocity (fps)				P-wave velocity (fps)			
		SLBEW	SBEE	SBEW	SUBEW	SLBEW	SBEE	SBEW	SUBEW
1	4.5	3418	4393	6975	8542	8372	10760	10869	13312
2	4	3418	4393	6975	8542	8372	10760	10869	13312
3	4	3418	4393	6975	8542	8372	10760	10869	13312
4	4	3443	4448	6975	8542	8433	10894	10869	13312
5	3.5	3483	4604	6975	8542	8531	11277	10869	13312
6	3.5	3567	4751	7115	8714	8738	11638	14811	18140
7	3.5	3795	5015	7156	8815	9296	12285	14897	18350
8	4	3948	5143	7415	9294	9670	12599	15435	19348
9	5	4185	5390	7436	9550	10251	13202	15480	19880
10	5	4305	5463	7622	9753	10544	13382	15867	20302
11	5	4247	5471	7562	9261	10402	13401	15741	19279
12	5	4080	5522	7692	9421	9995	13525	16013	19612
13	5	4067	5509	7899	9674	9961	13493	15053	18435
14	5	4305	5980	8080	9895	10545	14647	15397	18857
15	6	5193	6985	8288	10150	12719	17110	15239	18664
16	7	6052	7658	8376	10259	10782	13642	15402	18864
17	7	6972	8539	8546	10467	12422	15213	15714	19246
18	7	7129	8732	8552	10475	12701	15556	15726	19260
19	7	7129	8732	8715	10674	12701	15556	16025	19626
20	7	7159	8768	8857	10847	12754	15621	16285	19946
21	7	7217	8839	8960	10974	12858	15748	15963	19550
22	7	7349	9000	9098	11143	13092	16034	16208	19851
23	10	7453	9129	9143	11198	13279	16263	16288	19949

Layer	Thickness (ft)	S-wave frequency (Hz)				P-wave frequency (Hz)			
		SLBEW	SBEE	SBEW	SUBEW	SLBEW	SBEE	SBEW	SUBEW
1	4.5	152	195	310	380	372	478	483	592
2	4	171	220	349	427	419	538	543	666
3	4	171	220	349	427	419	538	543	666
4	4	172	222	349	427	422	545	543	666
5	3.5	199	263	399	488	487	644	621	761
6	3.5	204	271	407	498	499	665	846	1037
7	3.5	217	287	409	504	531	702	851	1049
8	4	197	257	371	465	484	630	772	967
9	5	167	216	297	382	410	528	619	795
10	5	172	219	305	390	422	535	635	812
11	5	170	219	302	370	416	536	630	771
12	5	163	221	308	377	400	541	641	784
13	5	163	220	316	387	398	540	602	737
14	5	172	239	323	396	422	586	616	754
15	6	173	233	276	338	424	570	508	622
16	7	173	219	239	293	308	390	440	539
17	7	199	244	244	299	355	435	449	550
18	7	204	249	244	299	363	444	449	550
19	7	204	249	249	305	363	444	458	561
20	7	205	251	253	310	364	446	465	570
21	7	206	253	256	314	367	450	456	559
22	7	210	257	260	318	374	458	463	567
23	10	149	183	183	224	266	325	326	399

PSFSV – Embedded Structure

Layer	Thickness (ft)	S-wave velocity (fps)				P-wave velocity (fps)			
		ELB	EBE1	EBE2	EUB	ELB	EBE1	EBE2	EUB
1	6	350	605	625	1033	1432	2271	2582	3686
2	6	388	646	703	1113	2054	3295	3677	5000
3	5.5	407	674	725	1141	2108	3436	3764	5000
4	5.585	415	693	741	1180	2155	3536	3914	5000
5	5.585	424	693	774	1244	2104	3533	3955	5000
6	5.5	410	730	776	1295	2238	3722	3978	5000
7	4.41	446	758	781	1336	2336	3865	4195	5000
8	4.5	3418	4393	6975	8542	8372	10760	10869	13312
9	4	3418	4393	6975	8542	8372	10760	10869	13312
10	4	3418	4393	6975	8542	8372	10760	10869	13312
11	4	3443	4448	6975	8542	8433	10894	10869	13312
12	3.5	3483	4604	6975	8542	8531	11277	10869	13312
13	3.5	3567	4751	7115	8714	8738	11638	14811	18140
14	3.5	3795	5015	7156	8815	9296	12285	14897	18350
15	4	3948	5143	7415	9294	9670	12599	15435	19348
16	5	4185	5390	7436	9550	10251	13202	15480	19880
17	5	4305	5463	7622	9753	10544	13382	15867	20302
18	5	4247	5471	7562	9261	10402	13401	15741	19279
19	5	4080	5522	7692	9421	9995	13525	16013	19612
20	5	4067	5509	7899	9674	9961	13493	15053	18435
21	5	4305	5980	8080	9895	10545	14647	15397	18857
22	6	5193	6985	8288	10150	12719	17110	15239	18664
23	7	6052	7658	8376	10259	10782	13642	15402	18864
24	7	6972	8539	8546	10467	12422	15213	15714	19246
25	7	7129	8732	8552	10475	12701	15556	15726	19260
26	7	7129	8732	8715	10674	12701	15556	16025	19626
27	7	7159	8768	8857	10847	12754	15621	16285	19946
28	7	7217	8839	8960	10974	12858	15748	15963	19550
29	7	7349	9000	9098	11143	13092	16034	16208	19851
30	10	7453	9129	9143	11198	13279	16263	16288	19949

Layer	Thickness (ft)	S-wave frequency (Hz)				P-wave frequency (Hz)			
		ELB	EBE1	EBE2	EUB	ELB	EBE1	EBE2	EUB
1	6	12	20	21	34	48	76	86	123
2	6	13	22	23	37	68	110	123	167
3	5.5	15	25	26	41	77	125	137	182
4	5.585	15	25	27	42	77	127	140	179
5	5.585	15	25	28	45	75	127	142	179
6	5.5	15	27	28	47	81	135	145	182
7	4.41	20	34	35	61	106	175	190	227
8	4.5	152	195	310	380	372	478	483	592
9	4	171	220	349	427	419	538	543	666
10	4	171	220	349	427	419	538	543	666
11	4	172	222	349	427	422	545	543	666
12	3.5	199	263	399	488	487	644	621	761
13	3.5	204	271	407	498	499	665	846	1037
14	3.5	217	287	409	504	531	702	851	1049
15	4	197	257	371	465	484	630	772	967
16	5	167	216	297	382	410	528	619	795
17	5	172	219	305	390	422	535	635	812
18	5	170	219	302	370	416	536	630	771
19	5	163	221	308	377	400	541	641	784
20	5	163	220	316	387	398	540	602	737
21	5	172	239	323	396	422	586	616	754
22	6	173	233	276	338	424	570	508	622
23	7	173	219	239	293	308	390	440	539
24	7	199	244	244	299	355	435	449	550
25	7	204	249	244	299	363	444	449	550
26	7	204	249	249	305	363	444	458	561
27	7	205	251	253	310	364	446	465	570
28	7	206	253	256	314	367	450	456	559
29	7	210	257	260	318	374	458	463	567
30	10	149	183	183	224	266	325	326	399

UHSRS

Layer	Thickness (ft)	S-wave velocity (fps)								P-wave velocity (fps)							
		SBEA	SBEB	SBEC	SBED	SLBA	SLBD	SUBA	SUBD	SBEA	SBEB	SBEC	SBED	SLBA	SLBD	SUBA	SUBD
1	7	6930	6930	5718	6930	5658	4298	8487	8487	10799	10799	9459	10799	8817	7950	13226	13226
2	5	6930	2705	2790	6930	5658	1782	8487	8487	10799	8726	5423	10799	8817	5000	13226	13226
3	8	6930	3110	2790	2790	5658	1874	8487	4630	10799	8875	5423	5423	8817	5000	13226	13212
4	7	2220	3110	5110	5110	1491	2089	3305	6854	7363	8875	9932	9932	5000	5961	10961	13321
5	7	2220	3110	5110	8755	1491	2089	3305	10723	7363	8875	9932	16379	5000	5961	10961	20060
6	7	2220	4160	5110	8755	1491	2794	3305	10723	7363	9158	9932	16379	5000	6151	10961	20060
7	7	2220	7460	5110	8755	1491	3810	3305	10723	7363	14810	9932	16379	5000	7405	10961	20060
8	5	2565	7460	5110	8755	1723	3810	3819	10723	10781	14810	9932	16379	7242	7405	16050	20060
9	5	2565	7460	5110	10565	1723	3810	3819	12939	10781	14810	9932	18299	7242	7405	16050	22412
10	10	4120	7460	8755	10565	2767	5562	6134	12939	9702	14810	16379	18299	6517	11042	14444	22412
11	10	6435	8800	8755	10565	4798	6561	8631	12939	14166	17470	16379	18299	10562	13026	18999	22412
12	5	7415	8800	8755	9405	5529	6561	9945	12939	15854	17470	16379	16755	11821	13026	21263	22412
13	5	8615	9850	8755	9405	6423	7148	11554	12939	16117	17296	16379	16755	12017	13373	21616	22412
14	10	9865	9850	10565	9405	8055	7679	12082	12939	17087	17296	18299	16755	13951	13681	20927	22412
15	10	8450	9850	10565	10760	6899	7667	10349	13178	15537	17296	18299	18894	12686	14097	19029	23140
16	10	9040	9390	10565	10760	7381	7667	11072	13178	17227	17266	18299	18894	14066	14097	21099	23140
17	25	9200	7675	10565	10760	7512	6267	11268	13178	17212	15237	18299	18894	14053	12441	21080	23140

Layer	Thickness (ft)	S-wave frequency (Hz)								P-wave frequency (Hz)							
		SBEA	SBEB	SBEC	SBED	SLBA	SLBD	SUBA	SUBD	SBEA	SBEB	SBEC	SBED	SLBA	SLBD	SUBA	SUBD
1	7	198	198	163	198	162	123	242	242	309	309	270	309	252	227	378	378
2	5	277	108	112	277	226	71	339	339	432	349	217	432	353	200	529	529
3	8	173	78	70	70	141	47	212	116	270	222	136	136	220	125	331	330
4	7	63	89	146	146	.43	60	94	196	210	254	284	284	143	170	313	381
5	7	63	89	146	250	43	60	94	306	210	254	284	468	143	170	313	573
6	7	63	119	146	250	43	80	94	306	210	262	284	468	143	176	313	573
7	7	63	213	146	250	43	109	94	306	210	423	284	468	143	212	313	573
8	5	103	298	204	350	69	152	153	429	431	592	397	655	290	296	642	802
9	5	103	298	204	423	69	152	153	518	431	592	397	732	290	296	642	896
10	10	82	149	175	211	55	111	123	259	194	296	328	366	130	221	289	448
11	10	129	176	175	211	96	131	173	259	283	349	328	366	211	261	380	448
12	5	297	352	350	376	221	262	398	518	634	699	655	670	473	521	851	896
13	5	345	394	350	376	257	286	462	518	645	692	655	670	481	535	865	896
14	10	197	197	211	188	161	154	242	259	342	346	366	335	279	274	419	448
15	10	169	197	211	215	138	153	207	264	311	346	366	378	254	282	381	463
16	10	181	188	211	215	148	153	221	264	345	345	366	378	281	282	422	463
17	25	74	61	85	86	60	50	90	105	138	122	146	151	112	100	169	185

ESWPT

Details of soil deposit modeling including soil layer thicknesses are presented in the following tables.

Layer	Thickness	Tunnel_ 1a_N					
		S-wave velocity (fps)			P-wave velocity (fps)		
		EBE	EUB	ELB	EBE	EUB	ELB
1	3.31	712	1098	423	1333	2054	792
2	3.31	693	1134	389	1296	2122	728
3	3.32	747	1180	417	3140	4328	1755
4	3.31	781	1263	450	3982	5000	2295
5	3.33	789	1285	463	4024	5000	2360
6	3.34	798	1309	477	4068	5000	2433
7	3.33	838	1380	476	4273	5000	2428
8	3.34	834	1365	484	4250	5000	2469
9	3.33	842	1414	492	4292	5000	2507
10	4.02	852	1468	490	4347	5000	2501
11	4.02	852	1468	490	4347	5000	2501
12	4.02	852	1468	490	4347	5000	2501
13	4.02	852	1468	490	4347	5000	2501
14	2	3785	5624	2187	9389	13952	6363
15	3	3785	5624	2187	9389	13952	6363
16	3	6628	8889	2187	13659	18319	6363
17	3	6628	8889	2187	13659	18319	6363
18	3	5397	7238	2187	11954	16033	6363
19	3	5397	7238	3345	11954	16033	7152
20	3	5397	7238	3345	11954	16033	7152
21	4	5397	7238	5831	11954	16033	11575
22	5	9145	11200	5831	16650	20392	11575
23	5	9145	11200	5831	16650	20392	11575
24	5	9145	11200	5831	16650	20392	11575
25	5	9145	11200	5831	16650	20392	11575
26	10	9145	11200	5831	16650	20392	11575
27	10	9145	11200	6250	16650	20392	12519
28	10	10064	12326	6250	17773	21767	12519
29	10	10064	12326	6250	17773	21767	12519
30	10	10064	12326	6880	17773	21767	12803
31	10	10064	12326	6880	17773	21767	12803
32	10	10064	12326	6880	17773	21767	12803
33	10	10047	12305	7421	17846	21857	13468
34	10	10047	12305	7421	17846	21857	13468
35	10	10047	12305	7421	17846	21857	13468
36	10	10047	12305	7421	17846	21857	13468
37	10	10047	12305	7512	17846	21857	14053
38	20	9200	11268	7512	17212	21080	14053
39	20	9200	11268	7512	17212	21080	14053
40	20	9200	11268	7512	17212	21080	14053
41	20	9200	11268	7512	17212	21080	14053
42	20	9200	11268	7512	17212	21080	14053

Layer	Thickness	Tunnel_1a_S							
		S-wave velocity (fps)				P-wave velocity (fps)			
		SBE-E	SBE-W	SLB	SUB	SBE-E	SBE-W	SLB	SUB
1	3.5	4393	6975	3418	8542	10760	10869	8372	13312
2	4	4393	6975	3418	8542	10760	10869	8372	13312
3	4	4393	6975	3418	8542	10760	10869	8372	13312
4	4	4448	6975	3443	8542	10894	10869	8433	13312
5	3.5	4604	6975	3483	8542	11277	10869	8531	13312
6	3.5	4751	7115	3567	8714	11638	14811	8738	18140
7	3.5	5015	7156	3795	8815	12285	14897	9296	18350
8	4	5143	7415	3948	9294	12599	15435	9670	19348
9	5	5390	7436	4185	9550	13202	15480	10251	19880
10	5	5463	7622	4305	9753	13382	15867	10544	20302
11	5	5471	7562	4247	9261	13401	15741	10402	19279
12	5	5522	7692	4080	9421	13525	16013	9995	19612
13	5	5509	7899	4067	9674	13493	15053	9961	18435
14	5	5980	8080	4305	9895	14647	15397	10545	18857
15	6	6985	8288	5193	10150	17110	15239	12719	18664
16	7	7658	8376	6052	10259	13642	15402	10782	18864
17	7	8539	8546	6972	10467	15213	15714	12422	19246
18	7	8732	8552	7129	10475	15556	15726	12701	19260
19	7	8732	8715	7129	10674	15556	16025	12701	19626
20	7	8768	8857	7159	10847	15621	16285	12754	19946
21	7	8839	8960	7217	10974	15748	15963	12858	19550
22	7	9000	9098	7349	11143	16034	16208	13092	19851
23	10	9129	9143	7453	11198	16263	16288	13279	19949
24	25	9129	9143	7453	11198	16263	16288	13279	19949
25	25	9129	9143	7453	11198	16263	16288	13279	19949
26	25	9129	9143	7453	11198	16263	16288	13279	19949
27	25	9129	9143	7453	11198	16263	16288	13279	19949
28	25	9129	9143	7453	11198	16263	16288	13279	19949
29	25	9129	9143	7453	11198	16263	16288	13279	19949

Layer	Thickness	Tunnel_1b					
		S-wave velocity (fps)			P-wave velocity (fps)		
		EBE-W	ELB	EUB	EBE-W	ELB	EUB
1	4.42	652	414	1107	1220	775	2070
2	4.42	651	402	1156	1629	1003	2788
3	4.41	711	442	1243	3625	2256	5000
4	4.17	746	466	1290	3805	2374	5000
5	4.17	769	477	1336	3922	2431	5000
6	4.17	785	479	1376	4001	2444	5000
7	4.16	830	492	1400	4233	2509	5000
8	4.02	848	490	1468	4326	2501	5000
9	4.02	848	490	1468	4326	2501	5000
10	4.02	848	490	1468	4326	2501	5000
11	4.02	848	490	1468	4326	2501	5000
12	3	3066	2187	5624	8918	6363	13952
13	3	3066	2187	5624	8918	6363	13952
14	4	3066	2187	8889	8918	6363	18319
15	4	3066	2187	8889	8918	6363	18319
16	5	3066	2187	7238	8918	6363	16033
17	3	4610	3345	7238	9856	7152	16033
18	3	4610	3345	7238	9856	7152	16033
19	3	7820	5831	7238	15525	11575	16033
20	3	7820	5831	11200	15525	11575	20392
21	5	7820	5831	11200	15525	11575	20392
22	5	7820	5831	11200	15525	11575	20392
23	5	7820	5831	11200	15525	11575	20392
24	5	7820	5831	11200	15525	11575	20392
25	10	7655	6250	11200	15333	12519	20392
26	10	7655	6250	12326	15333	12519	21767
27	10	7655	6250	12326	15333	12519	21767
28	10	8426	6880	12326	15680	12803	21767
29	10	8426	6880	12326	15680	12803	21767
30	10	8426	6880	12326	15680	12803	21767
31	10	9089	7421	12305	16495	13468	21857
32	10	9089	7421	12305	16495	13468	21857
33	10	9089	7421	12305	16495	13468	21857
34	10	9089	7421	12305	16495	13468	21857
35	20	9200	7512	12305	17212	14053	21857
36	20	9200	7512	11268	17212	14053	21080
37	20	9200	7512	11268	17212	14053	21080
38	20	9200	7512	11268	17212	14053	21080
39	20	9200	7512	11268	17212	14053	21080
40	20	9200	7512	11268	17212	14053	21080
41	20	9200	7512	11268	17212	14053	21080

Layer	Thickness	Tunnel_1b					
		S-wave velocity (fps)			P-wave velocity (fps)		
		EBE-W	ELB	EUB	EBE-W	ELB	EUB
42	20	9200	7512	11268	17212	14053	21080
43	20	9200	7512	11268	17212	14053	21080
44	20	9200	7512	11268	17212	14053	21080
45	20	9200	7512	11268	17212	14053	21080
46	20	9200	7512	11268	17212	14053	21080
47	20	9200	7512	11268	17212	14053	21080
48	20	9200	7512	11268	17212	14053	21080
49	20	9200	7512	11268	17212	14053	21080
50	20	9200	7512	11268	17212	14053	21080
51	20	9200	7512	11268	17212	14053	21080
52	20	9200	7512	11268	17212	14053	21080
53	20	9200	7512	11268	17212	14053	21080

Layer	Thickness	Tunnel_UHSRS PipeChase					
		S-wave velocity (fps)			P-wave velocity (fps)		
		EBE	ELB	EUB	EBE	ELB	EUB
1	3	908	608	1355	2333	1561	3488
2	4	1423	969	2089	4484	3055	6581
3	3	3762	2666	5307	9333	6615	13167
4	3	3762	2666	5307	9333	6615	13167
5	3	3762	2666	5307	9333	6615	13167
6	3	3762	2666	5307	9333	6615	13167
7	4	3762	2666	5307	9333	6615	13167
8	4	6628	4942	8889	13659	10184	18319
9	4	6628	4942	8889	13659	10184	18319
10	4	6628	4942	8889	13659	10184	18319
11	4	6628	4942	8889	13659	10184	18319
12	4	6628	4942	8889	13659	10184	18319
13	4	6628	4942	8889	13659	10184	18319
14	5	5397	4024	7238	11954	8913	16033
15	5	5397	4024	7238	11954	8913	16033
16	5	5397	4024	7238	11954	8913	16033
17	5	5397	4024	7238	11954	8913	16033
18	5	5397	4024	7238	11954	8913	16033
19	5	5397	4024	7238	11954	8913	16033
20	5	5397	4024	7238	11954	8913	16033
21	5	5397	4024	7238	11954	8913	16033
22	5	5397	4024	7238	11954	8913	16033
23	5	5397	4024	7238	11954	8913	16033
24	5	9087	7420	11129	16598	13552	20329
25	5	9087	7420	11129	16598	13552	20329
26	5	9087	7420	11129	16598	13552	20329
27	5	9087	7420	11129	16598	13552	20329
28	5	10161	8296	12445	17719	14467	21701
29	5	10161	8296	12445	17719	14467	21701
30	5	10161	8296	12445	17719	14467	21701
31	5	10161	8296	12445	17719	14467	21701
32	5	9807	8007	12011	17742	14486	21729
33	5	9807	8007	12011	17742	14486	21729
34	10	10114	8258	12387	17835	14563	21844
35	10	10114	8258	12387	17835	14563	21844

Layer	Thickness	Tunnel_2							
		S-wave velocity (fps)				P-wave velocity (fps)			
		SBE-E	SBE-W	SLB	SUB	SBE-E	SBE-W	SLB	SUB
1	3.5	4393	6975	3418	8542	10760	10869	8372	13312
2	4	4393	6975	3418	8542	10760	10869	8372	13312
3	4	4393	6975	3418	8542	10760	10869	8372	13312
4	4	4448	6975	3443	8542	10894	10869	8433	13312
5	3.5	4604	6975	3483	8542	11277	10869	8531	13312
6	3.5	4751	7115	3567	8714	11638	14811	8738	18140
7	3.5	5015	7156	3795	8815	12285	14897	9296	18350
8	4	5143	7415	3948	9294	12599	15435	9670	19348
9	5	5390	7436	4185	9550	13202	15480	10251	19880
10	5	5463	7622	4305	9753	13382	15867	10544	20302
11	5	5471	7562	4247	9261	13401	15741	10402	19279
12	5	5522	7692	4080	9421	13525	16013	9995	19612
13	5	5509	7899	4067	9674	13493	15053	9961	18435
14	5	5980	8080	4305	9895	14647	15397	10545	18857
15	6	6985	8288	5193	10150	17110	15239	12719	18664
16	7	7658	8376	6052	10259	13642	15402	10782	18864
17	7	8539	8546	6972	10467	15213	15714	12422	19246
18	7	8732	8552	7129	10475	15556	15726	12701	19260
19	7	8732	8715	7129	10674	15556	16025	12701	19626
20	7	8768	8857	7159	10847	15621	16285	12754	19946
21	7	8839	8960	7217	10974	15748	15963	12858	19550
22	7	9000	9098	7349	11143	16034	16208	13092	19851
23	10	9129	9143	7453	11198	16263	16288	13279	19949
24	25	9129	9143	7453	11198	16263	16288	13279	19949
25	25	9129	9143	7453	11198	16263	16288	13279	19949
26	25	9129	9143	7453	11198	16263	16288	13279	19949
27	25	9129	9143	7453	11198	16263	16288	13279	19949
28	25	9129	9143	7453	11198	16263	16288	13279	19949
29	25	9129	9143	7453	11198	16263	16288	13279	19949

Layer	Thickness	Tunnel_1a_N					
		S-wave frequency (Hz)			P-wave frequency (Hz)		
		EBE	EUB	ELB	EBE	EUB	ELB
1	3.31	43	66	26	81	124	48
2	3.31	42	69	24	78	128	44
3	3.32	45	71	25	189	261	106
4	3.31	47	76	27	241	302	139
5	3.33	47	77	28	242	300	142
6	3.34	48	78	29	244	299	146
7	3.33	50	83	29	257	300	146
8	3.34	50	82	29	254	299	148
9	3.33	51	85	30	258	300	151
10	4.02	42	73	24	216	249	124
11	4.02	42	73	24	216	249	124
12	4.02	42	73	24	216	249	124
13	4.02	42	73	24	216	249	124
14	2	379	562	219	939	1395	636
15	3	252	375	146	626	930	424
16	3	442	593	146	911	1221	424
17	3	442	593	146	911	1221	424
18	3	360	483	146	797	1069	424
19	3	360	483	223	797	1069	477
20	3	360	483	223	797	1069	477
21	4	270	362	292	598	802	579
22	5	366	448	233	666	816	463
23	5	366	448	233	666	816	463
24	5	366	448	233	666	816	463
25	5	366	448	233	666	816	463
26	10	183	224	117	333	408	232
27	10	183	224	125	333	408	250
28	10	201	247	125	355	435	250
29	10	201	247	125	355	435	250
30	10	201	247	138	355	435	256
31	10	201	247	138	355	435	256
32	10	201	247	138	355	435	256
33	10	201	246	148	357	437	269
34	10	201	246	148	357	437	269
35	10	201	246	148	357	437	269
36	10	201	246	148	357	437	269
37	10	201	246	150	357	437	281
38	20	92	113	75	172	211	141
39	20	92	113	75	172	211	141
40	20	92	113	75	172	211	141
41	20	92	113	75	172	211	141
42	20	92	113	75	172	211	141

Layer	Thickness	Tunnel_1a_S							
		S-wave frequency (Hz)				P-wave frequency (Hz)			
		SBE-E	SBE-W	SLB	SUB	SBE-E	SBE-W	SLB	SUB
1	3.5	251	399	195	488	615	621	478	761
2	4	220	349	171	427	538	543	419	666
3	4	220	349	171	427	538	543	419	666
4	4	222	349	172	427	545	543	422	666
5	3.5	263	399	199	488	644	621	487	761
6	3.5	271	407	204	498	665	846	499	1037
7	3.5	287	409	217	504	702	851	531	1049
8	4	257	371	197	465	630	772	484	967
9	5	216	297	167	382	528	619	410	795
10	5	219	305	172	390	535	635	422	812
11	5	219	302	170	370	536	630	416	771
12	5	221	308	163	377	541	641	400	784
13	5	220	316	163	387	540	602	398	737
14	5	239	323	172	396	586	616	422	754
15	6	233	276	173	338	570	508	424	622
16	7	219	239	173	293	390	440	308	539
17	7	244	244	199	299	435	449	355	550
18	7	249	244	204	299	444	449	363	550
19	7	249	249	204	305	444	458	363	561
20	7	251	253	205	310	446	465	364	570
21	7	253	256	206	314	450	456	367	559
22	7	257	260	210	318	458	463	374	567
23	10	183	183	149	224	325	326	266	399
24	25	73	73	60	90	130	130	106	160
25	25	73	73	60	90	130	130	106	160
26	25	73	73	60	90	130	130	106	160
27	25	73	73	60	90	130	130	106	160
28	25	73	73	60	90	130	130	106	160
29	25	73	73	60	90	130	130	106	160

Layer	Thickness	Tunnel_1b					
		S-wave frequency (Hz)			P-wave frequency (Hz)		
		EBE-W	ELB	EUB	EBE-W	ELB	EUB
1	4.42	30	19	50	55	35	94
2	4.42	29	18	52	74	45	126
3	4.41	32	20	56	164	102	227
4	4.17	36	22	62	182	114	240
5	4.17	37	23	64	188	117	240
6	4.17	38	23	66	192	117	240
7	4.16	40	24	67	204	121	240
8	4.02	42	24	73	215	124	249
9	4.02	42	24	73	215	124	249
10	4.02	42	24	73	215	124	249
11	4.02	42	24	73	215	124	249
12	3	204	146	375	595	424	930
13	3	204	146	375	595	424	930
14	4	153	109	444	446	318	916
15	4	153	109	444	446	318	916
16	5	123	87	290	357	255	641
17	3	307	223	483	657	477	1069
18	3	307	223	483	657	477	1069
19	3	521	389	483	1035	772	1069
20	3	521	389	747	1035	772	1359
21	5	313	233	448	621	463	816
22	5	313	233	448	621	463	816
23	5	313	233	448	621	463	816
24	5	313	233	448	621	463	816
25	10	153	125	224	307	250	408
26	10	153	125	247	307	250	435
27	10	153	125	247	307	250	435
28	10	169	138	247	314	256	435
29	10	169	138	247	314	256	435
30	10	169	138	247	314	256	435
31	10	182	148	246	330	269	437
32	10	182	148	246	330	269	437
33	10	182	148	246	330	269	437
34	10	182	148	246	330	269	437
35	20	92	75	123	172	141	219
36	20	92	75	113	172	141	211
37	20	92	75	113	172	141	211
38	20	92	75	113	172	141	211
39	20	92	75	113	172	141	211
40	20	92	75	113	172	141	211
41	20	92	75	113	172	141	211

Layer	Thickness	Tunnel_1b					
		S-wave frequency (Hz)			P-wave frequency (Hz)		
		EBE-W	ELB	EUB	EBE-W	ELB	EUB
42	20	92	75	113	172	141	211
43	20	92	75	113	172	141	211
44	20	92	75	113	172	141	211
45	20	92	75	113	172	141	211
46	20	92	75	113	172	141	211
47	20	92	75	113	172	141	211
48	20	92	75	113	172	141	211
49	20	92	75	113	172	141	211
50	20	92	75	113	172	141	211
51	20	92	75	113	172	141	211
52	20	92	75	113	172	141	211
53	20	92	75	113	172	141	211

Layer	Thickness	Tunnel_UHSRS PipeChase					
		S-wave frequency (Hz)			P-wave frequency (Hz)		
		EBE	ELB	EUB	EBE	ELB	EUB
1	3	61	41	90	156	104	233
2	4	71	48	104	224	153	329
3	3	251	178	354	622	441	878
4	3	251	178	354	622	441	878
5	3	251	178	354	622	441	878
6	3	251	178	354	622	441	878
7	4	188	133	265	467	331	658
8	4	331	247	444	683	509	916
9	4	331	247	444	683	509	916
10	4	331	247	444	683	509	916
11	4	331	247	444	683	509	916
12	4	331	247	444	683	509	916
13	4	331	247	444	683	509	916
14	5	216	161	290	478	357	641
15	5	216	161	290	478	357	641
16	5	216	161	290	478	357	641
17	5	216	161	290	478	357	641
18	5	216	161	290	478	357	641
19	5	216	161	290	478	357	641
20	5	216	161	290	478	357	641
21	5	216	161	290	478	357	641
22	5	216	161	290	478	357	641
23	5	216	161	290	478	357	641
24	5	363	297	445	664	542	813
25	5	363	297	445	664	542	813
26	5	363	297	445	664	542	813
27	5	363	297	445	664	542	813
28	5	406	332	498	709	579	868
29	5	406	332	498	709	579	868
30	5	406	332	498	709	579	868
31	5	406	332	498	709	579	868
32	5	392	320	480	710	579	869
33	5	392	320	480	710	579	869
34	10	202	165	248	357	291	437
35	10	202	165	248	357	291	437

Layer	Thickness	Tunnel_2							
		S-wave frequency (Hz)				P-wave frequency (Hz)			
		SBE-E	SBE-W	SLB	SUB	SBE-E	SBE-W	SLB	SUB
1	3.5	251	399	195	488	615	621	478	761
2	4	220	349	171	427	538	543	419	666
3	4	220	349	171	427	538	543	419	666
4	4	222	349	172	427	545	543	422	666
5	3.5	263	399	199	488	644	621	487	761
6	3.5	271	407	204	498	665	846	499	1037
7	3.5	287	409	217	504	702	851	531	1049
8	4	257	371	197	465	630	772	484	967
9	5	216	297	167	382	528	619	410	795
10	5	219	305	172	390	535	635	422	812
11	5	219	302	170	370	536	630	416	771
12	5	221	308	163	377	541	641	400	784
13	5	220	316	163	387	540	602	398	737
14	5	239	323	172	396	586	616	422	754
15	6	233	276	173	338	570	508	424	622
16	7	219	239	173	293	390	440	308	539
17	7	244	244	199	299	435	449	355	550
18	7	249	244	204	299	444	449	363	550
19	7	249	249	204	305	444	458	363	561
20	7	251	253	205	310	446	465	364	570
21	7	253	256	206	314	450	456	367	559
22	7	257	260	210	318	458	463	374	567
23	10	183	183	149	224	325	326	266	399
24	25	73	73	60	90	130	130	106	160
25	25	73	73	60	90	130	130	106	160
26	25	73	73	60	90	130	130	106	160
27	25	73	73	60	90	130	130	106	160
28	25	73	73	60	90	130	130	106	160
29	25	73	73	60	90	130	130	106	160

7) As stated in FSAR Part 11 Section 2.2, a ten layer half-space is used in the SASSI analysis. Section 2.2 will be expanded to explain that viscous dashpots are added at the base of the layers that simulate the half-space. Each half-space layer has a thickness of 1.5 Vs / f / number of half-space layers, where Vs is the shear wave velocity of the half-space and f is the frequency of analysis.

   FSAR Part 11 Section 2.2 will be revised to incorporate the above information.

8) The ESWPT is designed to resist in-plane shear due to longitudinal lateral demand, out-of-plane flexure and shear in walls for transverse lateral demand, and vertical demand resulting in out-of-plane flexure and shear in the roof slab and at the slab wall intersections. Adequate numbers of locations are selected to capture the seismic performance of the ESWPT.

   Similarly, for UHS and PSFSV, critical locations are selected based on the expected seismic behavior of these structures. The selected locations are sufficient to represent various locations throughout the building and include responses at peripheral locations to detect rocking and torsion.

   The selected locations for each structure are tabulated below.

PSFSV - Power Source Fuel Storage Vaults - Surface Structure

Node Name	Component	Node Number	X- Ordinate	Y- Ordinate	Z- Ordinate
VBM1	Basemat	1182	0	0	-9.67
VBM2		1194	0	86	-9.67
VBM3		1363	81.75	86	-9.67
VBM4		1351	81.75	0	-9.67
VBM5		1210	12.83	15.5	-9.67
VBM6		1262	36.83	15.5	-9.67
VBM7		1314	60.83	15.5	-9.67
VBM8		1214	12.83	43	-9.67
VBM9		1266	36.83	43	-9.67
VBM10		1318	60.83	43	-9.67
VBM11		1218	12.83	70.5	-9.67
VBM12		1270	36.83	70.5	-9.67
VBM13		1322	60.83	70.5	-9.67
VRF1	Roof	1723	0	0	20.39
VRF2		1735	0	86	20.39
VRF3		1904	81.75	86	20.39
VRF4		1892	81.75	0	20.39
VRF5		1807	36.83	43	20.39
VRF6		1809	36.83	56.75	20.39

Node Name	Component	Node Number	X- Ordinate	Y- Ordinate	Z- Ordinate
VSW1	South Wall	1723	0	0	20.39
VSW2		1729	0	43	20.39
VSW3		1735	0	86	20.39
VSW4		1651	0	15.5	11.36
VSW5		1655	0	43	11.36
VSW6		1659	0	70.5	11.36
VSW7		1182	0	0	-9.67
VSW8		1188	0	43	-9.67
VSW9		1194	0	86	-9.67
VNW1	North Wall	1892	81.75	0	20.39
VNW2		1898	81.75	43	20.39
VNW3		1904	81.75	86	20.39
VNW4		1712	81.75	15.5	11.36
VNW5		1716	81.75	43	11.36
VNW6		1720	81.75	70.5	11.36
VNW7		1612	81.75	7.5	2.33
VNW8		1619	81.75	56.75	2.33
VNW9		1351	81.75	0	-9.67
VNW10		1357	81.75	43	-9.67
VNW11		1363	81.75	86	-9.67
VWEW1	West External Wall	1735	0	86	20.39
VWEW2		1813	36.83	86	20.39
VWEW3		1904	81.75	86	20.39
VWEW4		1673	18.83	86	11.36
VWEW5		1685	36.83	86	11.36
VWEW6		1697	54.83	86	11.36
VWEW7		1194	0	86	-9.67
VWEW8		1272	36.83	86	-9.67
VWEW9		1363	81.75	86	-9.67
VWIW1	West Internal Wall	1731	0	56.75	20.39
VWIW2		1809	36.83	56.75	20.39
VWIW3		1900	81.75	56.75	20.39
VWIW4		1672	18.83	56.75	11.36
VWIW5		1684	36.83	56.75	11.36
VWIW6		1696	54.83	56.75	11.36
VWIW7		1190	0	56.75	-9.67
VWIW8		1268	36.83	56.75	-9.67
VWIW9		1359	81.75	56.75	-9.67

Node Name	Component	Node Number	X- Ordinate	Y- Ordinate	Z- Ordinate
VEIW1	East Internal Wall	1727	0	29.25	20.39
VEIW2		1805	36.83	29.25	20.39
VEIW3		1896	81.75	29.25	20.39
VEIW4		1671	18.83	29.25	11.36
VEIW5		1683	36.83	29.25	11.36
VEIW6		1695	54.83	29.25	11.36
VEIW7		1186	0	29.25	-9.67
VEIW8		1264	36.83	29.25	-9.67
VEIW9		1355	81.75	29.25	-9.67
VEEW1	East External Wall	1723	0	0	20.39
VEEW2		1801	36.83	0	20.39
VEEW3		1892	81.75	0	20.39
VEEW4		1670	18.83	0	11.36
VEEW5		1682	36.83	0	11.36
VEEW6		1694	54.83	0	11.36
VEEW7		1182	0	0	-9.67
VEEW8		1260	36.83	0	-9.67
VEEW9		1351	81.75	0	-9.67

PSFSV - Power Source Fuel Storage Vaults - Embedded Structure

Node Name	Component	Node Number	X- Ordinate	Y- Ordinate	Z- Ordinate
VBM1	Basemat	3609	0	0	-9.67
VBM2		3813	0	86	-9.67
VBM3		3826	81.75	86	-9.67
VBM4		3622	81.75	0	-9.67
VBM5		3645	12.83	15.5	-9.67
VBM6		3649	36.83	15.5	-9.67
VBM7		3653	60.83	15.5	-9.67
VBM8		3713	12.83	43	-9.67
VBM9		3717	36.83	43	-9.67
VBM10		3721	60.83	43	-9.67
VBM11		3781	12.83	70.5	-9.67
VBM12		3785	36.83	70.5	-9.67
VBM13		3789	60.83	70.5	-9.67
VRF1	Roof	4649	0	0	20.39
VRF2		4817	0	86	20.39
VRF3		4830	81.75	86	20.39
VRF4		4662	81.75	0	20.39
VRF5		4739	36.83	43	20.39
VRF6		4767	36.83	56.75	20.39

Node Name	Component	Node Number	X- Ordinate	Y- Ordinate	Z- Ordinate
VSW1	South Wall	4649	0	0	20.39
VSW2		4733	0	43	20.39
VSW3		4817	0	86	20.39
VSW4		4453	0	15.5	11.36
VSW5		4509	0	43	11.36
VSW6		4565	0	70.5	11.36
VSW7		3609	0	0	-9.67
VSW8		3711	0	43	-9.67
VSW9		3813	0	86	-9.67
VNW1	North Wall	4662	81.75	0	20.39
VNW2		4746	81.75	43	20.39
VNW3		4830	81.75	86	20.39
VNW4		4466	81.75	15.5	11.36
VNW5		4522	81.75	43	11.36
VNW6		4578	81.75	70.5	11.36
VNW7		4183	81.75	7.5	2.33
VNW8		4302	81.75	56.75	2.33
VNW9		3622	81.75	0	-9.67
VNW10		3724	81.75	43	-9.67
VNW11		3826	81.75	86	-9.67
VWEW1	West External Wall	4817	0	86	20.39
VWEW2		4823	36.83	86	20.39
VWEW3		4830	81.75	86	20.39
VWEW4		4596	18.83	86	11.36
VWEW5		4599	36.83	86	11.36
VWEW6		4602	54.83	86	11.36
VWEW7		3813	0	86	-9.67
VWEW8		3819	36.83	86	-9.67
VWEW9		3826	81.75	86	-9.67
VWIW1	West Internal Wall	4761	0	56.75	20.39
VWIW2		4767	36.83	56.75	20.39
VWIW3		4774	81.75	56.75	20.39
VWIW4		4540	18.83	56.75	11.36
VWIW5		4543	36.83	56.75	11.36
VWIW6		4546	54.83	56.75	11.36
VWIW7		3745	0	56.75	-9.67
VWIW8		3751	36.83	56.75	-9.67
VWIW9		3758	81.75	56.75	-9.67

Node Name	Component	Node Number	X- Ordinate	Y- Ordinate	Z- Ordinate
VEIW1	East Internal Wall	4705	0	29.25	20.39
VEIW2		4711	36.83	29.25	20.39
VEIW3		4718	81.75	29.25	20.39
VEIW4		4484	18.83	29.25	11.36
VEIW5		4487	36.83	29.25	11.36
VEIW6		4490	54.83	29.25	11.36
VEIW7		3677	0	29.25	-9.67
VEIW8		3683	36.83	29.25	-9.67
VEIW9		3690	81.75	29.25	-9.67
VEEW1	East External Wall	4649	0	0	20.39
VEEW2		4655	36.83	0	20.39
VEEW3		4662	81.75	0	20.39
VEEW4		4428	18.83	0	11.36
VEEW5		4431	36.83	0	11.36
VEEW6		4434	54.83	0	11.36
VEEW7		3609	0	0	-9.67
VEEW8		3615	36.83	0	-9.67
VEEW9		3622	81.75	0	-9.67

UHS - Ultimate Heat Sink Related Structures

Node Name	Component	Node Number	X- Ordinate	Y- Ordinate	Z- Ordinate
BAS1	Base Slab	1257	107.5	121.25	14.5
BAS2		871	83	7.6875	14.5
BAS3		862	2.5	7.6875	14.5
BAS4		1248	51	121.25	14.5
BAS5		705	8.5	7.6875	2.5
BAS6		1238	125.25	114.625	14.5
PRES1	Pump Room Elevated Slab	2484	2.5	77.75	73.5
PRES2		2414	8.5	21.5	55.5
PRES3		2374	71.25	-5.75	69.5
PRES4		2371	71.25	-20.75	35
PRES5		2411	2.5	21.5	60.5
PRES6		2481	8.5	69.4167	73.5
PRES7		2413	2.5	14.0625	55.5
PRRS1	Pump Room Roof Slab	3158	132	91.375	51.5
PRRS2		3098	34	14.0625	35
PRRS3		2998	94.75	-14.75	60.5
PRRS4		2995	94.75	-26.75	22.5
PRRS5		3095	132	91.375	22.5
PRRS6		3155	83	91.375	55.5
PRRS7		3145	2.5	98	22.5
PRRS8		3097	132	114.625	22.5
PRRS9		3037	83	77.75	51.5
CT1FS1	Cooling Tower 1 Fan Supported Slab	3292	71.25	60.25	60.5
CT1FS2		3192	21.25	77.75	55.5
CT1FS3		3186	27.5	130.25	51.5
CT1FS4		3286	71.25	130.25	51.5
CT1FS5		3236	51	130.25	51.5
CT1FS6		3202	15.5	2.5	55.5
CT1FS7		3232	66	130.25	22.5
CT1FS8		3283	45.75	-14.75	55.5
CT2FS1	Cooling Tower 2 Fan Supported Slab	3300	120.25	130.25	55.5
CT2FS2		3200	21.25	130.25	55.5
CT2FS3		3194	21.25	77.75	60.5
CT2FS4		3294	15.5	-26.75	60.5
CT2FS5		3244	58.5	60.25	60.5
CT2FS6		3203	15.5	2.5	51.5
CT2FS7		3240	51	2.5	22.5
CT2FS8		3284	45.75	-14.75	60.5
CT1MS1	Cooling Tower 1 Missile Shield Slab	3557	58.5	7.6875	112.5
CT1MS2		3478	15.5	2.5	35
CT1MS3		3476	132	98	28.75
CT1MS4		3555	51	7.6875	83.5
CT1MS5		3542	40.75	14.0625	83.5
CT1MS6		3516	45.75	2.5	28.75
CT1MS7		3490	21.25	130.25	43.25

Node Name	Component	Node Number	X- Ordinate	Y- Ordinate	Z- Ordinate
CT2MS1	Cooling Tower 2 Missile Shield Slab	3565	45.75	7.6875	112.5
CT2MS2		3484	34	130.25	43.25
CT2MS3		3482	15.5	77.75	43.25
CT2MS4		3563	66	39.5	112.5
CT2MS5		3548	76.25	26.8125	112.5
CT2MS6		3522	115	130.25	35
CT2MS7		3496	51	130.25	43.25
CT1RS1	Cooling Tower 1 Roof Slab	3704	83	-14.75	19.5
CT1RS2		3593	107.5	9.75	91.5
CT1RS3		3587	107.5	9.75	112.5
CT1RS4		3698	132	130.25	19.5
CT2RS1	Cooling Tower 2 Roof Slab	3712	100	-14.75	19.5
CT2RS2		3601	50.7503	33.1875	112.5
CT2RS3		3595	97.829	14.0625	91.5
CT2RS4		3706	76.25	-14.75	19.5
PRUWW1	Pump Room Upper West Wall	2862	45.75	43	69.5
PRUWW2		2874	58.5	43	60.5
PRUWW3		2908	100	2.5	69.5
PRUWW4		2964	115	-14.75	22.5
PRUWW5		2798	34	26.8125	69.5
PRUWW6		2756	21.25	2.5	35
PRUWW7		2666	132	121.25	51.5
PRUWW8		2612	76.25	60.25	69.5
B1WW1	Basin 1 West Wall	2306	45.75	2.5	112.5
B1WW2		1874	40.75	43	28.75
B1WW3		1446	100	39.5	83.5
B1WW4		1431	119.849	26.8125	83.5
B1WW5		1859	15.5	77.75	22.5
B1WW6		1865	27.5	77.75	35
B1WW7		2058	115	43	112.5
B1WW8		2291	66	60.25	51.5
PRLWW1	Pump Room Lower West Wall	2161	132	7.6875	103.5
PRLWW2		2279	51	43	96.8333
PRLWW3		1419	125.25	130.25	19.5
PRLWW4		187	2.5	51.25	9.5
PRLWW5		139	2.5	7.6875	9.5
PRLWW6		1777	83	2.5	35
PRLWW7		1789	89.75	-14.75	35
PRLWW8		1823	89.75	-5.75	69.5
PRLWW9		1369	132	69.4167	19.5

Node Name	Component	Node Number	X- Ordinate	Y- Ordinate	Z- Ordinate
PRUEW1	Pump Room Upper East Wall	2965	107.5	44.5	51.5
PRUEW2		2909	94.75	2.5	35
PRUEW3		2875	58.5	44.5	60.5
PRUEW4		2863	51	43	69.5
PRUEW5		2613	76.25	60.25	60.5
PRUEW6		2667	125.25	130.25	55.5
PRUEW7		2757	21.25	2.5	43.25
PRUEW8		2799	27.5	33.1875	73.5
CTUWW1	Cooling Tower Upper West Wall	3539	94.75	7.6875	83.5
CTUWW2		3513	58.5	2.5	28.75
CTUWW3		3474	132	108	28.75
CTUWW4		3338	15.5	39.5	55.5
CTUWW5		3347	15.5	26.8125	73.5
CTUWW6		3353	66	51.25	51.5
CTUWW7		3434	83	26.8125	28.75
CTUWW8		3431	34	51.25	28.75
CTUWW9		3425	2.5	98	28.75
PRLEW1	Pump Room Lower East Wall	2280	66	43	103.5
PRLEW2		2162	132	7.6875	90.1667
PRLEW3		1778	83	2.5	51.5
PRLEW4		144	34	7.6875	9.5
PRLEW5		192	34	51.25	9.5
PRLEW6		1420	15.5	55	14.5
PRLEW7		1824	76.25	-5.75	69.5
PRLEW8		1370	2.5	74.75	19.5
BIW1	Basin Interior Wall	2277	58.5	43	96.8333
BIW2		2020	132	51.25	51.5
BIW3		1397	2.5	121.25	19.5
BIW4		1432	125.25	21.5	83.5
BIW5		1447	94.75	39.5	83.5
BIW6		1875	51	43	22.5
BIW7		2059	100	43	112.5
BIW8		2307	45.75	43	83.5
BIW9		2292	58.5	-14.75	51.5
BIW10		1837	132	-14.75	51.5
BIW11		1860	15.5	77.75	28.75
CTUMW1	Cooling Tower Upper Middle Wall	3545	40.75	26.8125	112.5
CTUMW2		3519	100	130.25	35
CTUMW3		3480	15.5	2.5	28.75
CTUMW4		3339	15.5	43	55.5
CTUMW5		3348	15.5	60.25	73.5
CTUMW6		3354	58.5	51.25	60.5
CTUMW7		3435	83	33.1875	28.75
CTUMW8		3432	83	21.5	28.75
CTUMW9		3426	2.5	91.375	28.75

Node Name	Component	Node Number	X- Ordinate	Y- Ordinate	Z- Ordinate
B2EW1	Basin 2 East Wall	2278	51	43	90.1667
B2EW2		2021	132	51.25	60.5
B2EW3		1398	83	121.25	19.5
B2EW4		1433	120.44	21.5	83.5
B2EW5		1448	71.5	22.75	83.5
B2EW6		1876	51	43	35
B2EW7		2060	107.5	60.25	51.5
B2EW8		2308	45.75	43	73.5
B2EW9		2293	51	-14.75	51.5
B2EW10		1838	132	-14.75	35
B2EW11		1861	8.5	77.75	28.75
CTUEW1	Cooling Tower Upper East Wall	3551	76.25	33.1875	112.5
CTUEW2		3525	94.75	130.25	43.25
CTUEW3		3486	27.5	130.25	43.25
CTUEW4		3340	15.5	44.5	55.5
CTUEW5		3349	15.5	55	73.5
CTUEW6		3355	51	51.25	60.5
CTUEW7		3436	83	51.25	28.75
CTUEW8		3433	83	14.0625	28.75
CTUEW9		3427	34	21.5	28.75
B2NW1	Basin 2 North Wall	2323	71.25	2.5	96.8333
B2NW2		1463	94.75	14.0625	112.5
B2NW3		1469	120.25	25.2872	112.5
B2NW4		1896	83	60.25	55.5
B2NW5		1894	83	60.25	51.5
B2NW6		1892	66	43	35
B2NW7		2081	125.25	2.5	96.8333
B2NW8		2329	71.25	43	96.8333
B1NW1	Basin 1 North Wall	2310	45.75	43	103.5
B1NW2		1450	76.25	21.5	83.5
B1NW3		1461	97.829	14.0625	112.5
B1NW4		1887	34	7.6875	35
B1NW5		1884	71.25	43	28.75
B1NW6		1880	51	43	28.75
B1NW7		2070	115	-14.75	51.5
B1NW8		2321	71.25	2.5	103.5
PRUNW1	Pump Room Upper North Wall	2970	132	130.25	43.25
PRUNW2		2969	132	130.25	35
PRUNW3		2968	132	121.25	35
PRUNW4		2967	120.25	-5.75	35
PRUNW5		2801	51	7.6875	103.5
PRUNW6		2802	45.75	7.6875	103.5
PRUNW7		2803	71.25	7.6875	103.5
PRUNW8		2804	66	7.6875	103.5

Node Name	Component	Node Number	X- Ordinate	Y- Ordinate	Z- Ordinate
PRLNW1	Pump Room Lower North Wall	2287	51	60.25	55.5
PRLNW2		2284	51	43	112.5
PRLNW3		1852	132	-14.75	55.5
PRLNW4		1424	0	0	109.5
PRLNW5		1427	0	0	109.5
PRLNW6		1855	2.5	77.75	22.5
PRLNW7		1854	27.5	77.75	22.5
PRLNW8		2040	100	2.5	112.5
CT2UNW1	Cooling Tower 2 Upper North Wall	3567	71.25	7.6875	83.5
CT2UNW2		3564	45.75	7.6875	83.5
CT2UNW3		3561	58.5	39.5	112.5
CT2UNW4		3365	71.25	51.25	69.5
CT2UNW5		3368	45.75	21.5	103.5
CT2UNW6		3371	45.75	26.8125	103.5
CT2UNW7		3452	132	21.5	28.75
CT1UNW1	Cooling Tower 1 Upper North Wall	3559	66	7.6875	112.5
CT1UNW2		3556	66	7.6875	83.5
CT1UNW3		3553	76.25	14.0625	83.5
CT1UNW4		3357	58.5	51.25	69.5
CT1UNW5		3360	45.75	51.25	51.5
CT1UNW6		3363	71.25	51.25	51.5
CT1UNW7		3444	132	21.5	35
CT2USW1	Cooling Tower 2 Upper South Wall	3472	132	91.375	35
CT2USW2		3469	132	114.625	43.25
CT2USW3		3466	132	108	35
CT2USW4		3330	21.25	26.8125	73.5
CT2USW5		3333	21.25	69.4167	73.5
CT2USW6		3336	15.5	26.8125	55.5
CT2USW7		3417	2.5	108	43.25
CT1USW1	Cooling Tower 1 Upper South Wall	3464	132	77.75	28.75
CT1USW2		3461	132	74.75	35
CT1USW3		3458	132	84.75	35
CT1USW4		3322	21.25	43	55.5
CT1USW5		3325	21.25	60.25	55.5
CT1USW6		3328	21.25	14.0625	73.5
CT1USW7		3409	120.25	2.5	28.75
PRUSW1	Pump Room Upper South Wall	2844	45.75	43	51.5
PRUSW2		2843	71.25	2.5	69.5
PRUSW3		2842	71.25	2.5	43.25
PRUSW4		2841	71.25	2.5	35
PRUSW5		2591	83	60.25	35
PRUSW6		2592	83	60.25	43.25
PRUSW7		2593	83	55	35
PRUSW8		2594	83	55	43.25

Node Name	Component	Node Number	X- Ordinate	Y- Ordinate	Z- Ordinate
PRLSW1	Pump Room Lower South Wall	2143	120.25	-26.75	35
PRLSW2		2140	100	-5.75	69.5
PRLSW3		1524	125.25	21.5	112.5
PRLSW4		134	8.5	2.5	9.5
PRLSW5		137	27.5	2.5	9.5
PRLSW6		1527	125.25	26.8125	112.5
PRLSW7		1526	132	26.8125	112.5
PRLSW8		1952	89.75	-20.75	35

ESWPT

Node Name	Component	Node Number	X-Coordinate	Y-Coordinate	Z-Coordinate
Tun_1a_D_S-01	Bottom Slab	4614	-11.5	56	-36.25
Tun_1a_D_S-02		4620	11.5	56	-36.25
Tun_1a_D_S-03	Top Slab	5165	-11.5	56	-19.58
Tun_1a_D_S-04		5171	11.5	56	-19.58
Tun_1a_D_S-05	Exterior Wall 1	4761	-11.5	56	-32.92
Tun_1a_D_S-06		5022	-11.5	56	-22.91
Tun_1a_D_S-07	Interior Wall	4762	0	56	-32.92
Tun_1a_D_S-08		5023	0	56	-22.91
Tun_1a_D_S-09	Exterior Wall 2	4763	11.5	56	-32.92
Tun_1a_D_S-010		5024	11.5	56	-22.91
Tun_1a_SE_S-01	Bottom Slab	666	0	48	-26.33
Tun_1a_SE_S-02		672	23	48	-26.33
Tun_1a_SE_S-03	Top Slab	1089	0	48	-10.67
Tun_1a_SE_S-04		1095	23	48	-10.67
Tun_1a_SE_S-05	Exterior Wall 1	796	0	48	-22.42
Tun_1a_SE_S-06		952	0	48	-14.59
Tun_1a_SE_S-07	Interior Wall	797	11.5	48	-22.42
Tun_1a_SE_S-08		953	11.5	48	-14.59
Tun_1a_SE_S-09	Exterior Wall 2	798	23	48	-22.42
Tun_1a_SE_S-010		954	23	48	-14.59
Tun_1b_D_S_S-01	Bottom Slab	1456	5.75	4.79	-36.25
Tun_1b_D_S_S-02		1454	-5.75	4.98	-36.25
Tun_1b_D_S_S-03	Top Slab	2900	5.75	4.79	-19.58
Tun_1b_D_S_S-04		2898	-5.75	4.98	-19.58
Tun_1b_D_S_S-05	Exterior Wall 1	1818	11.5	4.69	-32.08
Tun_1b_D_S_S-06		2540	11.5	4.69	-23.75
Tun_1b_D_S_S-07	Interior Wall	1816	0	4.89	-32.08
Tun_1b_D_S_S-08		2538	0	4.89	-23.75
Tun_1b_D_S_S-09	Exterior Wall 2	1814	-11.5	5.08	-32.08
Tun_1b_D_S_S-010		2536	-11.5	5.08	-23.75
Tun_F-01	Bottom Slab	1451	-11.5	92	9.91
Tun_F-02		1457	11.5	92	9.91
Tun_F-03	Top Slab	2232	-11.5	92	25.58
Tun_F-04		2238	11.5	92	25.58
Tun_F-05	Exterior Wall 1	2002	-11.5	92	21.66
Tun_F-06		1726	-11.5	92	13.83
Tun_F-07	Interior Wall	2003	0	92	21.66
Tun_F-08		1727	0	92	13.83

Node Name	Component	Node Number	X-Coordinate	Y-Coordinate	Z-Coordinate
Tun_F-09	Exterior Wall 2	2004	11.5	92	21.66
Tun_F-010		1728	11.5	92	13.83
Tun_E_PipeChase-01	Bottom Slab	482	-12	28	-36.25
Tun_E_PipeChase-02		488	13	28	-36.25
Tun_E_PipeChase-03	Top Slab	690	-12	28	-25.58
Tun_E_PipeChase-04		696	13	28	-25.58
Tun_E_PipeChase-05	Exterior Wall 1	614	-12	28	-29.42
Tun_E_PipeChase-06		566	-12	28	-33.25
Tun_E_PipeChase-07	Interior Wall	615	0	28	-29.42
Tun_E_PipeChase-08		567	0	28	-33.25
Tun_E_PipeChase-09	Exterior Wall 2	616	13	28	-29.42
Tun_E_PipeChase-010		568	13	28	-33.25

9) The NEI check process is described in detail in FSAR Section 3OO.1.4. The NEI check and adjusted Foundation Input Response Spectra (FIRS) for the horizontal and vertical directions for Reactor Building (R/B) Complex are presented in Figures 3OO-235 and 3OO-236, respectively. Similar figures for East and West Power Source Buildings (PS/Bs) are presented in the response to RAI 5546, Question 03.07.02-3. As described in FSAR Section 3OO.1.1, the site specific Power Source Fuel Storage Vault (PSFSV) structures use the same SSI input motions as those of the PS/B and the same NEI check figures presented in response to RAI 5546, Question 03.07.02-3 for the East and West PS/Bs apply to the East and West PSFSVs. These figures are not repeated here.

   The NEI check and adjusted FIRS for East Essential Service Water Pipe Tunnel (ESWPT) in the horizontal and vertical directions are provided in Figure 1 and Figure 2, respectively. As described in FSAR 3OO.1.4, the adjusted FIRS are smoothed to obtain Soil Structure Interaction (SSI) input motions. The adjustment for horizontal spectrum occurs at frequencies between 2.4 Hz and 8.0 Hz with a maximum factor of 1.06. For the vertical spectrum the modification occurs at frequencies between 2.3 Hz and 6.2 Hz with a maximum factor of 1.03.

   The NEI check and adjusted FIRS for West ESWPT in the horizontal and vertical directions are provided in Figure 3 and Figure 4, respectively. Note that the adjusted FIRS for the East and West ESWPT are enveloped prior to smoothing to constitute the SSI input motion for the East and West ESWPT. The adjustment for horizontal spectrum occurs at frequencies between 2.2 Hz and 7.9 Hz with a maximum factor of 1.07. For the vertical spectrum the

modification occurs at frequencies between 2.0 Hz and 8.3 Hz with a maximum factor of 1.08.

The NEI check and adjusted FIRS for the Ultimate Heat Sink Related Structure (UHSRS) Pipe Chase in the horizontal and vertical directions are provided in Figure 5 and Figure 6, respectively. As described in FSAR 3OO.1.4, the adjusted FIRS are smoothed to obtain SSI input motions. The adjustment for horizontal spectrum occurs at frequencies above 4.0 Hz with a maximum factor of 1.04. For the vertical spectrum the modification is more pronounced and it occurs at frequencies above 4.8 Hz with a maximum factor of 1.22.

As described in FSAR Section 3OO.1.2, the UHSRS are analyzed as surface structures, thus the NEI check does not apply to the SSI input motions developed for them.

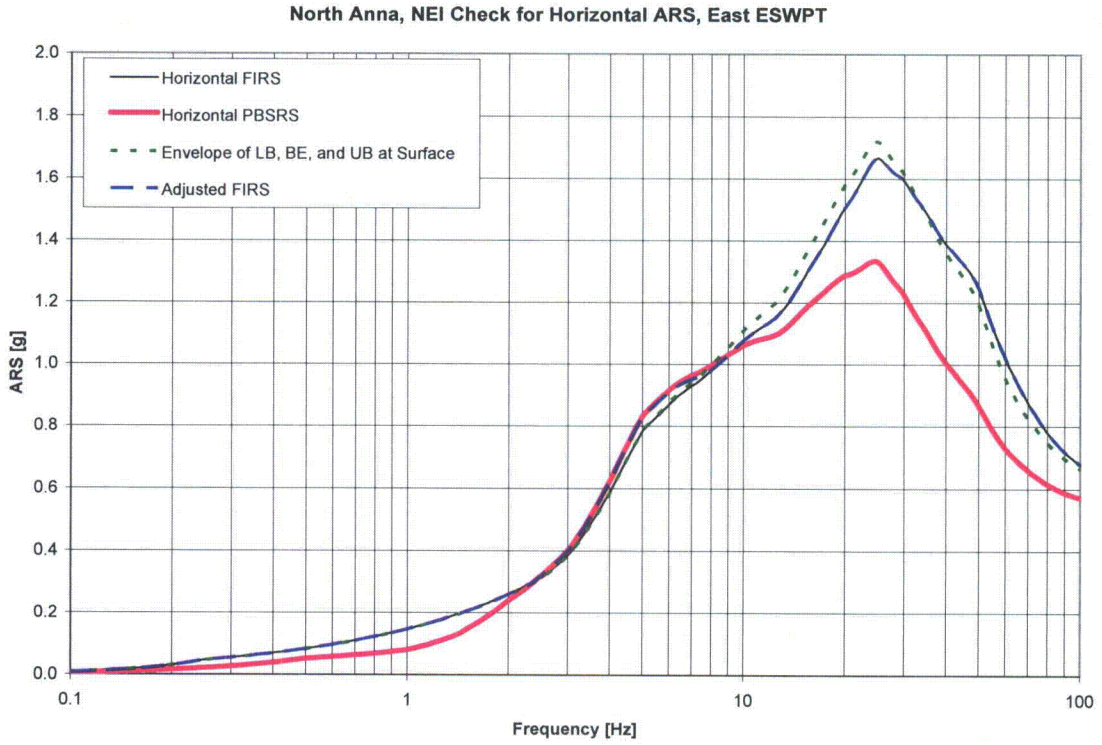

Figure 1 - NEI Check of Horizontal FIRS for East ESWPT

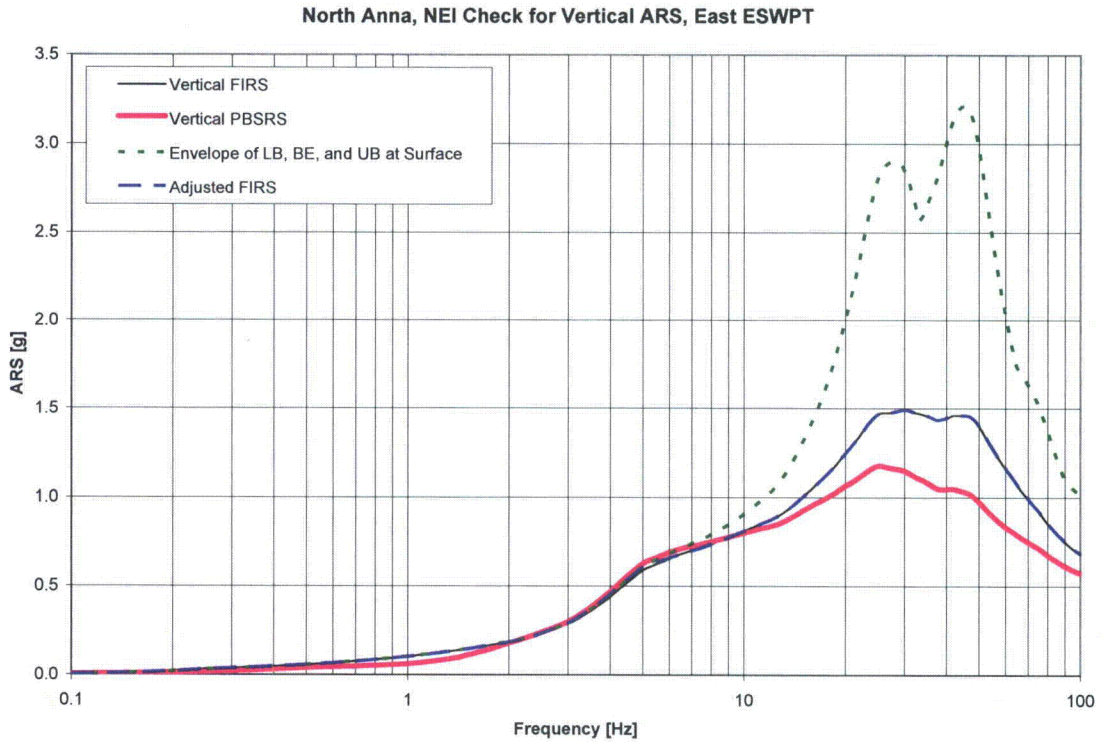

Figure 2 - NEI Check of Vertical FIRS for East ESWPT

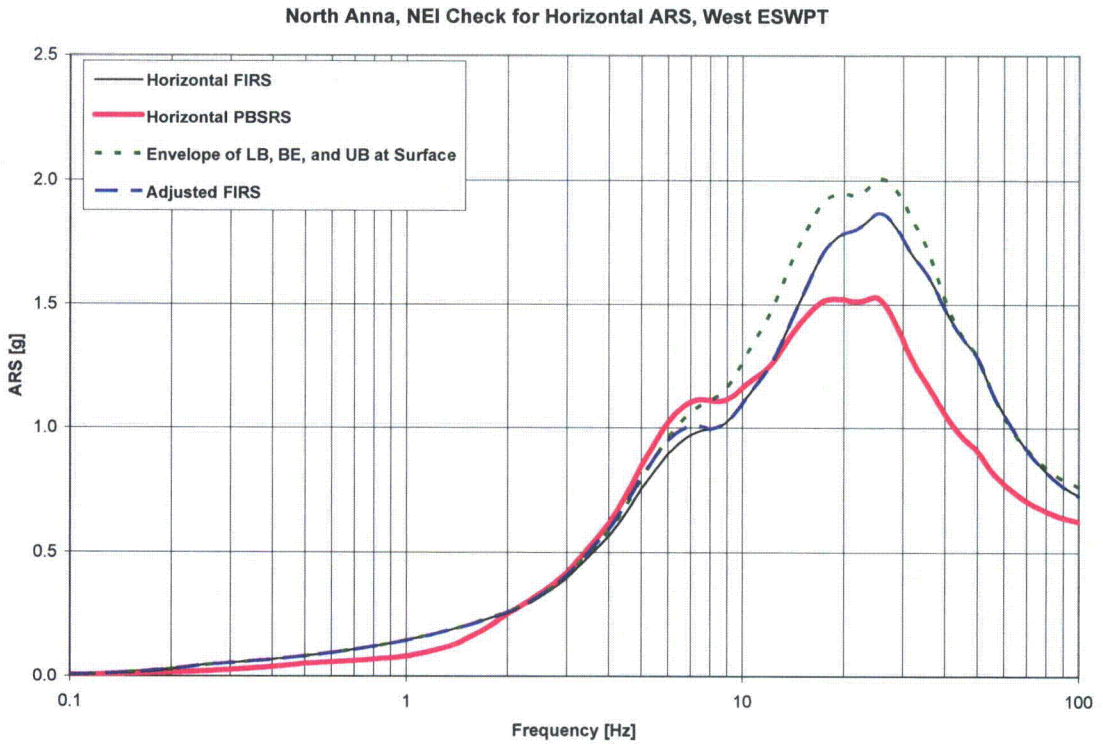

Figure 3 - NEI Check of Horizontal FIRS for West ESWPT

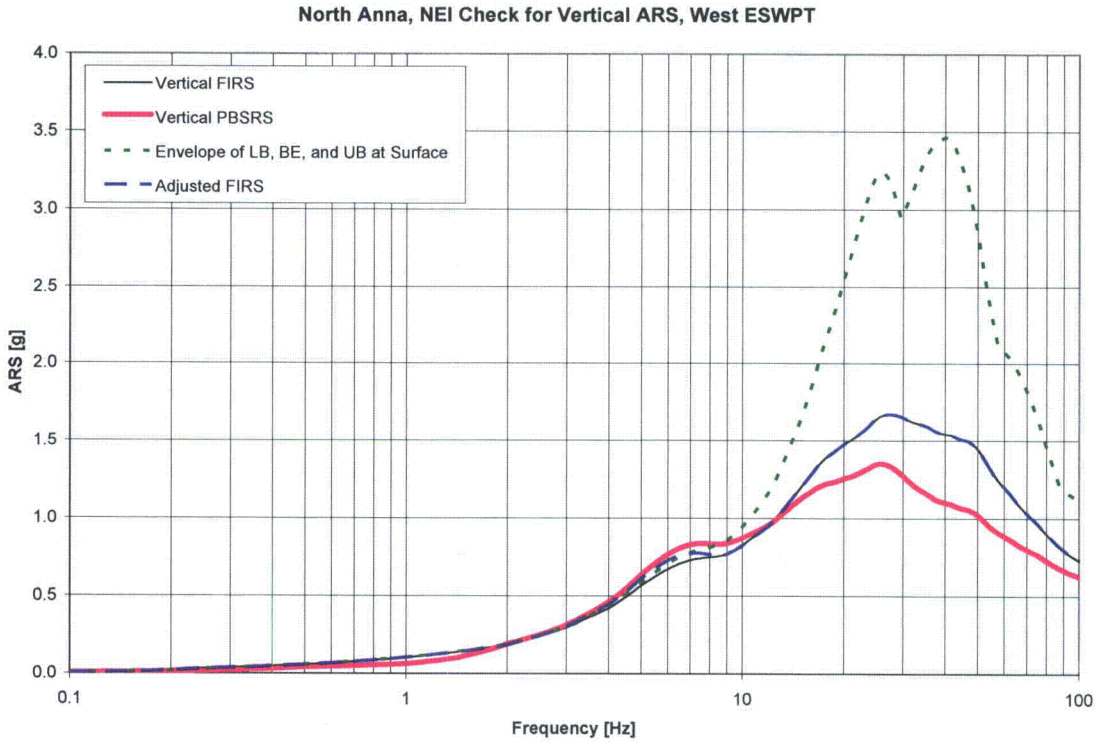

Figure 4 - NEI Check of Vertical FIRS for West ESWPT

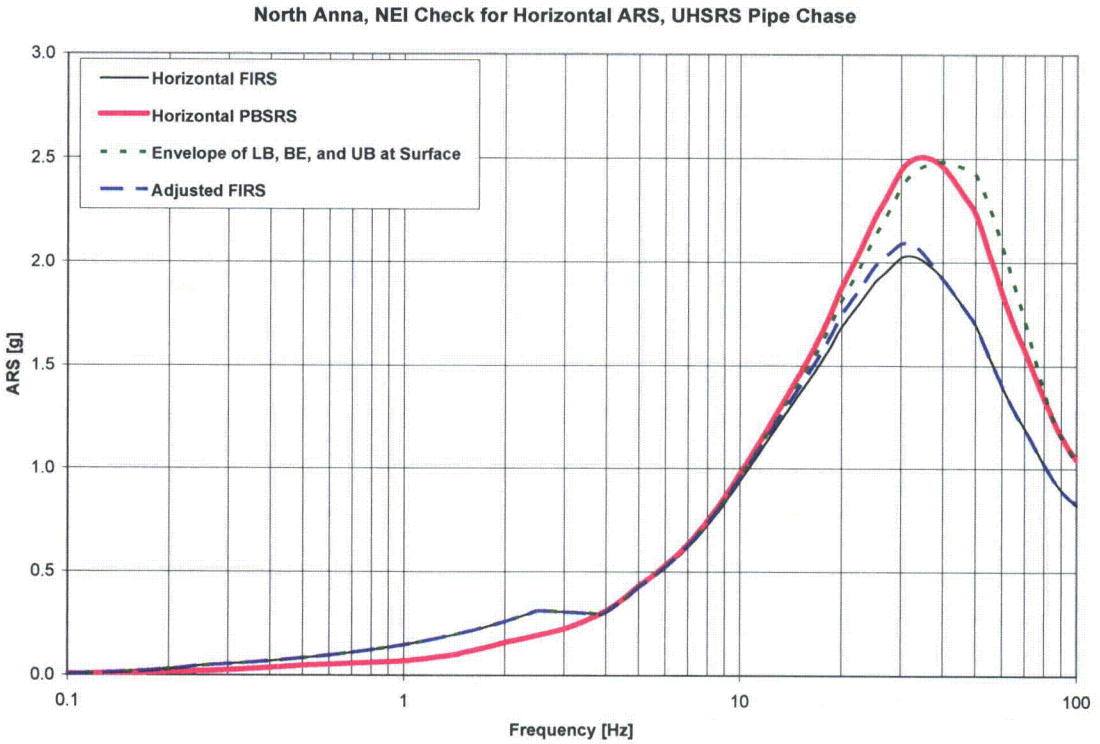

Figure 5 - NEI Check of Horizontal FIRS for UHSRS Pipe Chase

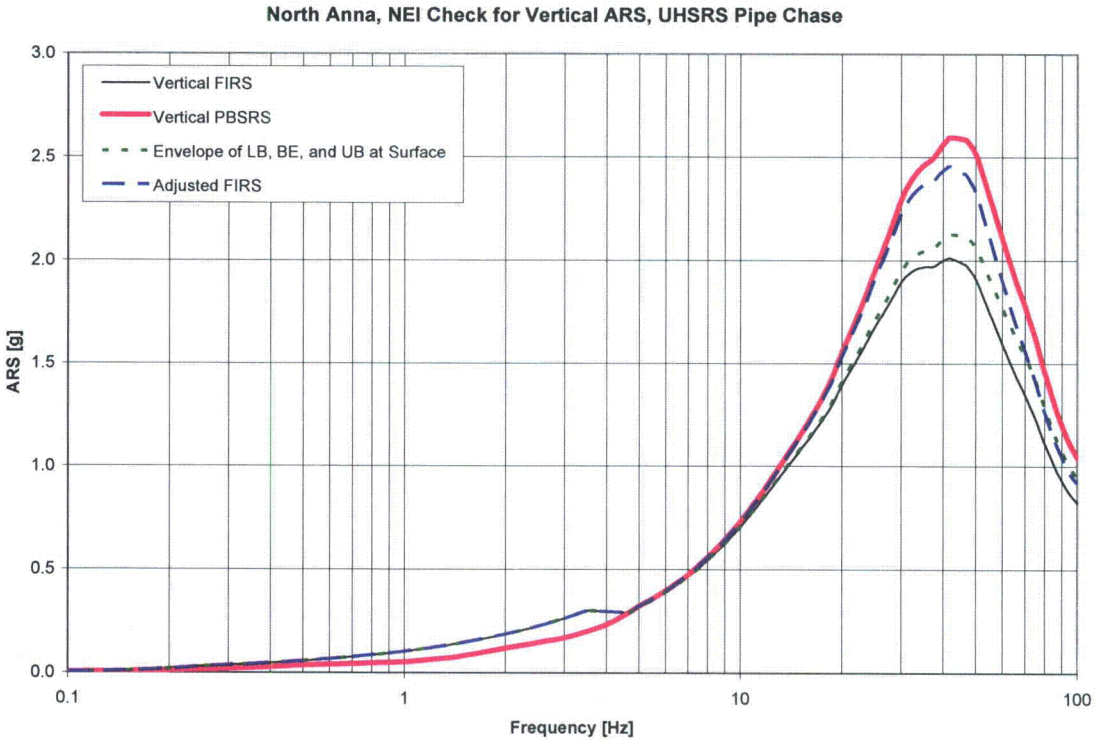

Figure 6 - NEI Check of Vertical FIRS for UHSRS Pipe Chase

Proposed COLA Revision

COLA Part 11 Sections 2.2, 3.1.3, 4.1.3, and 5.1.1 will be revised as indicated on the attached markup.

Markup of North Anna COLA

The attached markup represents Dominion's good faith effort to show how the COLA will be revised in a future COLA submittal in response to the subject RAI. However, the same COLA content may be impacted by revisions to the DCD, responses to other COLA RAIs, other COLA changes, plant design changes, editorial or typographical corrections, etc. As a result, the final COLA content that appears in a future submittal may be somewhat different than as presented herein.

2.0 SITE DESIGN CONDITIONS

2.1 Plant Layout

FSAR Figure 3.8-201 presents the layout of the North Anna Unit 3 US APWR Plant. All directions are with respect to plant north. The site-specific seismic Category I structures as shown in FSAR Figure 3.8-201 consist of four UHSRS, an east and a west PSFSV, and the ESWPT. The four units of UHSRS are located plant north of the R/B complex and are labeled as A, B, C and D, where UHSRS unit A and UHSRS unit D are located at the east and west ends of the plant respectively. UHS units B and C located east and west of the plant centerline and are connected by the UHSRS pipe chase. The UHSRS are founded on Zone III rock with a layer of concrete fill with a nominal thickness of 5 ft placed on the rock. The main basemat of the UHSRS basin is located at nominal elevation of 277'-0". The basemat of the UHSRS pit hosting the pump outlet is located at nominal elevation of 265'-0". The foundation of the UHSRS pipe chase is located at nominal elevation of 286'-0".

The east and west PSFSVs are located south of the east and west PS/Bs respectively. Fuel pipe access tunnels provide access between the PSFSVs and the PS/B. The basemats of the east and west PSFSVs rest on the surface of a thick block of fill concrete that is supported on the Rock III and IV. The nominal elevation of the PSFSVs foundations is 272'-3".

Refer to FSAR Figure 3.8-201 for the orientation of ESWPT segments. Two segments of the ESWPT, 1a located east of the R/B complex and 1b located west of the R/B complex, are connected to the UHSRS. ESWPT Segment 1a is divided into two portions: Segment 1a-S and Segment 1a-N. Segment 1a-N extends north of the east PS/B north wall and segment 1a-S extends south of the east PS/B north wall. The segment of the ESWPT south of the R/B complex and below the T/B is labeled as segment 2. This segment interfaces with the ESWPT that are integrally attached to the east and west PSFSV structures. The bottoms of the ESWPT segment 1a and 1b basemats are at nominal elevation of 259'-1", and the bottom of the segment 2 basemat is at nominal elevation 251'-2".

For details of the UHSRS refer to FSAR Figures 3.8-206, 3.8-208, 3.8-209, and 3.8-210; for the PSFSVs refer to FSAR Figures 3.8-204, 3.8-212, 3.8-213, and 3.8-214; and for the ESWPT refer to FSAR Figures 3.8-201, 3.8-202, 3.8-203, and 3.8-205.

The foundation excavations are backfilled with engineered fill material to establish the nominal elevation of the plant grade at 290 ft. All of the elevations are based upon NAVD88 system and it is noted that the difference between NGVD29 and NAVD88 is +0.86 ft.

2.2 Dynamic Soil Properties

In order to account for the variation of soil properties and the uncertainties in measurement methods, a range of properties are used for each set of SSI analyses. Besides best estimate (BE) values of subgrade and backfill properties, the site-specific analyses address the variation of the

subgrade properties by considering lower bound (LB) and upper bound (UB) properties. The layering and the dynamic properties of the subgrade materials such as unit weight, strain compatible S-wave and P-wave velocities and damping are obtained from the site response analyses. Identical damping values are assigned to the profiles used to model the dissipation of energy in the site soil, rock and fill concrete materials associated with both S-wave and P-wave velocities.

The site models for SSI analysis of the UHSRS, PSFSVs and ESWPT use infinitely horizontal layers to represent the dynamic properties of the embedment soil, the excavated soil and the top strata of subgrade materials. The properties of the subgrade at greater depths are represented by a half-space modeled by 10 visco-elastic layers. Each half-space layer has a thickness of:

$$\text{layer thickness} = \frac{(1.5Vs) \div f}{n}$$

where:

Vs = the shear wave velocity of the half-space
f = the frequency of analysis
n = the number of half-space layers

Viscous dashpots are modeled at the base of the simulated half-space. The profiles of the embedment soil strain compatible properties that are obtained directly from the site response analyses are adjusted to match the geometry of the finite element mesh of the SSI models. The S-wave and P-wave velocities of the backfill (Vs and Vp) are adjusted using the equivalent arrival time methodology as follows:

$$Vs = \frac{D}{\sum \frac{d_i}{Vs_i}} \quad \text{and} \quad Vp = \frac{D}{\sum \frac{d_i}{Vp_i}}$$

where: D is the thickness of the embedment soil layer in the SASSI site model, d_i are the thicknesses of the embedment soil layers in the site response analysis model, Vs_i and Vp_i are the strain-compatible S-wave and P-wave velocities corresponding to the layering of the site response model. The soil damping (Ds) and the unit density (ws) of the backfill layers in the SASSI site model is calculated as weighted average using the following formula:

$$Ds = \frac{\sum d_i \bullet Ds_i}{D} \quad \text{and} \quad ws = \frac{\sum d_i \bullet ws_i}{D}$$

where: Ds_i and ws_i are the damping and the unit weight of the soil corresponding to the layering of the model used for site response analysis.

Four sets of site properties are used for the analyses of Segment 2 of the ESWPT, and the east and a west PSFSV structures. These values are identical to those used for the SSI analyses of

3.1.3 SSI Analysis

The UHSRS is modeled in SASSI as a structure resting on the surface of the subgrade at elevation 277 ft, which coincides with the UHSRS basin main basemat bottom. The input motion is applied at the subgrade surface for all SSI analyses. The depth of the shallow 13 ft thick backfill embedment, which extends from elevation 277 ft to nominal plant grade elevation of 290 ft, is small relative to the height of the UHSRS. Therefore, the SSI analyses neglect the embedment effects of the engineered backfill. The SSI analysis of the UHSRS considers a total of eight subgrade profiles, as described in Section 2.0, to address variations and uncertainties in soil properties. The lower boundary used in the SASSI analysis is 368 feet below grade. The depth to the lower boundary is more than twice the size of foundation plus embedment (158' x 2 + 13' = 329') as recommended by SRP 3.7.2 (Reference 3).

The cutoff frequencies for all SASSI analyses are greater than 50 Hz (the cut-off frequency is 50 Hz per the US-APWR DCD) and the responses from a minimum of 101 modes are determined. The lowest frequency of analysis for all SASSI runs is 0.012 Hz. Acceleration transfer functions are interpolated using Option 2 in the ACS SASSI MOTION module input (Reference 3NN-1), and no smoothing of the transfer functions is applied. For each analysis, the amplitudes of the acceleration functions are plotted and inspected to check the accuracy of the interpolation and to ensure that the expected structural responses were observed. Frequencies of analyses were added if needed to improve the accuracy. Sufficient frequencies of analyses are selected to cover SSI and primary structural frequencies. SSE structural damping values of DCD Chapter 3 Table 3.7.3-1(a) are used in the site-specific SASSI analysis. The design of reinforced concrete members shows high level of design stresses that justifies the use of higher SSE damping values.

The following SSI analysis cases are used for calculating the seismic response of the UHSRS:

- A total of four analysis cases using four different BE subgrade properties to represent the conditions anticipated beneath UHSRS A through D.
- An analysis case using the LB subgrade properties to represent the conditions anticipated beneath UHSRS A, B, and C.
- An analysis case using the UB subgrade properties to represent the conditions anticipated beneath UHSRS A, B, and C.
- Two analysis cases using LB and UB subgrade properties to represent the conditions anticipated beneath UHSRS D.

Consideration of the above listed cases assures that the enveloped results presented herein capture all potential seismic effects of a wide range of subgrade properties.

The SSI analyses produce results including ISRS, maximum displacements relative to the top of the main basement and maximum displacements relative to the free field motion. The acceleration

4.1.3 SASSI SSI Model and Analysis

The SSI analyses of the PSFSV model are performed using methods and approaches consistent with ASCE 4 (Reference 5) and accounting for the site-specific stratigraphy and subgrade conditions as well as the backfill conditions around the embedded PSFSV structures.

Consideration of a total of four profiles, each, for both the embedded and surface conditions assures that the enveloped results from all eight sets of SSI analyses capture all potential seismic effects of a wide range of site conditions. The profiles represent the UB, LB, and BE of soil properties. Best estimate profiles are developed for both the east and west vaults. The following summarizes the eight soil profiles utilized in the SSI analyses:

SSI Soil Profiles:

Designation	Description
SBEE	Surface Model - BE, East Vault
SBEW	Surface Model - BE, West Vault
SUBEW	Surface Model - UB Estimate
SLBEW	Surface Model - LB Estimate
EBE1	Embedded Model - BE, East Vault
EBE2	Embedded Model - BE West Vault
EUB	Embedded Model - UB Estimate
ELB	Embedded Model - LB Estimate

SSE structural damping values of Table 1 of RG 1.61 (Reference 7) are used in the site-specific SASSI analysis. The seismic response of the PSFSV results in high stress levels for the reinforced concrete members. That warrants the use of higher SSE damping values to account for the dissipation of energy due to material damping.

The surface SSI model of the PSFSV has a cut-off frequency of 50 Hz and 101 frequency points for all four soil profiles. For the PSFSV embedded models, the flexible interface method, with interaction nodes at the foundation-soil interface, is used for the SSI analyses. This method provides particularly accurate results in the low-frequency range, which is important for capturing embedment effects. For the embedded models, the shear wave passing frequency for all layers below the base slab, based on layer thickness of 1/5 wavelength, ranges from 12 Hz for ELB to 34 Hz for EUB. The SASSI analysis frequencies are selected to cover the range between 0.05 Hz and the cutoff frequency of 50 Hz. This frequency range includes the SSI frequency and primary structural frequencies. It is verified that as the transfer functions approached the zero frequency (static input), the co-directional transfer function approached unity while the cross-directional terms approached zero. The acceleration transfer functions are interpolated using Option 2 in the ACS SASSI MOTION module input (Reference 3NN-1), and no smoothing of the transfer functions is

applied. For each analysis, the amplitudes of the acceleration functions are plotted and inspected to check the accuracy of the interpolation and to ensure that the expected structural responses were observed. Frequencies of analyses were added if needed to improve the accuracy. Table 4.0-7 shows the cut-off frequencies and numbers of frequency points for the embedded soil profiles.

4.2 Analysis Results

Table 4.0-4 presents the natural frequencies obtained from the modal analyses of the ANSYS detailed design model. Table 4.0-10 presents a summary of SSI effects on the seismic response of the PSFSVS.

Table 4.0-6 provides the summary of maximum displacements relative to the PSFSV basemat obtained from the response spectra analyses of ANSYS detailed design model and the SASSI analyses of the SSI model. The table shows the correlation of the results obtained from the two types of analyses. The values presented for the maximum relative displacements represent the envelope of the SSI analyses results of all soil cases considered. The SASSI analyses where the PSFSV is conservatively modeled as a structure supported by a 21.25 ft thick block of fill concrete resting on the surface of the rock subgrade provide the maximum relative displacement values that explains why in some cases SASSI analysis results exceed the ANSYS results.

Table 4.0-8 shows that the maximum displacements of the PSFSV relative to the free field ground motion are small (less than 0.10 inch), which confirms that the 4 inch gaps between the PSFSV and the adjacent structures and foundation are sufficient to ensure that no collision will occur during an earthquake.

Figures 4.0-14 through 4.0-16 provide profiles of the soil pressure distributions. These figures indicate that the upper bound soil profile for the embedded SSI model governs the out-of-plane pressure forces on the exterior walls.

Table 4.0-5 provides the ANSYS Design Model shears and reactions at the base of the walls. It is inaccurate to calculate the base reaction forces using the results of an SSRS combination of three directional response spectrum analysis results as in the procedure described above. This is due to the fact that the "directional" sense of forces and displacements is lost in the squaring procedure. The correct procedure to determine the total out-of-phase contribution to base reaction forces is to calculate the base reaction forces for each mode and then sum these modal values using the Lindley-Yow method. The total base shear and vertical reactions shown in Table 4.0-5 were determined in this manner.

Table 4.0-10 presents the overall factors of safety for the PSFSV structure against sliding, overturning and flotation.

5.0 ESWPT AND UHSRS PIPE CHASE

5.1 Model Description and Analysis Approach

The ESWPT is divided into segments separated by expansion joints that prevent interaction between them during seismic events. FSAR Figure 3.8-201 shows the plant layout with the extent of each ESWPT segment. Segments 1a-N and 1a-S run in the north-south direction and are located east of the R/B complex. Segment 1b with its straight and skewed portions runs in the north-south direction and is located west of the R/B complex. These segments are completely buried in backfill on all sides except for Segment 1a-S that is adjacent to the East Power Source Building. The SSI analyses of ESWPT Segment 1a-S consider the tunnel as a surface foundation due to the presence of a four-inch gap separating the tunnel from the adjacent PS/B.

Segment 2 of the ESWPT runs in the east-west direction. Segment 2 is located underneath the north end of the T/B. The exterior walls and the roof of Segment 2 are not in contact with soil.

The portion of the ESWPT that is located between the PSFSVs and PS/Bs is cast together with the basemat of the PSFSVs and are referred to as the PSFSV tunnels, as shown in FSAR Figures 3.8-212 and 3.8-213.

The structure located between the UHSRS B and C is a partially embedded pipe chase that is part of the UHSRS, and this structure is therefore labeled as the "UHSRS pipe chase." The pipe chase portions integrally attached to the UHSRS are designed as part of their respective UHSRS as previously mentioned in Section 1.0 and shown in FSAR Figures 3.8-206, 3.8-208, 3.8-209, and 3.8-210.

Two set of seismic response analyses are employed:

1. ANSYS response spectrum analyses of a fixed base model to calculate seismic demands for design of structural members for "UHSRS pipe chase" and ESWPT Segment 2; and

2. ACS SASSI SSI analyses to calculate ISRS used for design of Seismic Category I and II subsystems, components and equipment. The ACS SASSI analyses of Segments 1a-S, 1a-N and 1b provide maximum accelerations of the roof, interior and exterior wall and base slab of the tunnel. These maximum acceleration results serve as basis for development of equivalent static demands (inertia forces) that are used for the design of the structural members.

The results for maximum relative displacements obtained from ANSYS response spectra analyses and ACS-SASSI analyses of ESWPT Segment 2 and UHSRS pipe chase are compared to verify and confirm the accuracy of responses obtained from the two different types of analyses.

5.1.1 SSI Model and Analysis

To address differences in geometry/configuration, site conditions, input motion, and loading, SSI analyses of the ESWPT use a total of four models: one each for Segments 1a- N, 1a-S, 1b, and 2.

As previously addressed, there are also SSI models for the UHSRS pipe chase, the PSFSV which includes a pipe passage/tunnel for the essential service water piping, and the UHSRS model which includes a pipe chase for the essential service water piping. The SSI analyses considers tunnel Segments 1a-N and 1b as underground structures with subgrade at the bottom and backfill soil in contact with the exterior walls and roof of the tunnel. The seismic response of the ESWPT Segments 1a-S and 2 are obtained from the SSI analyses of surface foundations without soil at the sides and the top of the tunnel. The SSI analysis of the UHSRS pipe chase uses a SASSI model of a partially embedded structure. ESWPT segments adjacent to the UHSRS and the PSFSVs are connected to the UHSRS and PSFSV structures and analyzed using integrated models as described in Sections 3.0 and 4.0. However, the acceleration response spectra results obtained from the SSI analyses of the PSFSV segments of the tunnel and UHSRS pipe chases are used for development of ISRS defining seismic demands for design of Seismic Category I and II components and equipment located anywhere in the ESPWT or UHSRS pipe chases (see detail discussion in Section 5.3).

The SSI models for all ESWPT segments with the exception of the UHSRS and PSFSV portions are shown in Figures 5.0-1 through 5.0-4. The SSI model for the UHSRS pipe chase is shown in Figure 5.0-5. Shell elements model the roof, interior and exterior walls and the basemat. Brick elements model the backfill and fill concrete below the ESWPT basemat. Where the shell elements and brick elements are connected, the shell elements extend into the brick elements to transmit nodal rotations. The extended elements shares nodes with the corresponding face of the solid elements and are massless.

Table 5.0-1, 5.0-2 and 5.0-3, respectively, present the material properties, geometry and types of elements assigned to the structural components of the SASSI FE models of ESWPT Segments 1a, 1b and 2 and UHSRS pipe chase. Table 5.0-4 presents the fixed base natural frequencies of ESWPT Segment 2 and UHSRS pipe chase. The material properties of the walls, roof and base slabs of ESWPT Segments 1a and 1b are adjusted to consider the cracked concrete properties (adjusted values are not shown in the aforementioned tables). The out-plane stiffness for those members are reduced to one half of the uncracked flexural stiffness. Refer to Section 4.1.1 for description of the methodology used to adjust the material and geometrical properties of the members to take into account for cracked flexural stiffness. SSE damping values are used in the site-specific SASSI analysis.

Table 5.0-5 provides a summary of the main characteristics of the SSI models and analyses for the ESWPT and UHSRS pipe chase. For each set of SSI analyses, the table presents the profiles used of soil strain compatible dynamic properties as described in Section 2.4 and the type of SSI analyses. For the embedded models listed in Table 5.0-5, the flexible interface method, with interaction nodes at the foundation-soil interface, is used for the SSI analyses. This method provides particularly accurate results in the low-frequency range which is important for capturing embedment effects. The listed maximum frequencies show the ability of the different models to

transmit seismic waves with high frequency. Table 5.0-5 also presents for each set of SSI analyses the total number of frequencies of analyses used and the cut off frequency.

The results of the SASSI analyses are validated through reviews of the transfer functions and other output to make sure that adequate frequencies of analyses are used for calculation. It was verified that as the transfer functions approached the zero frequency, the co-directional transfer function approached unity while the cross-directional terms approached zero. The acceleration transfer functions are interpolated using Option 2 in the ACS SASSI MOTION module input (Reference 3NN-1), and no smoothing of the transfer functions is applied. Transfer functions are examined for each analysis to verify that the interpolation was reasonable and that the expected structural responses were observed. Frequencies of analyses were added if needed to improve the accuracy of the transfer function interpolations. Transfer functions, spectra, accelerations, and soil pressures are compared between the various soil profiles used in analyses to verify that the responses are reasonably similar between these cases except for the expected trends due to soil frequency changes.

The SASSI analyses produce results including peak accelerations, in-structure response spectra, seismic element demands, and seismic soil pressures. All results from SSI analyses represent the envelope of all soil conditions. The SASSI analysis results are used to produce the ISRS and provide confirmation of the inputs to the ANSYS design model.

5.1.2 ANSYS Static and Response Spectrum Analyses

The structural components in the ANSYS models used for static and response spectra analyses are modeled with finite elements that have the same properties and configuration as the ACS SASSI models. ANSYS shell type element 181 is used for roof, floor slab, exterior and interior walls. The 9'-11" thick foundation of ESWPT Segment 2 is modeled by ANSYS SOLID45 elements. COMBIN14 type elements are used to model the soil springs representing the stiffness of the subgrade under the foundation base.

The seismic demands for design of the tunnel structural members are obtained from two types of ANSYS analyses:

1. Equivalent static analyses of ESWPT Segments 1a and 1b.

2. Response spectra analyses of Segment 2 and UHSRS pipe chase.

The static analyses use input seismic forces that include self inertial loads and dynamic soil pressures on exterior walls and the roof of the tunnel. The seismic soil pressure demands are applied on the structural elements as equivalent static pressures. The pressures applied are of larger magnitude compared to the calculated elastic solution used in ASCE 4-98 based on J.H. Wood, 1973 (Reference 5) following the methodology described in Section 2.4. The magnitude and distribution of the dynamic pressures are validated through comparison with the SSI analyses results for dynamic pressures. Soil above the tunnel is accounted for with a shear force applied at

ENCLOSURE 5

Response to NRC RAI Letter 64

RAI 5546 Question 03.07.02-5

RESPONSE TO REQUEST FOR ADDITIONAL INFORMATION

North Anna Unit 3

Dominion

Docket No. 52-017

RAI NO.: 5546 (RAI Letter 64)

SRP SECTION: 03.07.02 – SEISMIC SYSTEM ANALYSIS

QUESTIONS for Structural Engineering Branch 1 (AP1000/EPR Project) (SEB1)

DATE OF RAI ISSUE: 4/7/2011

QUESTION NO.: 03.07.02-5

The NA3 FSAR on Page 3-196 states, "The shell elements of the walls extend into the basemat solid elements to enable transmittal of nodal rotations. Rigid 3D beam elements connect the top of the basement shear walls with lumped-mass stick model representing the above ground portion of the R/B and FH/A. This modeling approach enables the R/B-FH/A to be connected to the flexible part of the building basement and decoupled from the thick central part that serves as foundation to the PCCV and containment internal structure part of the building."

The description in the paragraph quoted above does not address the full range of possible element connectivity in a 3D model for all Category-I structures. To address this issue, the staff requests the applicant to provide detailed information accompanied by appropriate illustrations that address connectivity between different types of elements used in the analysis models, including connectivity between shells and solids, beams and solids, and shells and beams, and show how applicable degrees of freedom are transmitted at these connections.

Dominion Response

The development of the structural models used for North Anna Unit 3 site-specific SSI analysis of Category I structures considered the connectivity between the various finite element (FE) types to ensure where applicable an adequate transfer of forces and/or moments from one structural component to another.

In the case of the lumped mass stick model of the reactor building (R/B) complex, rigid shell elements are used to account for the thick portion of the basemat under the containment. Rigid beam elements are then used to connect the rigid shell elements at the top of the basement shear walls to the lumped mass stick model representing the above ground portion of the R/B complex and fuel handling area (FH/A) such as shown in Figure 1. Figure 2 shows the connectivity between the lumped mass stick model of the R/B complex with the FE model of the

basement that consists of rigid beams connecting each node of the basement exterior walls with the stick element representing the stiffness of the first floor of the reactor building.

The Advanced Computational Software for System Analysis of Soil-Structure Interaction (ACS SASSI program) solid element nodes have only three translational degrees of freedom and can therefore not transfer moments from shell or beam elements. Shell elements modeling walls and slabs in all 3-D models of Category I structures are extended into solid elements to enable a proper transfer of moments from walls and slabs to several layers of solid element nodes as shown in Figure 3. Shell elements providing the connection have identical stiffness properties as shell elements modeling walls and slabs but are assigned a zero mass.

Each node of the ACS SASSI shell elements has five degrees of freedom that enable the transfer of forces and bending moments from beam elements to shell elements but not torsional or drilling moments. In the cases when the transfer of moments from members modeled with beam elements to members modeled by shell or solid elements is an important contributor to the dynamic response of the structure, massless rigid beam elements are generated on the surface of the shell or solid elements. Figure 4 and Figure 5 show examples of techniques used to provide adequate transfer of moments in all three rotational degrees of freedom from beams to solid elements and shell elements, respectively.

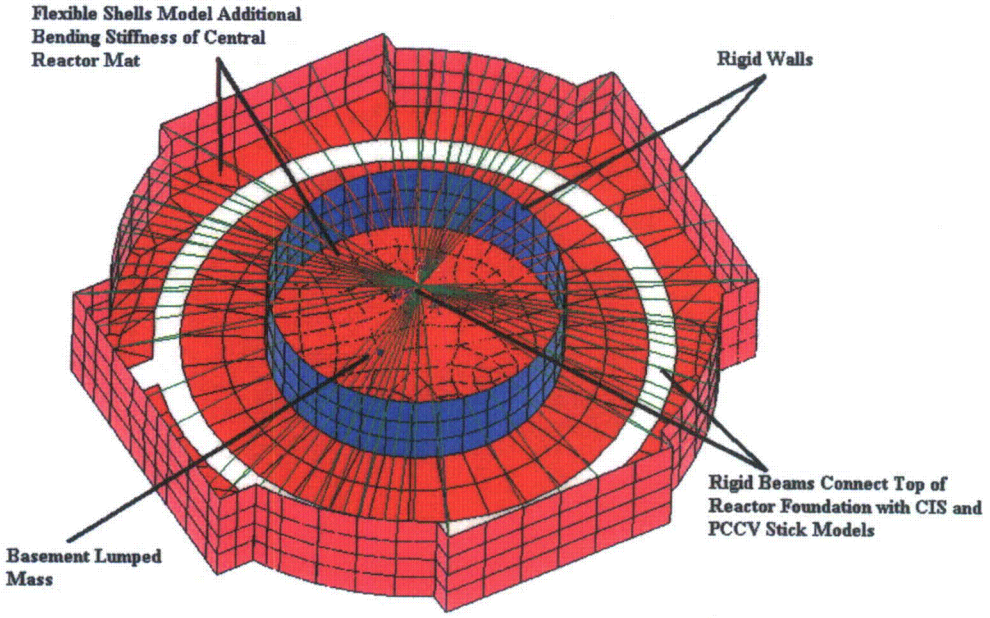

Figure 1 Element Connectivity Below the PCCV

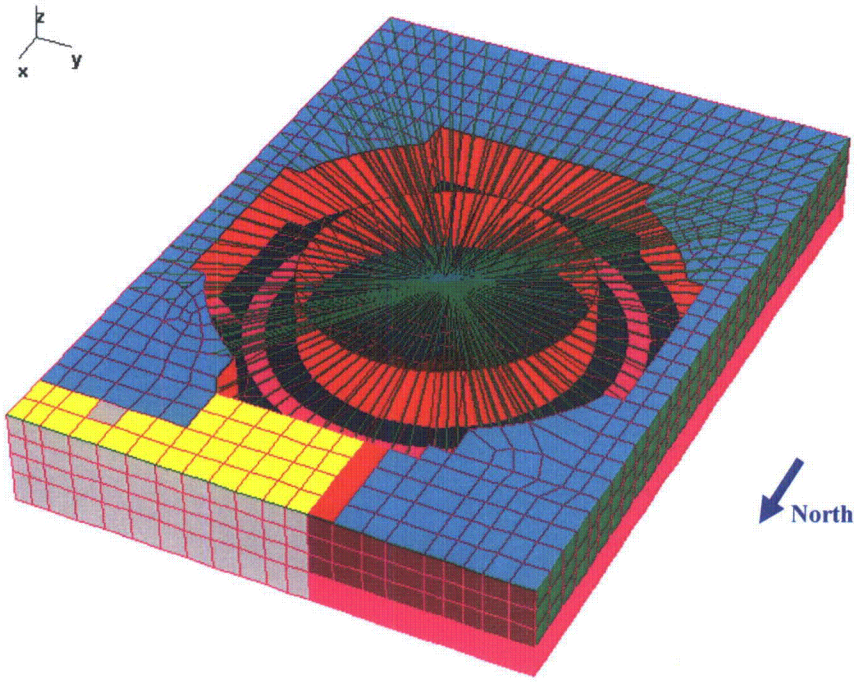

Figure 2 Connectivity of R/B Complex Lumped Mass Stick Model and Basement FE Model

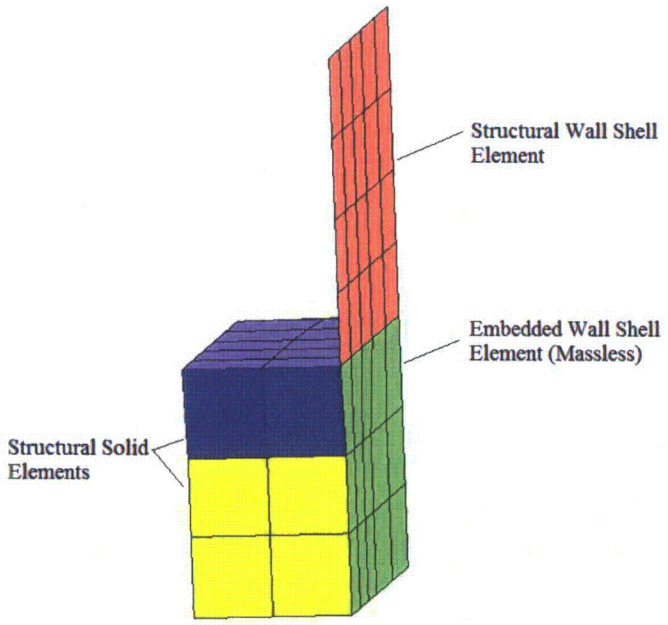

Figure 3 Connection of Shell to Solid Elements

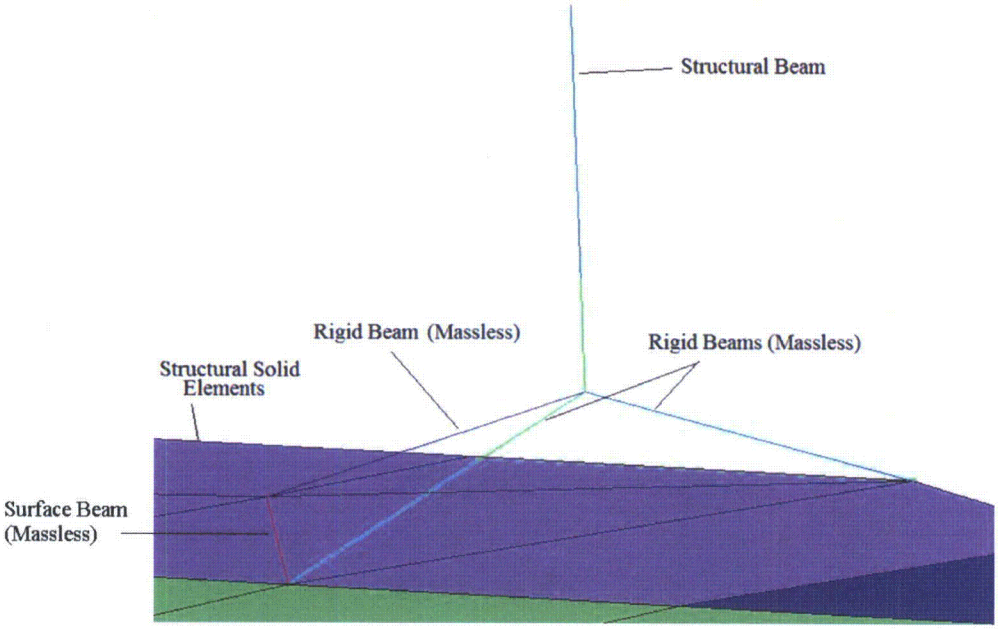

Figure 4 Connection of Beam to Solid Elements

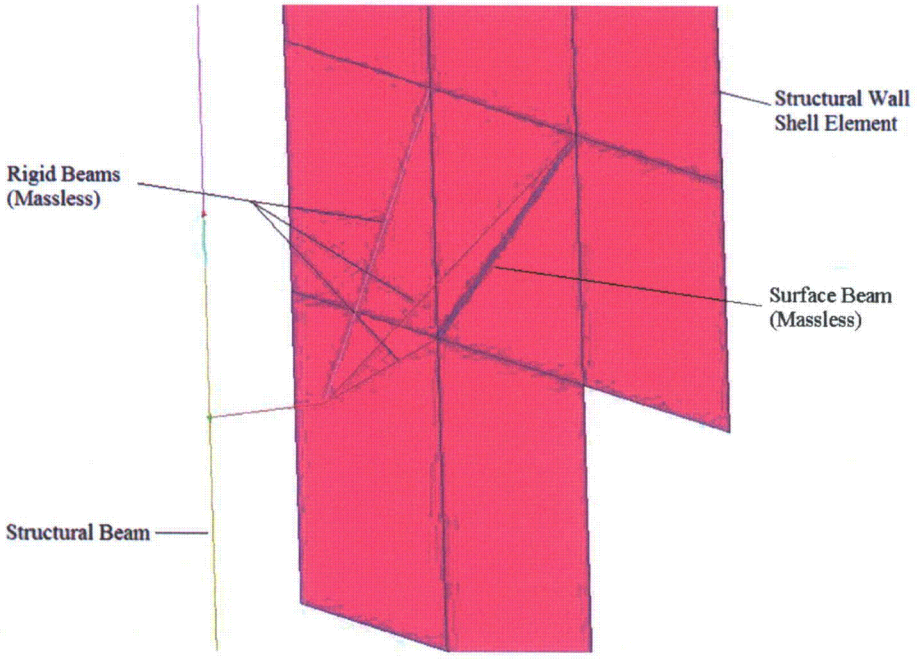

Figure 5 Connection of Beam to Shell Elements

Proposed COLA Revision

None

ENCLOSURE 6

Response to NRC RAI Letter 64

RAI 5546 Question 03.07.02-9

RESPONSE TO REQUEST FOR ADDITIONAL INFORMATION

North Anna Unit 3

Dominion

Docket No. 52-017

RAI NO.: 5546 (RAI Letter 64)

SRP SECTION: 03.07.02 – SEISMIC SYSTEM ANALYSIS

QUESTIONS for Structural Engineering Branch 1 (AP1000/EPR Project) (SEB1)

DATE OF RAI ISSUE: 4/7/2011

QUESTION NO.: 03.07.02-9

The staff understands that the dynamic soil-structure interaction analyses presented in the NA3 FASR do not account for potential separation and sliding between soil and structure under the design-basis earthquake ground motion. The SRP Section 3.7.2, "Seismic System Analysis" provides guidance that appropriate sensitivity studies should be performed to identify important parameters and to assist in judging the adequacy of the final results. These sensitivity studies can be performed by the use of well-founded and properly substantiated simple models to give better insight. The applicant is requested to provide information that addresses the effects of soil-structure separation and sliding on the results of seismic SSI analyses, including dynamic soil pressure and stability analyses, of Category I structures at the Unit 3 site.

Dominion Response

In order to account for the effect of the backfill on the seismic response of the structures, the North Anna Unit 3 site-dependent soil-structure interaction (SSI) analyses consider two bounding cases: 1) a surface foundation where the basement of the building is not in contact with the backfill surrounding it, and 2) a fully embedded foundation where all of the exterior walls of the basement are in full contact with soil at all times. The responses obtained from these two cases are enveloped in order to develop the bounding SSI responses for Unit 3. The seismic evaluation of Category I buildings ensures that sliding of Category I buildings during an earthquake will either not occur or will be resisted by structural elements designed to provide the required sliding resistance.

Sensitivity studies for backfill soil-structure separation were not performed specifically for Unit 3 but conclusions were derived based on the design bases analyses done to support the R-COLA (Reference 1), described as follows. The soil separation analyses are described for the UHSRS and PSFSV in Appendices 3KK and 3MM in the R-COLA. Tables 3KK-3 and 3MM-4 in those appendices state that soil separation effects on the SSI response are small. Information contained in the response to Question 03.07.01-06 of R-COLA RAI 193-5254 (Reference 2)

summarizes the surface foundation and embedment conditions considered. The R-COLA design basis analyses showed that separation of backfill soil did not produce significant changes in the design-basis ISRS. The ISRS were generally governed by the surface foundation condition. Where the surface foundation ISRS did not govern, the fully embedded foundation case governed or had only small differences from the embedded case with soil separation, and these differences were captured in the ISRS broadening process. Example Figures 1, 2, and 3 below, which show ISRS for the response of the R-COLA PSFSV at a typical node point near the center of the roof, demonstrate this point. In the horizontal directions shown in Figures 1 and 2, the ISRS for the surface condition govern. In the vertical direction shown in Figure 3, the embedded condition ISRS do exceed the surface condition ISRS at some resonant frequencies. This is mainly due to the fact that the acceleration time history of the minimum earthquake vertical outcrop motion was used as input motion for both the surface and embedded SSI analyses, as stated in R-COLA FSAR Section 3NN.2. This generally results in response amplitudes for the embedded analyses which are higher than would be obtained if within-layer motion were used as input motion. Where exceedances of the surface conditions ISRS do occur, the differences between the separated versus non-separated conditions are negligible. Another expected result shown in Figures 1, 2, and 3 is that ISRS for the separated soil typically are between the two extremes of the ISRS for the surface and fully embedded conditions. Similarly, soil separation considered in the R-COLA design basis analyses did produce changes to the dynamic soil pressure distributions, but resulted in only small differences in seismic demands and stability analyses which were captured by the margins present in the R-COLA design.

Further, the seismological conditions at the North Anna Unit 3 site are such that any displacements that are not captured by the site-specific SSI analyses, and are due to potential sliding or separation between the soil and the structure, will be of small amplitude and duration and will have insignificant effect on the seismic response of the US-APWR structures. The North Anna Unit 3 site-specific design ground motion is characterized by high frequency content and is of very low intensity at frequencies lower than 10 Hz. The displacements in the SSI dynamic system when subjected to this type of high-frequency excitation are of small amplitudes and durations. The comparison of results for maximum structural displacements relative to the free field motion in FSAR Tables 3NN-18 and 3NN-19 shows that the North Anna Unit 3 site-specific displacements are almost an order of magnitude lower than those calculated for the standard plant CSDRS-defined design motion. Therefore, potential sliding or separation at soil-structure interfaces can produce only insignificant shifts in the frequencies of the SSI responses. Any potential displacements in the SSI system larger than the elastic displacements calculated by the site-specific SSI analyses will be accompanied by higher dissipation of energy, reducing the responses at resonant frequencies.

In summary, soil-structure separation effects were investigated and included as part of the R-COLA design basis seismic analyses, and were not investigated further for the Unit 3 site-specific analyses, based on consideration of the North Anna Unit 3 site-specific conditions and design and the results obtained from the R-COLA. The US-APWR Category I buildings at the Unit 3 site are founded on rock and embedded in engineered fill material with much lower stiffness. The conditions at CPNPP with respect to the dynamic properties of the subgrade and the backfill material are very similar to those at Unit 3 site. However, since the site-specific design ground motion at the Unit 3 site is characterized by high energy content in the high-frequency range and very low energy content in the lower frequency range, separation between the soil and the structure will be small and short in duration. This leads to the conclusion that these effects will be considerably smaller than those for the case of design ground motion that is defined by CSDRS shape spectra and characterized with much energy content in the lower

frequency range, such as that at CPNPP. It is worth noting that the PSFSV and UHSRS at Unit 3 are founded on rock as in the R-COLA; however, these Unit 3 structures have much lower depths of embedment. This results in an actual condition at Unit 3 closer to a surface foundation condition, where the effects of the embedment and thus the effects of separation of backfill soil and the structure are much smaller than those at CPNPP site. These arguments demonstrate that the results of the sensitivity studies performed for the R-COLA are applicable for the Unit 3 site conditions.

References:

(1) Comanche Peak, Units 3 and 4 COLA, FSAR Revision 1, Luminant Generation Company, LLC, NRC Docket Nos. 52-034 and 52-035

(2) Comanche Peak, Units 3 and 4, Response to RAI 193-5254, Luminant Generation Company, LLC, Letter TXNB-11004 dated 1/27/2011

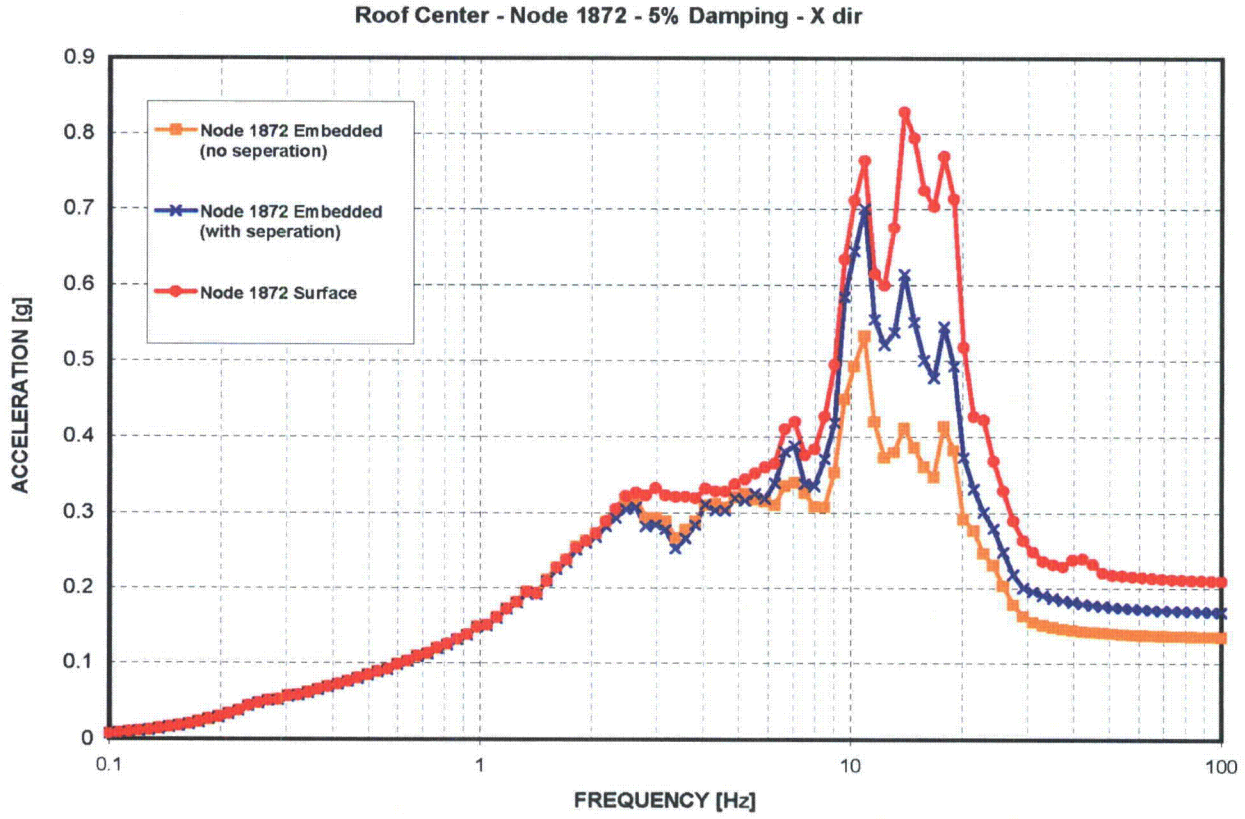

Figure 1 Horizontal (X-Direction) ISRS at Center of R-COLA PSFSV Roof

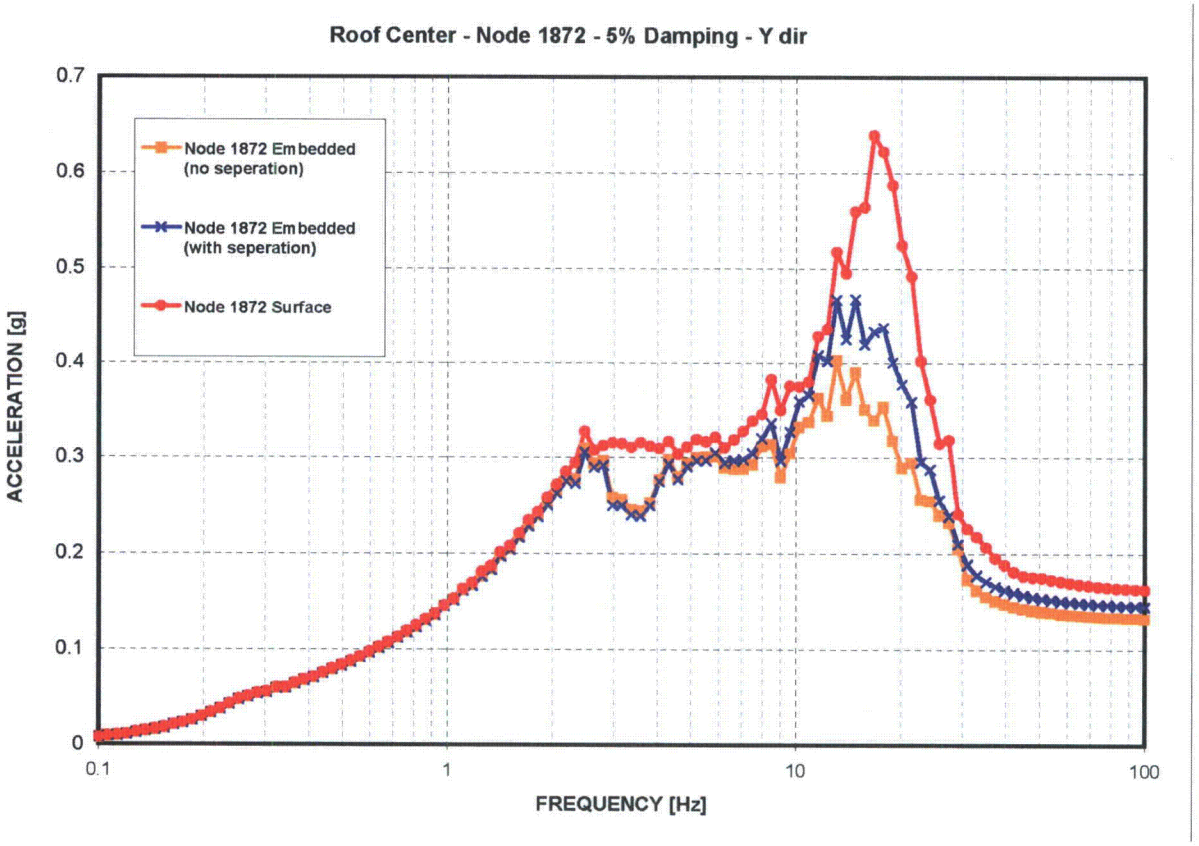

Figure 2 Horizontal (Y-Direction) ISRS at Center of R-COLA PSFSV Roof

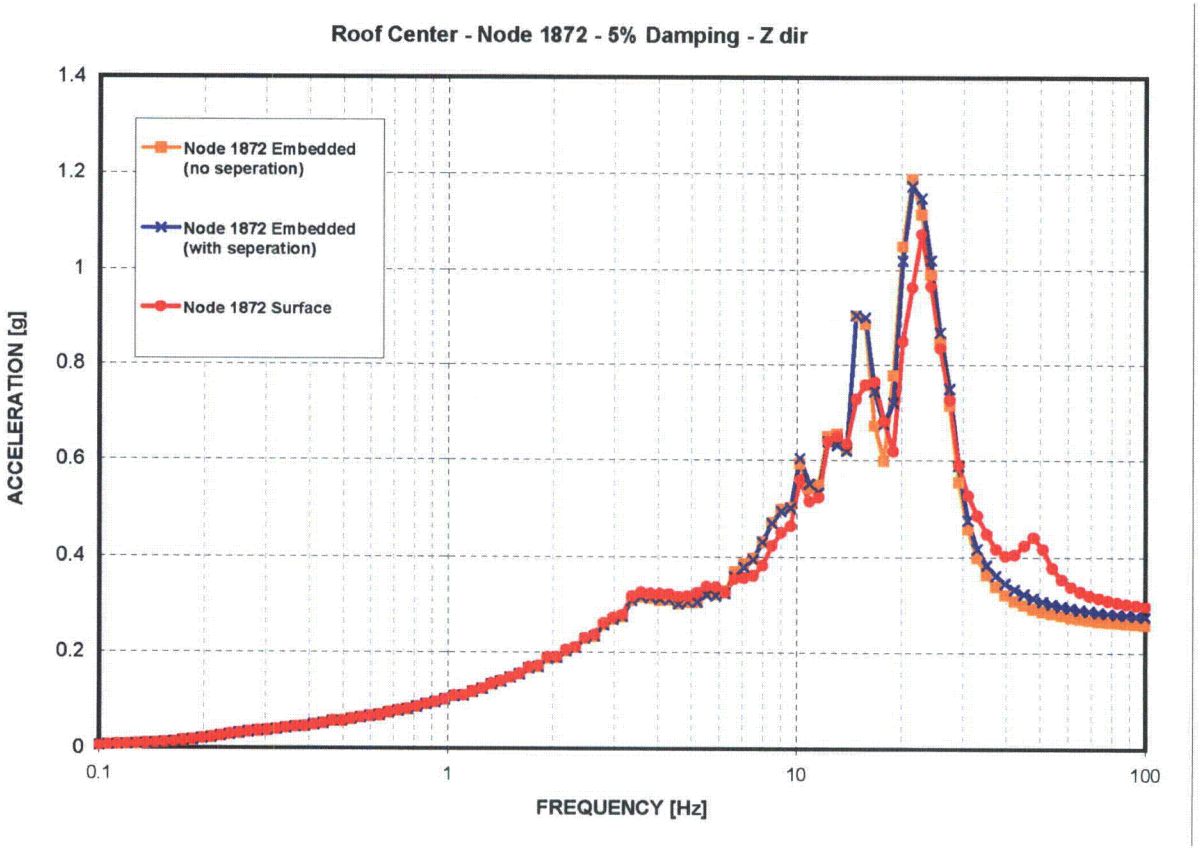

Figure 3 Vertical (Z-Direction) ISRS at Center of R-COLA PSFSV Roof

Proposed COLA Revision

None